EVALUATION OF COMBINED DEINKING PROCESS AND NOVEL UTILIZATION OF DEINKING SLUDGE

Ph.D. THESIS

by

SHILPA KULKARNI

DEPARTMENT OF PAPER TECHNOLOGY
INDIAN INSTITUTE OF TECHNOLOGY ROORKEE
ROORKEE- 247667 (INDIA)
SEPTEMBER, 2015

EVALUATION OF COMBINED DEINKING PROCESS AND NOVEL UTILIZATION OF DEINKING SLUDGE

A THESIS

Submitted in partial fulfilment of the requirements for the award of the degree of
DOCTOR OF PHILOSOPHY

by

SHILPA KULKARNI

DEPARTMENT OF PAPER TECHNOLOGY
INDIAN INSTITUTE OF TECHNOLOGY ROORKEE
ROORKEE- 247667 (INDIA)
SEPTEMBER, 2015

INDIAN INSTITUTE OF TECHNOLOGY ROORKEE
ROORKEE

CANDIDATE'S DECLARATION

I hereby certify that the work which is being presented in the thesis entitled **"EVALUATION OF COMBINED DEINKING PROCESS AND NOVEL UTILIZATION OF DEINKING SLUDGE"** in partial fulfilment of the requirements for the award of the Degree of Doctor of Philosophy and submitted in the Department of Paper Technology of the Indian Institute of Technology Roorkee is an authentic record of my own work carried out during a period from July, 2009 to September, 2015 under the supervision of Dr. Vivek Kumar, Associate Professor and Dr. M. C. Bansal, (Retd.) Professor, Department of Paper Technology, Indian Institute of Technology Roorkee, Roorkee, India.

The matter presented in the thesis has not been submitted by me for the award of any other degree of this or any other Institute.

(Shilpa Kulkarni)

This is to certify that the above statement made by the candidate is correct to the best of our knowledge.

(Vivek Kumar)
Supervisor

(M. C. Bansal)
Supervisor

The Ph.D Viva-Voce Examination of **Ms. Shilpa Kulkarni**, Research Scholar, has been held on .....

Chairman, SRC

External Examiner

This is to certify that the student has made all the corrections in the thesis.

Signature of Supervisor (s)

Head of the Department

Dated: .....

ABSTRACT

There is an increasing need for recycling. However, for recycling of paper, conventional method of chemical deinking is used but it needs further improvements to make the quality of recycled fibres reach up to that of virgin fibres, as far as possible. Hence, the present work is focused on evaluation of combined deinking process. Moreover, increase in recycling increases the production of waste called deinking sludge. This waste creates disposal problem. Hence, this work also focuses on the utilization of deinking sludge for useful energy recovery as well as for the production of building materials like brick. This research work is divided into four chapters:

Chapter 1 gives general introduction about the issues and challenges being faced by Indian recycled paper industry. It also discusses and highlights the objectives and scope of the present work.

Chapter 2 focuses on the studies on deinking processes using combined deinking and chemical deinking technologies. Combined deinking refers to the application of UV irradiation and ultrasound treatment on chemically deinked pulp. Photocopier waste paper was used as the raw material for this study. The optimization of duration of application of UV irradiation and ultrasound treatment was carried out to study their effects on the effectiveness of deinking processes. This was accomplished by evaluating various properties obtained after the application of selected treatments. The comparison of properties was carried out among all the three deinking processes. It appears that the combined deinking technology produced better results as compared to chemical deinking for most of the optical as well as strength properties. Hence, combined deinking technology can further improve the deinkability potential of chemical deinking.

Chapter 3 focuses on the thermal conversion of deinking sludge and its kinetics. This work is further divided into two parts. Two separate deinking sludge namely deinking sludge (A) and deinking sludge (B) were used as raw materials for section one and section two respectively. First part studies the effect of different heating rates on the pyrolysis and combustion of deinking sludge (A). In this section four heating rates namely 10, 20, 30 and 40 °C/min were applied under nitrogen and air atmospheres. Second part studies the thermal processing of deinking sludge (B), coal (C), rice husk (RH) and their blends under nitrogen and air atmosphere. In this section, 10 °C/min heating rate was applied throughout the experiment. It

was found that blending of deinking sludge with coal improves the ignition characteristics and shows higher reactivity compared to only coal. Hence, utilization of deinking sludge with coal can improve performance of the pyrolysis and combustion processes of coal. In addition, it was found that combustion improved the degradation process of deinking sludge, coal and rice husk. Blending of deinking sludge up to 20 wt% with coal displays almost similar combustion profile as that of coal. Thus deinking sludge can be used with coal in the existing combustion system. Moreover, it was observed that the deinking sludge required higher burnout temperature as compared to rice husk. The reactivity decreased with increment in amount of deinking sludge in the blend with rice husk. It was found that the rice husk replacement by deinking sludge up to 20 wt% showed almost similar pyrolysis profile as that of rice husk. The results obtained in such experiments may be used for effective design of thermal co-processing systems.

Chapter 4 investigates the utilization of deinking sludge in fired clay bricks. Initially the characterization of raw materials namely clay and deinking sludge was carried out using characterization techniques like XRF, XRD, TGA and SEM. Then different mixing proportions were prepared with deinking sludge with clay and fired at three different temperatures namely 900 °C, 950 °C and 1000 °C. Different properties of fired clay bricks were obtained using various codal standards for all temperatures. From the investigation, it was observed that the 15% deinking sludge addition in fired clay brick is optimum. Moreover, it is observed that the firing temperature of 950 °C is optimum. The values of compressive strength and water absorption were found too well under the limits mentioned in the standard IS 1077:1992. This lies under the class 10 that is suitable for brick masonry work. Also, it was noted that the thermal conductivity decreased with increase in the amount of deinking sludge addition. Reduction in thermal conductivity is suitable for energy saving purposes. Hence, deinking sludge can be effectively used in fired clay bricks, which can not only save energy but can also address the problem of disposal of deinking sludge.

LIST OF PUBLICATIONS

PUBLICATIONS

- Kulkarni, S., Chauhan, N., Kumar, V., and Bansal, M. C. (2012). Characterization of Deinking Sludge from Combined Deinking Technology. *IPPTA Journal*, *24* (3), 81-86.

- Bansal, M. C., Kumar, V., and Kulkarni, S. (2011). Combined Deinking Technology to Improve the Quality of Recycled Paper. *IPPTA Journal*, *23*(3), 145-148.

INTERNATIONAL CONFERENCES

- Kumar, V., Kulkarni, S., Singh, S. K., and Bansal, M. C. (2015). Reuse of Deinking Sludge from Recycled Paper Industry in Light Fired Clay Bricks. *15 AIChE Annual Meeting*, Salt Palace Convention Center, Salt Lake City, UT, USA, November 8-13, 2015 (Accepted for Oral Presentation).

- Kumar, V., Soni, Y., Kulkarni, S., Sharma, P., and Singh, S. K. (2015). Lime Sludge: An Emerging Alternate Construction Building Material for the Partial Replacement of Fine Aggregate. *15 AIChE Annual Meeting,* Salt Palace Convention Center, Salt Lake City, UT, USA, November 8-13, 2015 (Accepted for Oral Presentation).

- Kulkarni, S., Kumar, V., and Bansal, M. C. (2014). Pyrolysis Kinetics of Deinking Sludge. *14 AIChE Annual Meeting,* Marriott Marquis Atlanta, Atlanta, GA, USA, November 16-21, 2014 (Oral Presentation).

- Kulkarni, S., Kumar V., Singh, S. K., and Bansal, M. C. (2014). Experimental Investigations on Brick Specimens made from Deinking Sludge. *14 AIChE Anuual Meeting,* Marriott Marquis Atlanta, Atlanta, GA, USA, November 16-21, 2014 (Oral Presentation).

ACKNOWLEDGEMENTS

"Gurur Brahma, Gurur Vishnu, Gurur Devo Maheshvarah,
Gurur Sakshaat Param Brhama, Tasmai Shree Gurave Namaha"

Truly saying it is our teacher who guides us on the path of life and makes our valuable life meaningful. They not only mould us into a better person but also inculcate in us the capability to face the obstacles. I feel blessed to have great teachers and I am indebted to them. I am also thankful to almighty God who blessed me and saved me from all odds.

This research work would not have completed without the direction and efforts of some people. I am grateful to Dr. Vivek Kumar, Associate Professor, Department of Paper Technology, IIT Roorkee for his support and supervision during my research work. I am very grateful to him for conducting long discussions on the topic that benefitted me a lot for interpreting the obtained results and landing on a solid conclusion. His immense knowledge of the subject and constructive criticisms made my work technically sound. He helped me a lot in arranging all sorts of facilities for conducting my research work.

I place on record my sincere thanks to Dr. M.C. Bansal, Professor (Retd.), Department of Paper Technology, IIT Roorkee for giving me technical advice on my work. The help and support he extended to me was incredible. I am highly indebted to him for guiding me throughout my research work. His profound knowledge and vast experience of the subject helped me to accomplish the task easily.

It's been a great journey in the IIT and I feel fortunate that two great people Dr. M. C. Bansal and Dr. Vivek Kumar were an inseparable part of it.

I am thankful to Er. S. K. Singh, Principle Scientist, Structural Engg. Group & Associate Professor, Academy of Scientific & Innovative Research, CSIR-Central Building Research Institute, Roorkee, for guiding me on a quantum of my work. I am indebted to him for permitting me to work in his renowned institute and carry out experiments. His innovative ideas and practical approach to the problem inspired me a lot. I appreciate him for long scientific discussions. His experience, knowledge about the field and positive criticisms made my work valuable and channelled my research work towards a fruitful end.

I place on record my deepest gratitude to Dr. Thallada Bhaskar, Senior Scientist & Head, Biomass Thermocatalytic Processes Area (TPA), Bio-fuels Divison (BFD), CSIR - Indian Institute of Petroleum, Dehradun, for guiding me on a piece of my work.

I extend my sincere and cordial gratitude to Dr. Y. S. Negi (Professor In-charge), Dr. Satish Kumar (DRC Chairman), Dr. S. P. Singh, Dr. A. K. Ray, Dr. Dharm Dutt, Dr. Milli Pant

and all faculty members of DPT who guided me during my doctoral programme. I also place on record the support given by Dr. Ravi Kumar, Professor, Department of Mechanical and Industrial Engineering, IIT Roorkee for providing lab facilities.

The assistance given by various scientists and technical staff of CSIR-Central Building Research Institute, Roorkee is also deeply appreciated. In particular, I would like to thank Dr. Sukhdeo R. Karade, Principal Scientist and Co-ordinator (AcSIR**)** and Dr. L. P. Singh**,** Sr. Scientist, Environmental Science & Technology division for advising me and availing me required support. I would also like to thank Mr. Bhupal Singh, Sr. Technical Officer, SE division for helping me to carry out my experiments. I am also grateful to Ms. Usha Purohit and Ms. Geetika Mishra, Reserach Scholars as well as Mr. Sandeep and Mr. Amit, Project Fellows for assisting me in my research as well as availing me a friendly working environment. I would also appreciate Mr. Khalil Ahmed, Mr. Satya Pal and Mr. Arvind Kumar for assisting me during experiments.

It was a pleasant experience to work with seniors and colleagues (Prabhat, Amrish, Gaurav, Archana, Anushree, Laxmi, Amit, Asit) and all research scholars of DPT. I am also thankful to Ritesh and Jitendra for their help and support. I would also take this opportunity to thank Mr. Ratinesh Sinha, Mr. Anurag, Mr. Rakesh and all staff members of DPT for assisting me during my research work.

I also place on record my thanks to my institute IIT Roorkee for providing me all types of facilities for the completion of my doctoral programme. The quantum of my life that I spend in IIT will be cherished in my heart like sweet nostalgia. The financial assistance provided by MHRD is also acknowledged.

My special thanks to Mrs. Chitra Rekha Bansal (wife of Dr. M. C. Bansal) and Mrs. Shikha Agrawal (wife of Dr. Vivek Kumar) for caring and encouraging me through thick and thin.

I would like to extend my deepest gratitude to my parents Er. D. H. Kulkarni and Mrs. Sunanda Kulkarni for their love and blessings. I do not know how to thank my husband Er Archit for his invaluable affection and support. Without his sacrificial support and patience, completing my Ph.D would have been impossible. Last but not the least I would also like to extend my gratitude to my sister Mrs. Shweta Purkar and brother Swatantra for boosting my morale.

(**Shilpa Kulkarni**)

LIST OF CONTENTS

LIST OF FIGURES

LIST OF TABLES

ABBREVIATIONS

ASTM	American Society for Testing and Materials
BIS	Bureau of Indian Standards
CAGR	Compounded Annual Growth Rate
CER	Catalogue of European Residues
Cy	Pulp consistency
C	Coal
DF	Deinkability factor
DTG	Differential thermogravimetry
DTPA	Diethylene triamine pentaacetic acid
DS	Deinking sludge
IS	Indian standard
o.d.	Ovendried
RH	Rice husk
SD	Standard Deviation
SEM	Scanning electron microscope
TAPPI	Technical Association of the Pulp and Paper Industry
TG	Thermogravimetry
TGA	Thermogravimetric analysis
US	Ultrasound
UV	Ultraviolet
XRD	X-ray diffraction

CHAPTER 1
INTRODUCTION

1.1. Introduction

The journey of Indian paper industry got started centuries ago and is still going on and today about 715 pulp and paper mills have been setup with about 12.75 million tons capacity (Indian Paper Industry 2015, Pathak 2014). With increase in consumption, the production is increased. In 2010-2011, the production reached up to 10.11 million tons whereas the consumption reached up to 11.5 million tons (Paper: Report 2011).

According to a report by working group for 12th five-year plan of India, the consumption in India is expected to increase up to 43.9 million tons by 2026-2027. However, the production of paper is expected to increase only up to 39.7 million tons in 2026-27 as shown in Figure-1.1. This certainly points to the possible shortage of paper in coming years (Paper: Report 2011).

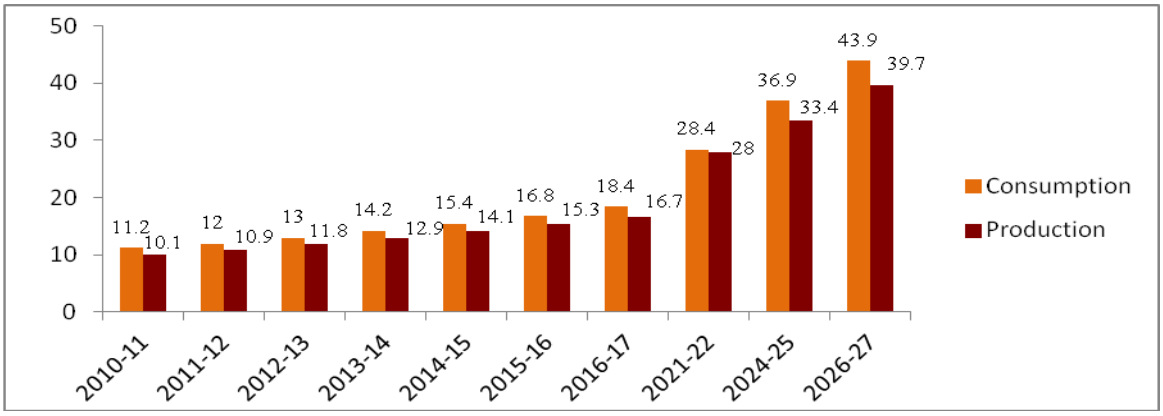

Figure-1.1 Projected Consumption and Production of Paper in India (Adapted from Paper: Report 2011)

According to another source, the CAGR (Compounded Annual Growth Rate) of paper production was 8.4% against CAGR of paper consumption of 9% in 2012-2013 (Indian paper industry at a glance 2014). The paper industry is one of the most important sectors in India such that it is presently growing at a CAGR of 9.6% for 2012-2017 with an annual turnover of Rs. 50,000 crores along with the contribution of Rs. 4500 crores to the national exchequer. In addition, this sector provides employment to about 2.0 million people directly or indirectly (Indian paper industry at a glance 2015, Indian Paper Industry 2015). Furthermore, the rising literacy rate and low per capita consumption of this country presents many opportunities for

further growth of this sector. Statistics shows that the per capita consumption of paper in India is about 5.4 kg/capita against the 38 kg/capita consumption of Asia and 52 kg/capita consumption of the world (Market facts 2014).

In spite of ample growth opportunities, most of the paper industries lack state-of –the-art technologies and therefore only about 5% mills are producing close to 60% of total production (Market facts 2014). Therefore, the technology and processes used in the mill needs to be enhanced. Many researchers have worked in this field (Chinnaraj et al. 2011, Rao and Kumar 1985, Subramanian et al. 2007, Subramanian et al. 2008). Moreover, the deforestation is increasing exponentially. Strict legislations along with the pressure from NGO's to conserve forests are becoming obstacles for the availability of raw material to paper industries. Today the daunting issue is the shortage of virgin fibres that will grow further in years to come (Dixit et al. 2010, Sankaralingam et al. 2013). Hence, the recycling of fibres needs to be increased in order to compensate the shortage of paper. Recycling is the process of converting wastepaper into paper products ready to use. Recycling of wastepaper will ultimately save the forests and fulfil the demand of paper. Moreover recycling facilitates to use resource out of thrash i.e. wastepaper. Hence recycling is suitable both economically and environmentally.

For recycling deinking is an important process. Deinking is such a process in which ink, fillers, stickies and other contaminants are separated from the printed wastepaper. This is achieved by formation of fibrous suspension using chemical, thermal and mechanical energy. It is a two-step process in which the ink particles are detached from fibres because of the action of mainly chemicals and then they are separated from the pulp suspension by froth flotation process (Agnihotri 2007).

With many merits of recycling, there are some demerits too (Agnihotri 2007)

- Deinking of papers specially printing and writing grades require complex system
- The quality of recycled paper doesn't reach up to the paper made by using virgin fibre
- There is shortage of even wastepaper for recycling because majority of wastepaper collection is in the hands of rag pickers and scrap dealers that is severely unorganised in India.

There are two types of printing process. One is impact printing and other is non-impact printing process. Impact printing is used in printing of newspaper and non-impact printing is used in laser printing, photocopying etc. However, in the present scenario the trend of using non-

impact printing processes is increasing day by day. Among various non-impact printing processes, photocopying is also used widely. Toner particles in non-impact printing get fused with the fibre and hence are difficult to remove whereas toner particles in case of impact printing doesn't get fused with fibre surfaces and hence are easy to remove. The toners of photocopier machine have different chemical composition than conventional ink. The conventional ink contains oil or water based carrier whereas toners used for photocopying usually consists of thermoplastic resins composed of a styrene-acrylate copolymer binder (85% to 90%) along with dispersed carbon black (10% to 15%), iron oxide for imparting magnetic characteristics and dry lubricants as well as some charge carriers. The toner of photocopier is transferred electro-statistically, fused because of high temperature as well as pressure and attaches to the fibre surfaces in a large, rigid flat shaped particle (Bhardwaj et al. 1997, Jeffries et al. 1994, Lee et al. 2013, Lee et al. 2011, Pala et al. 2004, Pala et al. 2006, Pathak et al. 2010). Therefore, it is difficult to detach these ink particles from the fibre surface using conventional deinking (Pathak 2014). Thus, chemical deinking needs further improvement or some new approach for the removal of ink particles (Kulkarni et al. 2012, Mathur et al. 2005, Jeffries et al. 1995). Hence, in this study, combined deinking technology i.e. chemical combined with UV irradiation treatment or ultrasound treatment is presented to further enhance the detachment of ink particles from fibre in case of non-impact printed-paper.

1.2. Thermal conversion of deinking sludge and its kinetics

Fossils are non-renewable sources of energy and therefore they are depleting. Moreover, energy and power demands are increasing because of growing population and industrialization. Hence there is a need to find out an effective, eco-friendly and economical power and heat generation system using alternative fuels (Singh and Shadangi 2011, Subramanian et al. 2012, Subramanian and Paulapuro 2006,). On the other hand, because of heavy industrialization, the quantity of solid waste is increasing exponentially (Pradhan and Singh 2012, Yu et al. 2002). It needs a proper waste management system (Dixit et al. 2012). Like several kinds of wastes, deinking sludge is also increasing day-by-day (Yanfen and Xiaoqian 2010). One ton of paper manufacturing produces about 160-500 kg wet deinking sludge (Lou et al. 2012). Deinking sludge contains short and degraded fibres along with fines, coatings, fillers, toner particles, additives etc (Mendez et al. 2009). The handling and disposal of the exponentially expanding amounts of these wastes is becoming a great concern (Vamvuka et al. 2009). Disposal of deinking sludge through landfilling is no longer a sustainable option because of decreasing landfilling sites, expensive disposal, environmental laws and regulations as well as adverse

effect on health (Vamvuka et al. 2009, Yu et al. 2002). Additionally, the application of deinking sludge in agriculture makes the crops nitrogen-deficient (Battaglia et al. 2003). However, biomass is regarded as the 3rd largest primary energy resource in the world (Vamvuka et al. 2003, Wang et al. 2011,). Biomass is becoming popular alternative source of energy because of carbon neutrality along with low sulphur content (Jain et al. 2011, Lee and Jeffries 2011, Park et al. 2010). Moreover, deinking sludge is clean and cheap source of energy. In addition, according to Catalogue of European Residues (CER) all wastes generated from cellulose and paper manufacturing are not dangerous (Garcia et al. 2008). Nevertheless, cellulosic wastes are easily available and that too at low cost (Lee et al. 2011, Singh et al. 2013). Combustion and pyrolysis of deinking sludge can minimize its quantity. Pyrolysis transforms waste of lower energy density to higher energy density (Bhuiyan et al. 2008). The co-processing of waste material with fuel like coal can be an interesting option as it allows the use of already existing infrastructures there by reducing the fossil fuel emission and consumption. Some changes in the systems may be required because of the differences in the characteristics of the fuels (Vamvuka and Kakaras 2011). Hence, the prior knowledge of the thermal behaviour of waste material (deinking sludge), fuel as well as their blends is very necessary for the effective operation of the unit (Vamvuka et al. 2009). Moreover, the investigation of chemical composition of the fuels must also be carried out as it affects the operation of the co-processing systems (Vamvuka and Kakaras 2011, Vamvuka et al. 2003, Vamvuka 1998, Vamvuka and Woodburn 1995). In country like India where the major source of livelihood is agriculture, the prospect of converting widely available huge quantity of agricultural residues like rice husk into fuel for energy recovery is very attractive (Vamvuka et al. 2003). The compatibility of deinking sludge with coal or rice husk should be properly monitored for the effective design and operation of thermo-chemical conversion systems. Moreover, the knowledge obtained from these experiments about the behaviour of fuels and their blends will help to solve the practical problems of co-processing like handling as well as feeding of biomass separately from other fuel and will be helpful in avoiding any catastrophic events (Vamvuka et al. 2003).

The thermochemical processes like pyrolysis and combustion of deinking sludge is accompanied by complex reactions (Yu et al. 2002). Therefore, studies related to the pyrolysis and combustion of deinking sludge and its blends with other fuels are rare. However, obtained data from thermal analysis techniques can be used for design and operation of co-firing units. In addition, it can provide valuable information for the promotion of biomass to be used as co-

fuels for energy generation (Vamvuka and Sfakiotakis 2011). The aim of the present research work is to study the thermal degradation behaviour of deinking sludge, coal, rice husk and the blends of coal with deinking sludge as well as rice husk with deinking sludge as well as its kinetics.

1.3. Utilization of deinking sludge in fired clay bricks

Bricks have been a prominent building material since the early stages of civilization. They became an indispensable part of development because of their interesting properties, low cost and abundant raw material (clay) used to manufacture them (Bories et al. 2014).Their use can be traced back to even pre-historic times. Investigators reveal that dried clay bricks were used for the first time in 8000 BC and fired clay bricks were invented around 4500 BC (Arshad and Pawade 2014, Zhang 2013). Moreover, these were produced at an industrial scale after the invention of brick press by Auguste Virebent in 1830 (Bories et al. 2014).

The demand for building materials like bricks is increasing. Today the production of bricks have reached up to 1391 billion units around the world (Arshad and Pawade 2014, Zhang 2013). Hence, there is a mismatch between the demand and supply of bricks (Rajput et al. 2012). Also because of heavy industrialization, problem of solid wastes is increasing. On the other hand, the world is facing energy crisis at present that is likely to grow more in the future. Hence, there is a need to conserve energy and build sustainably (Yazdi et al. 2014). Therefore, demand of high insulating bricks is increasing (Demir et al. 2005).

Building sector consumes significant amount of energy due to largest end users of energy as well as improving quality of lifestyle. This sector consumes energy mainly for heating and cooling purposes (Sutcu et al. 2014). It has been found that about half of the total energy consumed by buildings gets lost. This energy loss can be reduced by lowering the thermal conductivity of the brick (Sutcu and Akkurt 2009). Moreover, because of clay as a raw material in the fired clay brick, brick acquires heterogeneous nature and thus it can accommodate different waste materials (Dondi et al. 1997*)*. High insulation capacity in the brick can be imparted with the help of addition of pore forming agents into the brick (Demir et al. 2005). Pore forming agent burns off during firing stage and leave the voids or pores behind them (Phonphuak 2013). Moreover, porosity hinders the heat transfer. Thus thermal conductivity decreases. Decrease in the thermal conductivity ultimately decreases the heat loss through the walls (Sutcu and Akkurt 2009). Pore forming agents are mainly of two types – organic and inorganic. Organic pore formers are cheaper and contribute in firing the furnace. Inorganic pore

formers are costlier and increase the demand for water in order to maintain the plasticity. Organic pore formers are more popular than inorganic ones. Organic pore formers include waste from paper industry and recycle paper industry, sewage sludge, sawdust, coal etc. (Demir et al. 2005).

Of total recycle paper mills operating in India, 30% of them are engaged in recycling producing about 15% waste annually. This waste is called deinking sludge and is generally land filled (Rajput et al. 2012). Nevertheless, because of decreasing land filling sites this option is becoming expensive day by day. Moreover, this waste can be utilized instead of just dumping. Utilizing this waste will reduce the amount of non-renewable naturally occurring material (clay) used in bricks (Arshad and Pawade 2014, Sutcu and Akkurt 2009). In addition, since it is porous and fibrous in nature, so it will impart lightweight character in the brick that will also reduce the transportation cost (Raut et al. 2012). Moreover, the force of earthquake is proportional to the mass of the building. Hence, reduction in the weight of the materials used in the building will reduce the damage caused by the earthquakes (Mehmannavaz et al. 2014). This deinking sludge contains mainly cellulose fibres and some inorganic contents. Moreover, it is a waste so it will reduce the overall cost of manufacturing or producing the bricks. Also with the addition of sludge content, the physical and mechanical properties of brick can be controlled. By increasing the deinking sludge (recycle paper mill sludge), the porosity can be increased. Porosity also depends on the type of clay used in manufacturing and the temperature of firing (Johari et al. 2010). By increasing the porosity, water absorption capacity of the brick can be increased. With increase in the water absorption capacity, the shock absorption capacity as well as the insulation will be increased (Phonphuak 2013, Raut et al. 2012). Hence by using the deinking sludge along with the clay for making the fired clay bricks will not only conserve the natural resource (clay) and compensate the shortage of bricks but will also address the problem of solid waste (deinking sludge). Moreover, utilization of deinking sludge in fired burnt clay bricks will save the energy.

1.4. Problem statement

The demand for paper is increasing and the production is unable to fulfil it. In addition deforestation and strict legislations possess problem for the availability of raw material to the paper industry. Therefore recycling of fibres is required to address this problem. Moreover the quality of paper after recycling by conventional method doesn’t match to the paper made using virgin fibres. Hence, there is a need to improve the method of conventional recycling.

Application of Ultraviolet (UV) irradiation and Ultrasound treatment on chemical deinking can be a potential solution to the above problem.

Moreover the solid wastes like deinking sludge are increasing due to industrial activities. They possess disposal problems because of decreasing land filing sites, strict environmental laws and expensive disposal. These wastes require proper management system.

There is a need to find out an alternative way for fulfilling the increasing energy demands because of depletion of conventional fuels. There is also a need for reducing fossil fuel emission and consumption. Moreover rice husk which is a useless waste from rice mills needs proper disposal option through proper usage. Hence utilizing deinking sludge in energy recovery options can address its disposal problem. Furthermore, co-processing of deinking sludge with coal or rice husk can reduce the consumption of former and can address the disposal problem of later.

On the other hand demand of building materials like brick is increasing. Whereas the clay used to manufacture fired clay brick is decreasing. However, buildings consume a lot of energy due to large end users because of improved quality in life. It has been found that about half of the energy used by building gets wasted. This energy loss can be reduced by increasing thermal insulation of the bricks by adding pore formers like deinking sludge. Hence, utilizing deinking sludge in fired burnt clay bricks can be a potential option for waste utilization and energy conservation.

1.5. Summary of research gap

1. This work will investigate the application of Ultraviolet irradiation and Ultrasound treatment to improve the performance/ efficiency of chemical deinking.

2. It will investigate the thermal degradation behaviour of deinking sludge in different atmosphere at various heating rates and its co-processing with coal and rice husk.

3. It will also calculate kinetic parameters obtained from the various models.

4. It will study the incorporation of deinking sludge in fired clay burnt clay bricks to make them more energy efficient.

1.6. Scope of work

The scope of the work highlights the application of Ultraviolet (UV) and Ultrasound (US) treatment on chemically deinked pulp of copier paper. A commercial grade copier paper provided by an Indian paper mill will be printed by a photocopier machine. The chemicals and UV tubes will be procured from Indian suppliers. Then chemical deinking, chemical deinking followed by UV-irradiation and chemical deinking followed by Ultrasound treatment will be performed separately. Both US and UV treatments will be applied for different durations. All these processes will be followed by flotation. Then hand sheets will be prepared and properties like brightness, opacity, ink elimination, dirt count, deinkability factor, tensile index, tear index and burst index will be tested. Finally the results will be compared and best method with optimum duration will be selected.

The work will also be focussed on the potential of thermal conversion of deinking sludge and its kinetics for energy recovery purpose. Two deinking sludges (A) and (B) will be procured from a recycle paper industry in Punjab (India). Coal and Rice husk will be collected from local area of Saharanpur (India). Characterization of all the raw materials will be performed initially. The characterization will include proximate and ultimate analysis. Then the thermogravemetric analysis of deinking sludge (A) will be performed under four heating rates and two different atmospheres upto 900 °C. After that regression coefficient will be calculated using four different models proposed by previous researchers. The kinetic parameters will be calculated using the model that will give best fit of the data. Finally the results will be interpreted. In section B, thermogravemetric analysis will be carried out using three raw materials namely coal, deinking sludge (B) and rice husk under nitrogen atmosphere at 10 °C/min heating rate. Co-pyrolysis of coal sample and deinking sludge (B) will be performed under nitrogen atmosphere with same heating rate. Co-pyrolysis of rice husk sample and deinking sludge (B) will also be performed under same atmosphere and at same heating rate. The same procedure mentioned above for deinking sludge (B) will be performed under oxygen to study the combustion procedure. Regression coefficient will be calculated using four different models of different previous researchers. The model that will present best fit of data will be used for determining kinetics parameters in both Pyrolysis and combustion process.

The potential of using deinking sludge in fired burnt clay brick specimens will be investigated. The deinking sludge will be procured from one of the recycle paper industry in Punjab and clay will be obtained from local area in Roorkee, Uttrakhand, India. Initial characterization of raw

materials will be done. This will include particle size analysis, XRF, XRD, SEM and TGA. After this brick specimens having different proportions of deinking sludge will be prepared and will be fired in a laboratory type electrical furnace at different temperatures. Then various test methods will be performed to evaluate different properties of fired burnt clay brick specimens. The properties such as compressive strength, water absorption, mass loss, shrinkage, density, apparent porosity and thermal conductivity of brick specimens will be tested. Then SEM and XRD of the fired burnt clay brick specimens will be performed. Then results will be interpreted and data of different compositions will be compared on the basis of IS standards and optimum firing temperature and deinking sludge addition will be chosen.

1.7. Contribution of work

This work will improve the conventional method of chemical deinking by the application of UV and US treatments. It will also present the possibility of using the deinking sludge in energy recovery options through Pyrolysis and combustion. In addition, this work will also highlight the usage of deinking sludge incorporation in fired burnt clay bricks to make the buildings more energy saving.

1.8. Objectives

Hence the objectives of this study are:

1. To present a evolutionary field of combined deinking technology
2. To examine the thermal behaviour of deinking sludge
3. To examine the thermal behaviour of deinking sludge in combination with other fuels.
4. To evaluate the thermal behaviour and kinetics of deinking sludge and its blends with other fuels namely coal and rice husk.
5. To determine the usability of deinking sludge in the building product (fired burnt clay brick), which should be sustainable and energy efficient.

To cover the above objectives

Chapter 2 covers combined deinking technology applied on copier waste paper

Chapter 3 covers thermal conversion of deinking sludge and its kinetics and

Chapter 4 covers utilization of deinking sludge in fired clay bricks

Hence an effort has been made to cover all the objectives in the above three chapters. Suitable experiments have been planned, data has been generated, analyzed and results have been discussed with possible reasons.

CHAPTER 2

COMBINED DEINKING TECHNOLOGY APPLIED ON COPIER WASTE PAPER

2.1. Introduction

Chemical deinking is the removal of ink from the fibres using chemicals. But the quality of this process needs to be improved further to reach upto the virgin fibres. Hence, combined deinking technology is used to further enhance the efficiency of chemical deinking process in removal of ink. Combined deinking technology refers to the applications of UV-irridations and Ultrasound treatment on chemical deinking separately. The combined deinking technology has been applied presently on 75 gsm office copier waste paper generated in our own photocopier section. The combined deinking technologies cover pulping (deinking) of the waste paper followed by flotation operation. Suitable chemicals have been added and pulping has been carried out at optimum operating conditions. Then Ultraviolet irradiation (UV- irradiation) and Ultrasonic vibration (US treatment) have been applied separately with chemical deinking process. The results indicate improvement in properties under optimum operating conditions.

2.2. Literature review

This section presents an account of various works carried out on different topics related to this research.

2.2.1. Pulping

Pulping is known as the first stage of deinking. In this stage, de-fibering of wastepaper is carried out. The attached ink is detached and dispersed. This operation is carried out in alkaline environment (pH 9-11) and the temperature is usually kept from 45 °C to 75 °C (Agnihotri 2007). This operation can be carried out in batch or continuous mode. In this operation, mainly chemical and mechanical actions are utilized to detach the ink particles from the fibre surfaces. Chemicals are added to break the fibre-ink bond and disperse the ink particles as well as to prevent them to redeposit on the fibre surfaces. Mechanical action of rotor moves the pulp suspension and provides hydrodynamic force to facilitate friction between fibres for the removal of ink attached to the fibre surfaces (Agnihotri 2007). Effective pulping operation facilitates effective ink removal and ultimately effective deinking. The effectiveness of any deinking technique depends on how well it detaches the ink particles from fibres and removes them from pulp suspension thereby imparting sufficient optical, physical and mechanical

properties to the recycled stock. However, the effectiveness highly depends on the kind of ink required to be removed, kind of printing technique used, pulp composition, operating conditions and much more (Lee et al. 2013).

2.2.2. Flotation operation

The process of bringing dispersed and detached ink particles from pulp suspension to the surface with the help of rising air bubbles and skimming off the black froth formed at the surface of cell is called flotation deinking. It is a selective complex separation process of fibres and ink particles along with other contaminants. It is generally used for 10-150 µm sized particles (Pala et al. 2004). According to Zhao et al. (2004), a flotation process can be called successful if it fulfils three objectives: the separation of toner particles from fibres, the effective sticking of detached and dispersed toner particles to the air bubble and the removal of froth containing toner particles from the flotation cell. According to Jiang and Ma (2000), the effectiveness of flotation deinking depends on flotation consistency, ink/fibre particle size, pH, chemicals used and temperature. Moreover, Jiang and Ma (2000) have reported that the optimal range of consistency is usually 0.7-1.2 %. In flotation stage the flotation chemicals makes the dispersed ink particles into hydrophobic in nature and thus enhance their floatability. Because of the hydrophobicity these ink particles get attached to the rising air bubbles and are brought up to the upper surface containing froth (Varshney et al. 2007). Finally, the froth containing the ink particles is skimmed off. However, the hydrophilic fibres remain in the suspension (Jiang and Ma 2000).

2.2.3. Deinking chemicals

In the chemical deinking technology, different chemicals are used for carrying out different functions in deinking. The chemicals along with their functions are as follows:

2.2.3.1. Sodium hydroxide

Sodium hydroxide is used to adjust the pH for ink detachment. It makes the pH to the alkaline level that makes fibres to swell. Swelling in the fibres makes them more flexible and soft. Softness in the fibres facilitates breaking of inter fibre bonds and removal of toner ink (Lehmann et al. 1990). It is used to saponificate and/or hydrolyze the resin of the toner. The alkalinity must be sufficiently high to have flexible fibres and better saponification of resins.

However, the addition of NaOH increases yellowness and makes them dark. High alkali content gives rise to the chromophore groups. These chromophore groups are responsible for making the pulp yellow and making them dark. However, it can be prevented by hydrogen peroxide (Wallberg et al. 1998). Jiang and Ma (2000) have mentioned 0-5% sodium hydroxide dosing for all grades of paper. However, researchers (Imamoglu 2006, Pathak et al. 2011 and Tatsumi et al. 2000) have optimized the dose of NaOH and found 2% as optimum.

2.2.3.2. Sodium silicate

Sodium silicate prevents the decomposition of hydrogen peroxide and acts as a stabilizer. This is achieved by forming the colloids with heavy metal ions. Sodium silicate also prevents the detached ink particles to be re-deposited on the fibre surfaces. Moreover, it is also known for its buffering effect on pH and acts as a source of alkalinity. However, excessive amount of sodium silicate can cause alkali darkening which causes yellowness (Wallberg et al. 1998, Agnihotri 2007). Hence, researchers (Agnihotri 2007, Pathak 2014) have optimized the dosing of sodium silicate and they used 2-3% Na_2SiO_3.

2.2.3.3. Hydrogenperoxide

The main role of H_2O_2 is to prevent the yellowness caused by NaOH. This is achieved by discolouring the chromophore groups originated by the alkalinity of the pulp. It also reduces the darkening caused by sodium hydroxide. The prehydroxyl anion HOO- is responsible for bleaching. Its concentration is influenced by pH, temperature, H_2O_2 dosing and metal ions like Fe, Mn and Cu. In presence of heavy metal ions, H_2O_2 gets decomposed. However, the decomposition can be prevented by the use of stabilizers like DTPA, EDTA or Na_2SiO_3 (Wallberg et al. 1998, Agnihotri 2007). Pathak (2014) has used photocopier paper as raw material, Tatsumi et al. (2000) used laser printed office paper and Imamoglu (2006) has used waste office paper (printed using duplicating machine) as raw material. They have optimized the dosing of H_2O_2 and found 1% H_2O_2 as optimum dose in chemical deinking.

2.2.3.4. Chelating agents

The function of chelating agent is metal ion chelation. It forms complexes with heavy metals that are solvable in nature. It also stabilizes hydrogen peroxide. Commonly used chelating agents are DTPA (diethylenetriaminepentaacetic acid) and EDTA (ethylenediaminetetraacetic acid) among whom DTPA produces better results because of its five-legged structure against

the four-legged structure of EDTA. Hence, DTPA is mostly used (Wallberg et al. 1998). Jiang and Ma (2000) have recommended to use 0-0.5% DTPA or EDTA for all grades of paper.

2.2.3.5. Surfactants

A chemical that contains both hydrophilic and hydrophobic ends having surface activity is called surfactant. Hence according to this definition foaming agents, de-foamers, collectors and dispersants can be called surfactants. However, most of the surfactants play multiple roles. Surfactants are of various types-cationic, anionic, non-ionic or amphoteric. Non-ionic and anionic surfactants are more popular. The structure of the surfactants can be straight chain, double or simple bindings, branched chain, long or short chain and many more (Wallberg et al. 1998). Surfactants perform three roles generally during the deinking process. It generates froth at the top of pulp suspension in the flotation cell to remove the detached ink particles. It acts as dispersant to separate the ink particles from the fibre surface and ensure that the detached ink particles must not redeposit on the fibre surfaces. Surfactant also facilitates the swelling of fibre surface and thus releases the ink particle. It is believed that surfactant reduces the surface tension of water and thus penetrates between the ink and fibre surface. With the help of mechanical forces, this action isolates the ink particle into the water medium (Agnihotri 2007). Moreover, it acts as a collector to collect the small, dispersed ink particles and form their agglomerates (Kanhekar et al. 2005). In addition, it changes the hydrophilic nature of ink particles to hydrophobic one. As mentioned earlier it has two components- a hydrophilic and a hydrophobic. The hydrophilic or water loving part remains suspended into water medium whereas the hydrophobic part attaches with the ink particle. Thus, surfactant action forms micelles. Though the surfactants play a significant role in the removal of ink, they might get adsorbed on the fibre surfaces and may reduce the fibre bonding as well as cause the foaming problems in paper machines. However, surfactants should be used appropriately because not all types of surfactants are required for deinking of all types of inks. Like use of collector is not necessary while deinking the hydrophobic ink such as toners used in photocopy machines. Likewise, a separate dispersant may be unnecessary if the ink can be detached by chemicals like sodium hydroxide, sodium silicate or by mechanical action. Moreover, conditions used for deinking the ink particles like water hardness; pH, temperature etc. differ from mill to mill. Hence, the surfactant that works well for a raw material of one mill might not work with that effectiveness for raw material of another recycle paper mill (Zhao et al. 2004).

2.2.4. Ultrasound deinking

Ultrasound deinking is a new technology in the field of deinking. Although ultrasound treatment is in its evolutionary stage but it offers many advantages over conventional deinking. Ultrasound treatment is carried out at 20 kHz and above frequency. In this method, the device produces periodic compression and expansion waves. These waves generate friction and vibration that separates the ink particles from the fibre surface. However, detached ink particles may redeposit on the fibre surface because of excessive treatment (Tatsumi et al. 2000 and Zhenying et al. 2009).

Ultrasound is a sound having frequency higher than what a human can hear. A human ear can hear from 20 Hz to 20 kHz. Therefore, the ultrasound frequency starts from 20 kHz. Its upper limit is not sharply defined (Josefsson 2010). However, ultrasound can be divided into three categories based on frequency- power ultrasound, high frequency ultrasound and diagnostic ultrasound. Diagnostic ultrasound is characterized by low power and high frequency ranging from 1 MHz to 500 MHz. High frequency ultrasound posses frequency from 100 kHz to 1 MHz. Power ultrasound is sound of high energy and low frequency ranging from 20kHz to 100 kHz (Wu et al. 2013). Power ultrasound is used in this study. It imparts chemical as well as physical changes in the pulp suspension by subsequent generation and destruction of bubble cavities in the medium. It is a mechanical wave that propagates through a material medium setting the molecules in vibratory motion around their mean position. The vibratory motion is transferred from a molecule to its adjacent molecule. A molecule comes back to its original position after transferring its kinetic energy to its adjacent molecule. When there is a succession of waves then oscillation occur which give rise to compression and rarefaction alternatively. Due to these phenomenons, alternate occurrences of pressure variation occur in the area where the compression and rarefaction takes place. Higher pressure occurs in the compression areas in which liquid molecules are pushed towards each other whereas low pressure occurs in expansion (rarefaction) areas where the liquid molecules are pulled apart. These alternating pressures give rise to the phenomenon called cavitation. This phenomenon can be used judiciously in many industrial applications (Josefsson 2010).

The phenomenon of cavitation occurs at the low pressure regions. The generated cavitation serves as the region of concentration of sound energy. When the powers of rarefaction cycles become sufficiently higher, then it overcomes the attractive forces of liquid molecules and gives birth to cavitation bubbles (Mason and Cordemans 1996). Nevertheless, magnitude of the

low pressure needed to overcome the attractive forces of the liquid, depends on its purity. It is said that it is not possible to generate cavities in a pure liquid with the ultrasound systems available today. Moreover, real liquids are not very pure and hence the creation of cavities in them is relatively easy (Josefsson 2010). The impurities in the liquid act as weak hot spots and serve as the starting point for the cavitation bubbles formation. There are two types of cavities – stable and transient. Stable cavities survive for many cycles whereas the transient cavities grow in size because of the absorption of energy from every compression phenomenon until they ultimately implode. This implosion takes place at sufficiently high temperatures of about 4000 K and high pressure of around 100 MPa accompanied by shorter life times below 0.1 µs and cooling rates above 10^{10} K/s (Mason and Cordemans 1996). The collapse of bubble is so powerful and quick that it gives rise to the shear forces that are sufficient to break the chemical bonding of any polymeric material in the liquid. This should be the reason behind the reduction of large detached ink particles into floatable sizes. It produces significant mechanical effects. This generates jet stream having very high velocity of about 400 km/hr (Josefsson 2010). Implosion proceeds in the spherical region but if it is near to the surface than it will be directed towards the surface. This is equivalent to high pressure jetting. The shock waves generated by cavitation phenomenon are sufficiently strong to detach the ink particles from the fibres. In addition, the evolution of tremendous amount of heat due to cavitation helps in melting the polymer binder of the toner (Ikonomou et al. 1995). That is the region why ultrasound is considered so powerful for cleaning the surfaces, refining the pulp fibres, detaching the ink particles from the fibres and many more (Mason and Cordemans 1996). Cavitation depends on several factors namely viscosity of the medium, surface tension, vapour pressure, temperature etc (Josefsson 2010). Furthermore, according to Fricker et al. (2007), the toner particles are firstly broken down and then they are separated from the fibres. This reveals that the energy required to breakdown the cohesive forces among the toner particles is less as compared to the energy needed to break down the adhesive forces among the toner particle and fibre. Ultrasound treatment facilitates fibrillation of fibres as well as is able to detach and reduce the toner size into the floatable range (Manning and Thompson 2002, Fricker et al. 2007).

The simplicity of application of ultrasound and its potential in deinking makes this technique interesting.

2.2.5. Ultraviolet deinking

Like ultrasound deinking, ultraviolet deinking is also a new approach to remove the toner particles from the fibre surfaces. In fact, hardly any significant work is done in this field for its application in the removal of ink from waste papers as compared to even ultrasound. In this treatment, ultraviolet rays irradiate fibre surfaces containing ink particles for a certain period. The UV rays decompose the toner by initiating its degradation or breaking it into pulverization. Thermosetting resins used in toner of non impact printing technology are difficult to remove with conventional technology because they get fused with fibres because of high pressure and temperature (Pala et al. 2006). Hence, ultraviolet treatment can be used successfully in this area. However, the effectiveness of this treatment heavily depends on the time of illumination because its excessive exposure can impart yellowness and reduce the brightness of the deinked pulp (Zhenying et al. 2009). Since this technique is in its evolutionary stage, therefore a lot of study is required for analyzing the mechanism of UV irradiation assisted detachment of ink particles from waste papers. The economic and commercial considerations are yet to be fully worked out.

2.3. Materials and methods

2.3.1. Materials

2.3.1.1. Raw material

A commercial-grade copier paper (75 g/m^2) having size 210x297 mm^2 produced by an Indian paper mill was used for the study. The sheets were printed using WorkCentre 5335 photocopier by Xerox with Xerox black toner (006R01060). The sample sheet has been enclosed as Annexure-1 that shows high density of printed text than is normally available in the office copier waste. This has given more stringent condition for deinking. The age of the raw material was less than six months and was printed the same day as the experiment. The print format used in the sheets that were used in all sets of experiment is shown in Annexure-1 of which one line is as follows:

abcdefghijklmnopqrstuvwxyzABCDEFGHIJKLM20123456789!@#$%^&*(){}[]?<>

2.3.1.2. Chemicals

All chemicals were supplied by Qualigens Fine Chemicals (AR grade).

2.3.1.3. UV tubes

UV Philips tubes of 18 W each emitting UV radiations of 365 nm wavelength was used. Model no. of tubes was Philips TL-D 18W, BLB, Holland.

2.3.2. Methods

2.3.2.1. Parameters used in chemical deinking

The quantity of various chemicals and conditions used in carrying out the chemical deinking has been shown in Table-2.1 that have been taken from the works of earlier studies (Agnihotri 2007, Pathak et al. 2011, Imamoglu 2006, Jiang and Ma 2000) except pulp consistency, pulping time, flotation time, dose of surfactant and air flow rate. Pulp consistency was optimized between 6-16 % for the lab pulper used for the study. Moreover, pulping time (20min, 25min and 30min), flotation time (1min, 5min and 10 min) and air flow rate (5 L/min, 10 L/min and 15 L/min) were also optimized. Moreover, surfactant (oleic acid) concentration was optimized for 0.2%, 0.6% and 0.8%. In addition, combination of oleic acid (0.2%, 0.6%, 0.8%) and Tween 80 (0.2%, 0.6%, 0.8%) were also optimized. Nevertheless, the optimum dosing of individual oleic acid came out to be most significant. The optimum dosing of all parameters have been documented in Table-2.1.

2.3.2.2. Optimization of parameters used in combined deinking

The time of exposure of UV irradiation and the duration of the ultrasonic treatment have been optimized. The experiments were carried out with time interval of 1min, 5min, 10min, 15min and 20 min for both UV irradiation as well as ultrasound treatment as shown in Table-2.2 and Table-2.3 respectively.

Table- 2.1. Conditions for various treatments

Specification	Chemical deinking
Pulp consistency (%)	8
Pulping time (min)	25
End pH±0.1 (Hydrapulping)	10
Pulping Temperature (°C)	65
Agitation rate during pulping (rpm)	650
NaOH (%) on o.d. paper	2
Na_2SiO_3 (%) on o.d. paper	2.5
H_2O_2 (%) on o.d. paper	1.0
DTPA (%) on o.d. paper	0.5
Oleic acid (%) on o.d. paper	0.6
Flotation time (min)	5
Agitation rate during flotation (rpm)	1400
Air flow rate (L/min)	10

2.3.2.3. Deinking experimental procedure

The experimental procedure shown in Figure-2.1 is used in this study.

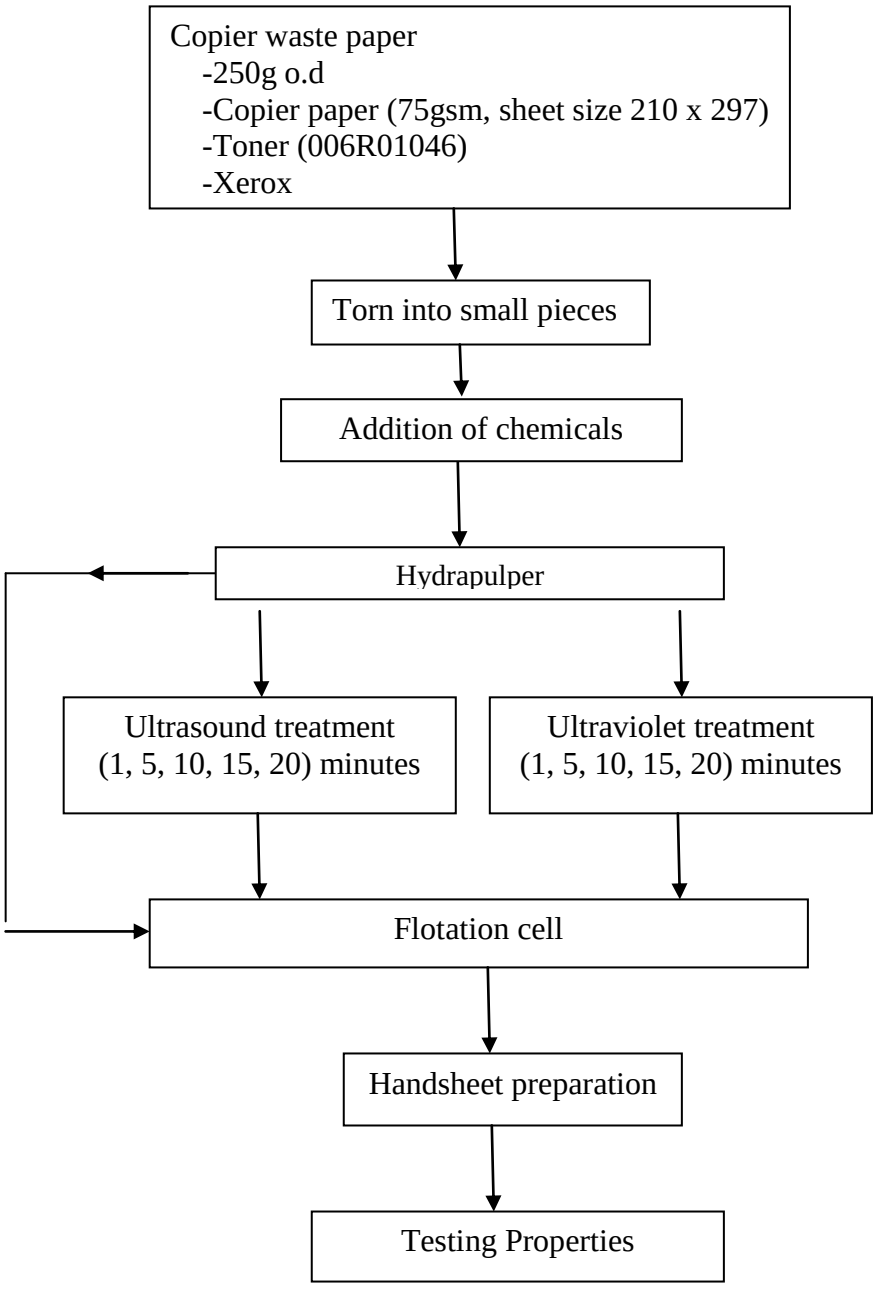

Figure-2.1 Flow diagram for combined deinking technologies

2.3.2.4. Hydrapulping

A laboratory Helico pulper was used for carrying out all repulping operations. Initially the wastepapers were torn manually. The size of torn pieces was around 4x4 cm squares. 250 g o.d. paper was used for carrying out the hydrapulping. Dosages of different chemicals and process variables used in hydrapulping are shown in Table-2.1. After the completion of hydrapulping, hand sheets were prepared and different optical and strength properties were measured.

2.3.2.5. Flotation process

However, flotation was carried out in a Voith type flotation cell having 1% consistency with 25 liters capacity with flotation time of 5 min in all treatments. After the flotation treatment, the deinked fibers were separated by a muslin cloth from the drain valve of flotation cell and handsheets were prepared. All process parameters related to the flotation cell have been documented in Table-2.1.

2.3.2.6. Ultrasonic treatment

The ultrasonic treatment was applied on chemical deinking. The ultrasonicator UTS-120 from Unitech Ultrasonic Mumbai (India) with ultrasonic wattage of 150 W, ultrasonic frequency of 40±3 kHz and having capacity of 6 L was used for the treatments. The instrument had a power supply of 220 volt, Ac 50 Hz, single phase. The pulp mixture was kept in a chamber made up of stainless steel. The ultrasonic treatment was carried out for different durations as mentioned in Table-2.3.

2.3.2.7. UV Irradiation treatment

The UV irradiation treatment was applied on chemical deinking. The pulp mixture was kept in a container kept in wooden chamber having 77 x 36 x 71 cm^3 size with 4 UV tubes. The distance between the UV tubes and the specimen was 15 cm. The instrument had a facility of a fan for dissipating the heat generated. The UV irradiation was applied on chemically deinked pulp for various durations as mentioned in Table-2.2.

2.3.2.8. Handsheet preparation

After flotation, the handsheets were prepared using TAPPI Test method T 218 sp-02 for reflectance testing. TAPPI Test Method T 205 sp-95 was used to make hand sheets for testing of physical properties. The hand sheets were made using a British handsheet former unit. Fifteen hand sheets (60 gsm) per run were prepared.

2.3.2.9. Testing of properties

2.3.2.9.1. Optical properties

Brightness and opacity were measured using a brightness tester (Model: Spectrophotometer CM-3630, KONICA MINOLTA, UK) at various places on both sides of the handsheets following TAPPI Test Method T452 om-92. Deinkability factor was calculated according to the formula mentioned in section 2.4.2. Dirt count was done by dirt analyzer (Model: DOMAS Scanner System P24100, Frank-PTI, Germany). Ink elimination was calculated by same brightness tester (Model: Spectrophotometer CM-3630, KONICA MINOLTA, UK) using INGEDE method.

2.3.2.9.2. Strength properties

Tensile index, burst index and tear index were determined by TAPPI Test Method T404 om-92, T403 om-97 and T414 om-98 respectively.

2.3.2.10. Comparison of various processes

After evaluating different properties of sheet made from different techniques used, comparison was done between chemical deinking, combined deinking of chemical and UV irradiation and combined deinking of chemical as well as ultrasound treatment.

2.4. Results and discussion

This section presents the results obtained after chemical deinking, combined deinking of chemical and UV irradiation treatment as well as combined deinking of chemical and ultrasound treatment. Table 2.2 shows the comparison of results of chemical deinking and UV-irradiation treatment whereas Table 2.3 shows the comparison of results of chemical deinking and Ultrasound treatment.

Table-2.2. Effect of chemical deinking and combined deinking with UV irradiation treatment on properties

Parameters	Brightness (%)	Opacity (%)	Ink elimination (%)	Dirt count reduction (%)	Deinkability factor (%)	Tensile index (N.m/g)	Tear index ($mN.m^2/g$)	Burst index ($kPa.m^2/g$)
Chemical deinking	83.60 (0.25)	86.33 (1.97)	28.10 (6.37)	36.38	57.79	31.44 (1.01)	5.63 (1.62)	0.70 (0.26)
UV-1 min	83.81 (0.31)	88.05 (0.84)	29.20 (5.40)	44.6	59.54	32.77 (1.28)	5.88 (0.48)	1.07 (0.06)
UV-5 min	85.52 (4.43)	88.34 (4.76)	34.74 (5.54)	46.73	65.76	35.15 (0.85)	5.77 (1.15)	1.17 (0.26)
UV-10 min	87.57 (4.71)	86.51 (1.34)	44.21 (2.48)	55.64	76.80	35.45 (1.43)	6.36 (0.20)	1.06 (0.18)
UV-15 min	82.34 (0.19)	85.47 (2.33)	33.36 (6.00)	52.88	39.63	33.21 (0.66)	5.60 (0.88)	1.05 (0.05)
UV-20 min	83.19 (0.35)	83.19 (0.66)	26.97 (4.48)	49.86	44.16	32.66 (0.56)	5.33 (0.45)	1.03 (0.12)

Note: 1. UV = Ultraviolet

2. Digits in parenthesis indicate standard deviation

Table-2.3. Effect of chemical deinking and combined deinking with Ultrasound treatment on properties

Parameters	Brightness (%)	Opacity (%)	Ink elimination (%)	Dirt count reduction (%)	Deinkability factor (%)	Tensile index (N.m/g)	Tear index ($mN.m^2/g$)	Burst index ($kPa.m^2/g$)
Chemical deinking	83.60 (0.25)	86.33 (1.97)	28.10 (6.37)	36.38	57.79	31.44 (1.01)	5.63 (1.62)	0.70 (0.26)
US-1 min	83.17 (0.47)	88.01 (0.02)	23.71 (3.59)	36.66	48.70	31.44 (1.06)	5.99 (0.47)	1.07 (0.12)
US-5 min	85.29 (0.14)	87.88 (0.04)	34.72 (3.13)	43.57	61.40	32.73 (0.56)	6.13 (1.07)	1.06 (0.10)
US-10 min	85.91 (3.53)	89.15 (0.05)	35.51 (5.51)	38.12	69.00	37.72 (0.10)	6.47 (0.14)	1.10 (0.11)
US-15 min	84.28 (0.65)	88.48 (0.12)	30.97 (3.03)	38.60	58.60	36.90 (0.20)	5.90 (0.15)	1.08 (0.12)
US-20 min	82.65 (0.18)	87.81 (0.12)	26.43 (2.60)	37.60	48.29	36.01 (0.88)	5.30 (0.29)	0.98 (0.09)

Note: 1. US = Ultrasound

2. Digits in parenthesis indicate standard deviation

2.4.1. ISO brightness (%)

It is observed that the maximum ISO brightness of the pulp after being treated by combined deinking of chemical and UV irradiation for different durations is found to be 87.57±4.71% after 10 minutes exposure. It is 3.97% better than ISO brightness obtained with only chemical deinking as mentioned in Table-2.2.

ISO brightness increases with increase in UV irradiation exposure as evident from Table-2.2. The reason behind this phenomenon is that the UV irradiation partially decomposes or degrades

the toner of the photocopier paper that contains thermosetting resin that gets fused to the paper fibres due to intense heat and pressure. This results in the loosening of the particle and weakening of the bond between ink and fibre. Then the toner particle can be easily detached from the fibre surfaces. Moreover, UV irradiation can further break the large specks of detached ink particles into floatable size (Zhenying et al. 2009).This is the reason behind better performance of combined deinking with UV-irradiation than chemical deinking.

However, after attaining an optimum value the ISO brightness showed reduction even with increase in the exposure time. This can be due to the development of yellowness in the pulp because of excessive exposure of UV irradiation (Zhenying et al. 2009). These processes are highly dynamic in nature and hence an optimised duration of UV irradiation treatment is necessary.

It is observed that ultrasound treatment produced 85.91± 3.53% as optimum value. It is 2.31% better than ISO brightness obtained only with chemical deinking. It is also obtained after 10 minutes duration of treatment. The effectiveness of ultrasound treatment in combined deinking technology can be traced in its mechanism. Treatment of the pulp suspension by ultrasound generates large quantity of microscopic bubbles. The bubbles grow in size and ultimately implode after a short span of few milliseconds. The shock waves generated by this implosion are so powerful that they possess sufficient energy to break down the bonding between the toner and fiber and thus facilitate their separation (Ikonomou et al. 1995). Hence, brightness increases as is evident from Table-2.3. Moreover, during implosion of bubbles, tremendous amount of localized heat takes place that further melts the polymeric resin of the toner and reduces the large detached particles (Ikonomou et al. 1995). However, after an optimum duration, ultrasonic treatment seems unfavorable. The reason behind decrement in ISO brightness is that excessive treatment may be making the detached toner thinner and excessively reduced in size thereby increasing their chances of re-deposition on the fiber matrix (Zhenying et al. 2009).

After examining the results of both combined deinking technologies of UV and US treatments, it can be mentioned that UV irradiation produces better result than US treatment at optimum duration. However, both produces better results than chemical deinking in terms of ISO brightness.

2.4.2. Deinkability factor (%)

The deinkability factor varies on a scale of 0-100%. Closure the value of deinkablity factor (D_F) % approaches 100, better is the efficiency of the treatment to carry out deinking. A 100% deinkability factor represents a perfectly deinked sample (Imamoglu et al. 2006). It shows the effectiveness of any treatment in removal of ink. The formula used to calculate the deinkability factor in this study is

D_F (%) = [(B_F – B_P)/ (B_{UP} – B_P)] x 100

Where B_F= ISO brightness of paper after flotation

B_P = ISO brightness of paper after pulping

B_{UP} =ISO brightness of unprinted paper which is 90.70%

The maximum deinkability factor is obtained with 10 minutes treatment of UV irradiation on the chemically deinked pulp. The deinkability factor obtained with 10 minutes exposure is 76.8% that is 19.01% more than the chemical deinking. The results have been shown in Table-2.2. The deinkability factor of combined deinking technology of chemical and UV irradiation treatment initially increases up to a maximum value. However, after an optimum duration of exposure, the deinkability factor starts decreasing. The excessive exposure of paper to UV irradiation turns it yellow, reducing its ISO brightness and the deinkability factor too.

The maximum deinkability is achieved after the application of 10 minutes of exposure to the ultrasonic treatment. The deinkability obtained after 10 min. duration is found to be 69.0% that is 11.21% more than the chemical deinking. The deinkability factor of the combined deinking of chemical deinking as well as ultrasonic treatment shows increment and then reduction after reaching a maximum value same as in the case of combined effect of chemical and UV irradiation.

The maximum deinkability factor obtained with UV irradiation treatment is 76.8% whereas the maximum deinkabilty factor obtained with ultrasonic treatment is 69.0% that is 7.8% lesser than UV irradiation treatment as evident from Table-2.2 and Table 2.3. Hence, the combined deinking with UV treatment appears better than combined deinking with US treatment. However, the effectiveness highly depends on the ink formulation and pulp composition. Hence, optimization of duration of treatment is required for every pulp individually.

2.4.3. Dirt count (ppm)

The insertion of foreign matter in the paper sheet having contrasting color more than 10% of full scale relative to the local background around any individual dirt speck is called dirt (Pathak 2014). The dirt count is evaluated more specifically by computing the dirt reduction (DR) using following formula

$DR\% = [(D_P - D_F)/ (D_P)] \times 100$

Where D_P = Dirt count (ppm) of the paper after pulping

D_F= Dirt count (ppm) of the paper after flotation

More the reduction in dirt, cleaner will be the pulp. With chemical deinking, 36.38% dirt reduction is observed whereas with optimum duration of UV irradiation treatment, 55.64% dirt reduction is observed. It is 19.26% better than only chemical deinking. Moreover in other durations also UV irradiation treatment shows higher dirt reduction than chemical deinking. Hence, it can be said that it removes the dirt better than chemical deinking. The possible reason behind this phenomenon can be the effective removal of dirt by UV irradiation from the fibre matrix by initiating the degradation of polymer or even leaving it into pulverized form and making it lose so that it can be easily removed during flotation stage (Zhenying et al. 2009). However, its effectiveness decreases after optimum duration of exposure. This might be due to the excessive exposure causing excessive breakage of the unwanted particles, even less than floatable size that resulted in their re-deposition. Hence, it looks that the combined treatment of chemical as well as UV irradiation can clean the pulp more effectively if the duration of treatment is optimized.

On comparing the dirt count reduction of chemical deinking and combined deinking of chemical along with Ultrasound treatment, it emerges that almost similar results appears at various durations of Ultrasound treatment except with optimum duration. At optimum duration of 5 minutes, 43.57% dirt reduction is observed that is 7.19% more than chemical deinking. The reason for the effective removal of dirt by ultrasonic waves is the generation of vibration and friction due to the compression and expansion which makes the unwanted particles loose and thus they can be removed in subsequent stages (Zhenying et al. (2009).

On comparing the dirt removal efficiency of both the technologies, it can be said that the UV irradiation treatment proves better than ultrasound treatment.

2.4.4. Ink elimination (%)

The ink elimination has been obtained by using the results of combined deinking of chemical and UV irradiation treatment or combined deinking of chemical and US treatment. The results have been obtained by using INGEDE method. Application of both technologies showed better removal of ink as compared to chemical deinking but only upto 15 minutes duration. UV irradiation produced 16.11% better ink elimination whereas ultrasound produced 7.41% better ink elimination at 10 min. duration as compared to chemical deinking. However both UV irradiation treatment and US treatments produced optimum results at 10 minutes duration. The increment in ink removal with UV or US treatment occurs because of their mechanism. After attaining an optimum value, the value starts reducing. Hence, excessive exposure in US or UV treatment is not helpful for good ink elimination. Therefore, optimization of treatment is required. Hence, based on above facts it is evident that the application of UV irradiation treatment and US treatment in addition to chemical pulping shall give better results. However, if the effectiveness of both treatments is considered, than the UV irradiation treatment appears better than US treatment.

2.4.5. Opacity

From the Table-2.2, it appears that the opacity increases initially with the increase in UV exposure duration and after reaching optimum it starts decreasing. Hence, excessive exposure of UV irradiation results in reduction of opacity. Maximum opacity of 88.34% is obtained with 5 minutes UV exposure. It is 2.01% more than opacity obtained with chemical deinking. The reason behind this phenomenon could be the mechanism of the UV irradiation in deinking process. Same trend is also observed with ultrasound treatment as can be seen from Table-2.3. Maximum opacity of 89.15% is observed with 10 minutes duration of treatment. It is 2.82% more than opacity obtained with chemical deinking. Here also excessive exposure is reducing the opacity.

2.4.6. Strength properties

The combined deinking of chemical and UV irradiation treatment produces better results for tensile index as compared to chemical treatment. Maximum tensile index of UV irradiation treatment is found to be 12.75% more than chemical deinking as shown in Table-2.2. The reason behind improvement in tensile index property may be the increment in fibrillation of the fibre surface by UV irradiations. The fibrillation facilitates increase in surface area for bonding

between the fibres and hence imparts sufficient tensile index (Josefsson 2010). However, the tensile index decreases after optimum duration of application of treatment. Hence, it appears that optimization of duration of UV irradiation treatment can be helpful for imparting better tensile index. However, the results highly depend on the ink formulation and type of pulp composition. On the other hand, for tear index also UV irradiation is producing almost similar trend. It is evident from the results that the tear index increases until optimum is achieved. Optimum duration of UV irradiation treatment results in 12.97% increment in tear as compared to chemical deinking. Moreover, after optimum, it showed reduction. The reason behind decrement in tear index may be the breakage of fibres. However, more study is required to study the mechanism to explain the effect of UV irradiation on strength properties. Moreover, UV irradiation produced higher burst index as compared to chemical deinking in all durations tested.

The tensile index obtained after the ultrasonic treatment also shows better results as compared to chemical deinking as shown in Table-2.3. Like UV treatment, it also shows increment up to optimum value with increase in duration of application of treatment. It produced 19.97% higher tensile index at 10 minutes duration of treatment. This duration comes out to be optimum. The reason for the improvement in tensile property is due to the increase in external fibrillation of the fiber due to the beating effect of the ultrasonic treatment. This results in fibre swelling that increases the contact area of the fibres. A large contact area facilitates inter-fibre bonding and increases the paper strength (Josefsson 2010, Manning and Thompson 2002, Manfredi et al. 2013). Hence optimization of duration is required. However, all the durations of ultrasound treatment produced higher tensile index than chemical deinking except 1 min. As far as tear is considered, ultrasonic treatment shows improvement in tear index as compared to chemical deinking until 15 minutes duration of treatment. However it showed maximum tear index at 10 minutes duration that is found to be 14.92% higher than the chemical deinking. Moreover, Manfredi et al. (2013) also got improved tear index with this treatment. Although, the tear index reduced after an optimum duration of 10 minute. The possible cause behind this could be the breakage of fibres because of excessive vibrations and friction. Ultrasound treatment showed higher burst index than chemical. Ultrasound treatment enhances the burst index. It improves with the removal of fines which improves inter fibre bonding and facilitates hydrogen bonding.

The maximum tensile index found with ultrasonic deinking is 37.72 $N.mg^{-1}$, whereas the maximum tensile index observed with UV irradiation is 35.45 $N.mg^{-1}$. Hence, ultrasound

treatment seems slightly better than UV irradiation treatment. Moreover, ultrasound produces better results than UV irradiation treatment regarding tear index also. Nevertheless, both treatments shows better burst index as compared to chemical deinking. In addition, it can be said both UV irradiation as well as ultrasound treatment show almost similar effect on burst index. Hence, it can be concluded that ultrasound treatment appears to be better than UV irradiation treatment if strength properties are considered.

2.4.7 Energy consumption

With increase in the duration of UV irradiation or Ultrasound treatment, the energy consumption will increase. From the results documented in Table-2.2 and Table-2.3, it is evident that various properties show improvement with increase in energy dosage. However, after optimum values of duration of treatment, reduction is observed. Hence, it can be said that the effectiveness of UV irradiation and US treatment are sensitive to energy dosage.

2.5. Conclusions

This chapter covers the effect of combined deinking of chemical pulping with UV or US treatments. Many optical properties as well as some strength properties have been estimated considering the effects of duration of treatments. Then comparison is carried out among all three deinking processes. It is observed that combined deinking of UV irradiation as well as US treatment showed improvement in deinking efficiency. UV and US treatments showed improvement in optical as well as strength properties over only chemical deinking. Hence, combined deinking technology can further enhance the deinking efficiency of conventional deinking. However, among both UV irradiation and US treatment, it is found that UV irradiation showed better enhancement in optical properties whereas US treatment produced higher improvement in strength properties. It is observed from the results that both UV irradiation and US treatment are sensitive to the energy dose. In both cases, deinking improves with increase in energy dose but starts decrease after reaching to an optimum value. However, the relative advantage of US or UV treatment is mainly property and material specific and no generalization is possible. However, in the present work no specific studies have been carried out to understand the mechanism of ink removal in UV irradiation and US treatment. Furthermore, little amount of work is carried out on ultrasound treatment and hardly any study is done in UV irradiation in this field. Hence, further investigation is required to clearly understand the mechanisms of these technologies.

CHAPTER 3

THERMAL CONVERSION OF DEINKING SLUDGE AND ITS KINETICS

3.1. Introduction

In this chapter, the thermal behaviour of deinking sludge and its kinetics is studied. This work is mainly divided into two parts. First part focuses on the effect of heating rate and atmosphere on the thermal behaviour of deinking sludge (A). Second part evaluates the possibility of co-processing of coal and rice husk with deinking sludge (B) under two different atmospheres. Initially the characterization of raw materials namely deinking sludge, coal and rice husk is carried out. Then their individual thermal behaviour is studied under air and nitrogen atmosphere. After that, the thermal behaviour of the blends of deinking sludge with coal and deinking sludge with rice husk is also studied. Kinetic parameters are calculated after evaluating the thermal behaviour.

The deinking sludge is procured from same recycle paper mill but at different point of time. Moreover most of the time mill raw material gets changed. That is why two deinking sludges namely deinking sludge (A) and (B) are different.

3.2. Literature review

In this section, the account of various works has been presented related to different aspects of the present study.

3.2.1. Raw material characterization

3.2.1.1. Proximate and Ultimate analysis

The determination of volatile matters, fixed carbon, ash content and moisture content is called proximate analysis. It is practical and a quick method of knowing the quality and type of fuel. Volatile matters convert in the form of gas, tars and hydrocarbons. As far as ash is concerned, it also reduces the heating value. It consists of many minerals like salts of calcium, silica, potassium and magnesium (Singh et al. 2011). Ultimate analysis is the determination of carbon as well as hydrogen in the specimen, as found in gaseous products of the complete combustion

of material and determination of sulphur, nitrogen as well as ash as a whole and calculating oxygen by difference (ASTM E 870-82 2006).

Wang et al. (2014) stated that the deinking sludge they used contained high volatile matter (50.39 %) and low fixed carbon (4.09 %). Hence, according to them it can be utilized as fuel. They also observed significant amounts of C (25.31 %), H (2.50 %) and O (28.88 %) elements which as they stated came from fibres or may have came from ink and fillers.

Vamvuka and Kakaras (2011) studied the ash properties and environmental impact of coal fuels and various biomass including paper sludge as well as their blends. They found that all the biomass tested displayed high volatile content that could be considered favourable for combustion or gasification process. Their ultimate analysis revealed that the hydrogen content in all samples was comparable but the carbon content was lower in all types of biomass as compared to coal. Moreover, the sulphur content of all samples was very low implying the SOx emissions during the combustion stage would not be a cause of concern.

Yanfen and Xiaoqian (2010) have also conducted study on the co-pyrolysis of paper sludge and coal. After carrying out the proximate analysis, they found that coal displayed higher fixed carbon content and lower ash content as compared to paper sludge. For coal, the obtained values of fixed carbon content and ash content were 45.31 wt% and 21.57 wt% respectively. For paper sludge, the values of fixed carbon content and ash content were 6.01 wt% and 45.25 wt% respectively. However, they observed that paper sludge showed higher oxygen contents and more volatiles than coal. The values of oxygen content and volatile matter obtained for paper sludge were 25.01 wt.% and 48.74 wt% respectively. For coal, the values of oxygen content and volatile matter were 8.20 wt.% and 33.12 wt% respectively. Since these are the vital elements for initiation of ignition, hence they recommended the use of their blends for more significant results.

Mendez et al. (2009) carried out proximate and ultimate analysis of different paper mill wastes. They found that all samples showed more than 50 wt% volatile content. They stated that it might be due to the organic matter and/or decomposition of $CaCO_3$. Fixed carbon varied from 1.05 wt% to 11.95 wt% in all the samples. Wastes from the paper industries displayed least amount of ash whereas the deinking sludge from recycle paper industries displayed significant amount of ash content up to 40.94%.

Vamvuka et al. (2009) carried out the proximate and ultimate analysis of paper sludge and sub-bituminous coal as well as the blends of both the fuels. Both paper sludge as well as coal displayed low sulphur content. For paper sludge, the sulphur content was 0.1% whereas for coal sample the value of sulphur content was 0.3%. The SO_x emissions during the combustion do not become a cause of concern if the sulphur content is low. In addition, the proximate analysis of both fuels showed high amounts of volatile matter. However, coal displayed low ash content and high fixed carbon content as compared to paper sludge. The corresponding values of ash content and fixed carbon content in coal were 5.6 % and 44.7 % respectively. For paper sludge, the corresponding values of ash content and fixed carbon content were 51.0% and 1.3% respectively. Moreover, their blend showed almost same amount of volatile matter but varying percentage of fixed carbon and ash content as compared to paper sludge and coal. The ultimate analysis displayed the high carbon and hydrogen content in sub-bituminous coal as compared to paper sludge. The carbon content in coal and paper sludge was 64.6% and 23.0 % respectively. The hydrogen content in coal and paper sludge was 5.8% and 2.8% respectively.

Mansaray and Ghaly (1999) carried out the proximate and ultimate analysis of four varieties of rice husk. The volatile matter ranged from 67.30 – 63.00 % and fixed carbon ranged from 18.80 – 24.60 % depending upon the variety of rice husk. The ash content ranged from 18.20 – 20.00 %. In the ultimate analysis, the carbon content varied from 37.60 – 42.60 % and the oxygen content varied from 31.37 – 36.56 % depending on the rice husk sample. The sulphur content in all the samples was less than 0.04%.

3.2.2. Thermal conversion of Paper/Deinking sludge

3.2.2.1. Pyrolysis

Various researchers have conducted TGA to understand the thermal degradation of materials like paper sludge, agricultural wastes etc.

Wang et al. (2014) studied the effect of different heating rates on the pyrolysis of deinking sludge. They applied 5, 10, 20, 30 and 40 °C/min heating rate under nitrogen atmosphere having flow rate of 60 ml/min. They observed that the pyrolysis profile of deinking sludge consist three stages *viz.* moisture loss, release of volatiles and residual decomposition. They found increment in the starting temperature, final temperature as well as temperature at which maximum weight loss occurred with increase in heating rate.

Lou et al. (2012) conducted the pyrolysis of deinking sludge sample at 20 °C/min heating rate. The TG-DTG curve showed three stages. First stage showed peak at 71 °C representing the mass loss. Second stage indicating the de-volatilization showed peak at 361 °C ranged from 100 °C to 550 °C. Third stage indicated decomposition of calcium carbonate. It occurred from 550 °C to 800 °C. This stage showed peak at 772 °C.

Yanfen and Xiaoqian (2010) conducted the pyrolysis of paper sludge at three different heating rates *viz.* 10, 20 and 30 K/min. They found two individual stages in the pyrolysis of paper sludge apart from moisture loss. First stage indicating de-volatilization occurred from 500 K (226.85 °C) to 900 K (626.85 °C). Other stage appeared from 1000 K (726.85 °C) to 1200 K (926.85 °C) with maximum weight loss rate at 1120 K (846.85 °C). This stage represented the decomposition of calcium carbonate.

Vamvuka et al. (2009) studied the pyrolysis of paper sludge. They applied heating rate of 10 °C/min in their study of pyrolysis of paper sludge. They observed two stages beside moisture loss. First stage representing de-volatilization started from 280 ºC to 550 ºC. Another stage occurred at still higher temperatures from 550 ºC indicating the decomposition of calcium carbonate in the paper sludge.

Bhuiyan et al. (2008) carried out the TGA of waste newspaper. They used three heating rates *viz.* 5, 10 and 20 K/min under nitrogen atmosphere with flow rate of 200 ml/min and at atmospheric pressure. They observed three stages in the TG profile of their sample. First stage started at 38 °C and ended at 142 °C with 5.4% weight loss. This stage represented the evaporation of moisture. Second stage that represented the release of volatiles started at 291 °C and ended at 429 °C with 63.2% weight loss. Third stage occurred between 657 °C and 743 °C with 16.1% weight loss leaving the residue. They observed that with increase in the heating rate, decomposition rate was increased.

3.2.2.2. Combustion

Liu et al. (2010) studied the effect of oxygen concentration on the thermal degradation of paper sludge. Various heating rates were applied *viz.* 10, 20 and 40 °C/min with 20 vol% oxygen concentration. DTG profiles showed two major peaks. First peak occurred at 326.0 °C, 326.8 °C and 345.0 °C for 10, 20 and 40 °C/min heating rates respectively. Second peak occurred at 752.9 °C, 786.9 °C and 805.4 °C for 10, 20 and 40 °C/min heating rates respectively. Moreover, oxygen concentration was also increased from 20 vol% to 80 vol% at constant

heating rate of 20 °C/min. Two peaks were observed in the DTG profile of various concentration of oxygen. First peak centred around 320 – 350 °C and other centred around 780 – 795 °C in all the different oxygen concentrations. First weight loss represented de-volatilization and second weight loss represented combustion of fixed carbons. It was found that with increase in the oxygen concentration, the initial decomposition temperature of paper sludge sample decreased. This indicated improvement in the ignition characteristic of paper sludge. Hence paper sludge would combust more completely and thus reducing residual weight.

Yanfen et al. (2010) carried out the combustion of their paper sludge sample with 10, 20 and 30 K/min heating rate under air atmosphere. The experiment was conducted from 310 K to 1300 K. From the DTG curve, two stages in the combustion profile of the paper sludge were observed. First stage represented burning of combustible matter and the second stage represented decomposition of mineral matter. First stage started from 400 K and ended at 900 K whereas second stage range from 900 K to 1200 K. Moreover, it was observed that as the heating rate was increased, the peaks of the combustion profile shifted towards higher temperature. However, the peak height corresponding to different heating rates remained almost same.

3.2.3. Thermal conversion of coal

3.2.3.1. Pyrolysis

Yanfen and Xiaoqian (2010) carried out the pyrolysis of semi-anthracite coal. In the pyrolysis of coal, the decomposition started at 600 K (326.85 °C) and ended at 1200 K (926.85 °C) with maximum weight loss at 743 K (469.85 °C). They observed two regions. First one depicting the mass loss due to vaporization, disruption of hydrogen bonds and transport of non-covalently bonded molecular phase released by reduction in hydrogen bonds and evaporation in the temperature range of 200 – 400 °C (Solomon et al. 1992). Another stage represented the primary decomposition reaction.

Vamvuka et al. (2009) carried out pyrolysis of sub-bituminous coal at 10 °C/min heating rate from ambient to 850 °C. They found that pyrolysis profile of coal extends over wide range of temperature. They observed that the decomposition of coal started at 166 °C and continued until the end of the experiment. They observed a small peak centred at 300 – 550 °C in the pyrolysis of coal sample.

3.2.3.2. Combustion

Vamvuka and Sfakiotakis (2011) did the combustion of lignite using TGA from 25 – 800 °C with 3 °C/min heating rate. From the DTG profile of their sample, they observed that lignite consisted of two components having different reactivity. A high combustible material that decomposes between 300 – 550 °C and a low combustible material that decomposes in higher range (550 – 750 °C). They also stated that the presence of low reactive char component is the reason for the incomplete combustion in lignite-fired power plants and for unburnt carbons left in the ash particles.

Yanfen and Xiaoqian (2010) carried out the combustion of semi-anthracite coal at 10 K/min heating rate. They observed a single peak at 715 K. They also studied the effect of oxygen concentration on the combustion profile of the coal sample. They found that as the concentration of oxygen was increased, the peak value indicating the reactivity got increased. Moreover, peaks corresponding to the combustion profile in different O_2 concentration shifted towards lower temperatures as the concentration of oxygen was increased.

Vamvuka et al. (2009) presented the burning profile of the sub-bituminous coal. They carried out the TGA of their coal sample at 10 °C/min heating rate from 25 – 850 °C with flow rate of 60 ml/min. They observed bimodal DTG curve indicating the presence of structures with different reactivity. The decomposition occurred from 400 – 550 °C with maximum weight loss at 476 °C.

3.2.4. Thermal conversion of Blends

3.2.4.1. Pyrolysis

Vamvuka et al. (2009) carried out the pyrolysis of sub-bituminous coal and paper sludge blend at 10 °C/min heating rate in the nitrogen atmosphere. The coal- paper sludge ratio was taken as 90:10. The DTG profile of the pyrolysis of coal and its blend with paper sludge showed almost same peak height as that of the DTG profile of the pure coal. The only difference was in the position of the peak. The peak shifted backwards towards low temperature, indicating that the presence of paper sludge in the blend increased the reactivity. Since they considered that, the peak height was directly proportional to the reactivity, whereas the corresponding temperature of the peak height was inversely proportional to the reactivity.

3.2.4.2. Combustion

Yanfen and Xiaoqian (2010) analysed the combustion profiles of semi-anthracite coal and paper sludge blends. They carried out the TGA on these samples with three heating rates *viz.* 10, 20 and 30 K/min at temperatures ranging from 310 K to 1300 K. In the combustion profile of the coal and paper sludge blend, they observed three stages in the DTG curve. This blend consisted of 10 wt% paper sludge. They stated that three stages represented the decomposition of organic compounds present in paper sludge, coal and mineral matter respectively. They also observed as the percentage of paper sludge was increased in the blend, the combustion profile became more similar as that of the paper sludge.

3.2.5. Thermal conversion of Biomass (Rice husk)

3.2.5.1. Pyrolysis

Mansaray and Ghaly (1998) studied the thermal degradation of rice husk under N_2 atmosphere. They took four varieties of rice husk (Lemont, ROK 14, CP 4 and Pa Potho). These samples were subjected to different heating rates *viz.* 10 °C/min, 20 °C/min and 50 °C/min. Samples were heated from ambient to 700 °C with flow rate of 50 ml/min. In the thermogravimetric analysis of rice husk samples, it was observed that a slight weight loss occurred from ambient to 100 °C. This could be because of the removal of physically bonded water or water bounded by surface tension. Then there was a major weight loss starting at 180 °C - 240 °C depending on the heating rate applied and rice husk variety used. This stage indicated the evolution of volatile compounds because of degradation of hemicelluloses and cellulose. This stage essentially ended at 360 – 380 °C according to the rice husk variety. This stage was regarded as active pyrolysis. Another stage that ended at 470 – 500 °C for different varieties was regarded as the passive pyrolysis. In this stage degradation of lignin occurred. It was also found that the degradation rate increased with increase in the heating rate.

3.2.5.2. Combustion

Mansaray and Ghaly (1999) conducted the combustion of four different rice husk samples (Lemont, ROK 14, CP 4 and Pa Potho) at 20 °C/min from ambient to 700 °C under oxygen atmosphere. They observed weight loss due to loss of water molecules in their sample from ambient to 100 °C. The weight loss in this stage was 4.0 – 4.7% depending upon the variety of rice husk. They observed very heavy decomposition starting from 203 – 218 °C because of rapid evolution of volatile matter. This stage ended at 291 – 295 °C according to the rice husk

variety. Total degradation and degradation rate in this stage were 60.35 - 68.90% and 16.50 - 19.70 %/min respectively. After this stage, a small peak was also observed that ended at 453 - 467 °C with total degradation 5.2 – 7.2% depending on the rice husk sample.

3.2.6. Thermal conversion of pure substance

Stylianos et al. (2014) studied the lingo-cellulosic biomass pyrolysis through pyrolysis of hemicelluloses, cellulose as well as lignin. Pyrolysis of samples was performed with constant heating rate of 10 °C/min under nitrogen atmosphere. The experiment was conducted in a temperature range of 28 – 840 °C. All the samples were dried at 105 °C for 4 h prior to use. Hemicellulose decomposed in lowest range of temperature from 200 °C to 320 °C. This can be attributed to its highly amorphous and branched structure. Cellulose decomposed over slightly higher range of temperature from 280 °C to 360 °C. This well defined decomposition of cellulose which is higher than hemicelluloses is because of its structure. It has long chain of D-glucose units with no branches. Lignin decomposed in a wide range of temperature ranging from 140 °C to 600 °C. It showed a very low intensity peak around 380 °C. This is because of its structure. It consists of cross-linked aromatic molecules that are difficult to decompose.

Shen and Gu (2009) studied the mechanism of thermal decomposition of cellulose. Initially cellulose sample as a white powder was dried in a furnace at 100 °C for 2 h before experiment. Then the sample was heated in TG analyzer from 20 °C to 800 °C at heating rates of 5, 20 and 60 K/min in nitrogen atmosphere. The flow rate was 60 ml/min. The TG-DTG curves of the sample showed a heavy weight loss in a small temperature range. This stage was observed between 294 °C to 377 °C with peak value at 348 °C. This temperature range was observed with 5 K/min heating rate. However, with 20 and 60 K/min, this temperature range started at 312 °C and 329 °C respectively and ended at 404 °C and 424 °C respectively. It means with increase in heating rate the DTG peaks shifted towards higher temperature.

Yang et al. (2007) studied the thermal decomposition characteristics of hemicelluloses, cellulose and lignin using TGA. They carried out the pyrolysis of these materials from ambient to 900 °C with 10 °C/min heating rate. Hemicellulose decomposed easily as compared to others. The DTG profile of it showed a major weight loss from 220 – 315 °C with maximum weight loss at 268 °C. Decomposititon of cellulose occurred at higher temperatrure range (315 – 400 °C) with maximum weight loss at 355 °C. However, the pyrolysis of lignin occurred at slowest rate compared to hemicelluloses and cellulose. Its decomposition happened from 100°C to 900 °C. The difference in the decomposition characteristics of these three components

is because of their structures. Hemicellulose composed of many saccharides. It has random and amorphous structure with many branches. These branches are easy to be removed from the main stem and get decomposed. Cellulose composed of long polymer of glucose without branches. Hence, it shows better thermal stability than hemicelluloses. Lignin consists of aromatic rings. The activity of chemical bonds in the structure of lignin covers a wide range of temperature. Therefore, lignin decomposes in a wide range of temperature.

Galan et al. (2013) studied the decomposition of calcium carbonate. The TG analysis was performed in nitrogen atmosphere under three heating rates *viz.* 5, 10 and 20 °C/min. From the TGA curve of the sample it was observed that with increase in the heating rate there was an increase in the temperature zone where the decomposition of the calcium carbonate takes place. However, the TG curves of all heating rates showed a heavy degradation after around 650 °C.

3.2.7. Kinetics

The thermal degradation kinetics can be described by following global model (Gangavati et al. 2005).

$$xX\ (s) \longrightarrow yY\ (s) + zZ\ (g) \quad (1)$$

The decomposition of solid biomass can be well described by a general expression as

$dx/dt = kf(x)$

Using the Arrhenius equation, the fundamental equation of thermal degradation can be framed as:

$$dx/dt = A \exp(-E/RT)\, f(x) \quad (2)$$

Where t=time (min)

A=pre-exponential factor (mg $^{1-n}$ min^{-1})

E=activation energy (kJ/mol)

R=gas constant

T=temperature (°C)

x = fractional conversion of A at time t

If the linear constant heating rate is taken as $\beta = dT/dt$ (°C/min), then Eq. 2 can be written as:

$$dx/dT = A/\beta \exp(-E/RT)\, f(x) \quad (3)$$

Where $f(x) = (1-x)^n$

Then, Eq. 3 can be written as:

$$dx/dT = A/\beta \exp(-E/RT)\, (1-x)^n \quad (4)$$

Where n=order of reaction

Because the first-order Arrhenius law can be used to describe the kinetics of the decomposition reaction, Eq. 4 becomes

$dx/dT = A/\beta \exp(-E/RT)(1-x)$ (5)

Several researchers have modelled different expressions using Eq. (5) for the determination of kinetic parameters.

Table -3.1 Kinetics models by various researchers

Reference	Raw material	Method	Kinetic model used
Yanfen and Xiaoqian (2010)	semi-anthracite coal, paper sludge and their blends	Iso-conversional integral method	$\ln\left(\frac{\beta}{T^2}\right) = \ln\left(\frac{AR}{Eg\,(\alpha)}\right) - \frac{E}{R}\,\frac{1}{T}$
Vamvuka et al. (2009)	Sub-bituminous coal, paper sludge and their blends	Independent First order reactions' model	$-\frac{dm}{dt} = \sum_i C_i \frac{da_i}{dt}$ i=1, 2, 3..... $\frac{da_i}{dt} = A_i \exp(-\frac{E_i}{RT})(1 - a_i)$
Bhuiyan et al., (2008)	Newspaper	Friedman method	$log\left[-\frac{1}{w_0 - w_f}\frac{dw}{dT}\right] = \log\left(\frac{A}{\beta}\right) - \frac{E}{2.3\,RT} + nlog\left[\frac{w-w_f}{w_0 - w_f}\right]$
Mansaray and Ghaly (1999)	Rice husk	Friedman method	$log\left[-\frac{1}{w_0 - w_f}\frac{dw}{dT}\right] = \log\left(\frac{A}{\beta}\right) - \frac{E}{2.3\,RT} + nlog\left[\frac{w-w_f}{w_0 - w_f}\right]$

3.3. Materials and methods

This section provides the information of the raw materials and the detailed experimental plan used in the present research work.

3.3.1 Materials

3.3.1.1 Raw materials

The deinking sludge (A) was procured from one of the recycle paper industries located in Punjab (India). The industry produces writing and printing-grade paper using coated duplex board and mixed office waste. The procured deinking sludge was sun-dried first and then further oven-dried at 105 ºC for 2 h. Dried sludge was crushed in a laboratory ball mill and sieved through a 75-µm sieve. Finally, the sieved sludge was stored in a polythene bag for further use. Deinking sludge (B) was procured from the same industry but after a period of time and it was also oven dried at 105 ºC for 2 h. Same ball mill was used to crush this sample and it was passed through 75-µm sieve. Coal and rice husk samples were collected from a local area of Saharanpur (India). Lignite grade coal used in the present study was oven dried at 105 ºC for 5 h. Then it was milled and sieved to make particle size less than 250 µm. Rice husk sample was also crushed and sieved to particle size less than 75 µm. After these procedures, samples were stored in a polythene bag for further use.

3.3.1.2 Characterisation of samples using different techniques

Proximate analyses of the samples were carried out using standard procedure ASTM D3172-13 (2013). Proximate analysis determines the amount of fixed carbon and volatile matters, which contributes to the heating value of the sample. The ultimate analyses were carried out using a CHNS Elemental Analyzer (Flash 2000, Thermo Fisher Scientific, UK). Thermogravimetric analysis (TGA) was performed using a Thermogravimetric Analyzer SII Seiko Instrument EXSTAR (Model no: TG/ DTA 6300, Tokyo, Japan) with a balance sensitivity of 0.1µg and balance accuracy better than 0.02%. In every set of experiments, the same quantity of sample (approximately 10 g) was used to avoid mass and heat transfer effects. For plotting of TGA/DTG curves, OriginPro (8.6) software was used.

3.3.2 Methods

The present study is divided into two parts. Section A focuses on the effect of heating rate on the pyrolysis and combustion of deinking sludge (A). Initially the raw material was characterized using above techniques. Four heating rates namely 10, 20, 30 and 40 °C/min were applied under nitrogen and air atmospheres separately with purge gas flow rate of 200 mL/min. The sample was heated from ambient to 900 °C. Section B focuses on the pyrolysis and combustion of deinking sludge (B), coal (C), rice husk (RH) as well as their blends. Initially the characterization of raw materials was carried out and thermogravimetric analysis was carried out for individual raw materials under nitrogen and air atmospheres separately. Then the blends containing 10%, 20%, 40% and 50% deinking sludge with coal (C) and rice husk (RH) were subjected to TG analysis under nitrogen and air atmospheres. Heating rate of 10 °C/min was applied in all the experiments of this section. The purge gas flow rate was 200 mL/min throughout the experiment. Then the TG-DTG curves were plotted using software. After this regression coefficient (R^2) was calculated using different models and then kinetic parameters were calculated using the model giving best regression coefficient (R^2) in both the sections.

3.4. Results and discussion

3.4.1. Section A-Effect of heating rates on deinking sludge (A)

3.4.1.1. Characterization of raw material

The proximate and ultimate analyses of deinking sludge (A) have been carried out and are presented in Table-3.2 and Table-3.3 respectively.

Table-3.2 Proximate analysis of deinking sludge (dry basis)

Parameters (%)	Sludge Sample
Volatile matter	54.20
Ash	41.02
Fixed carbon	4.78

Table-3.3 Ultimate analysis of deinking sludge (dry basis)

Parameters (%)	Sludge Sample
C	26.25
H	2.50
N	0.31
S	0.18
O	29.74

From Table-3.2, it can be observed that the deinking sludge (A) contains high amount of volatile materials. In addition, Table-3.2 also shows that sludge sample contains high ash content and low fixed carbon content. Moreover obtained values of moisture content, volatile matter, ash, and fixed carbon are in close approximation to that reported in Mendez et al. (2009).. Table-3.3 shows that the sludge contained sulphur. However, it is in small quantity, which may not be a cause for concern during combustion.

3.4.1.2. Thermal decomposition characteristics

In this section, the pyrolysis and combustion characteristics of deinking sludge (A) are investigated.

3.4.1.2.1. Pyrolysis

The TG-DTG profiles of the pyrolysis of deinking sludge (A) under nitrogen atmosphere are shown in Figure-3.1 to Figure-3.2 and thermal degradation behaviour is documented in Table-3.4.

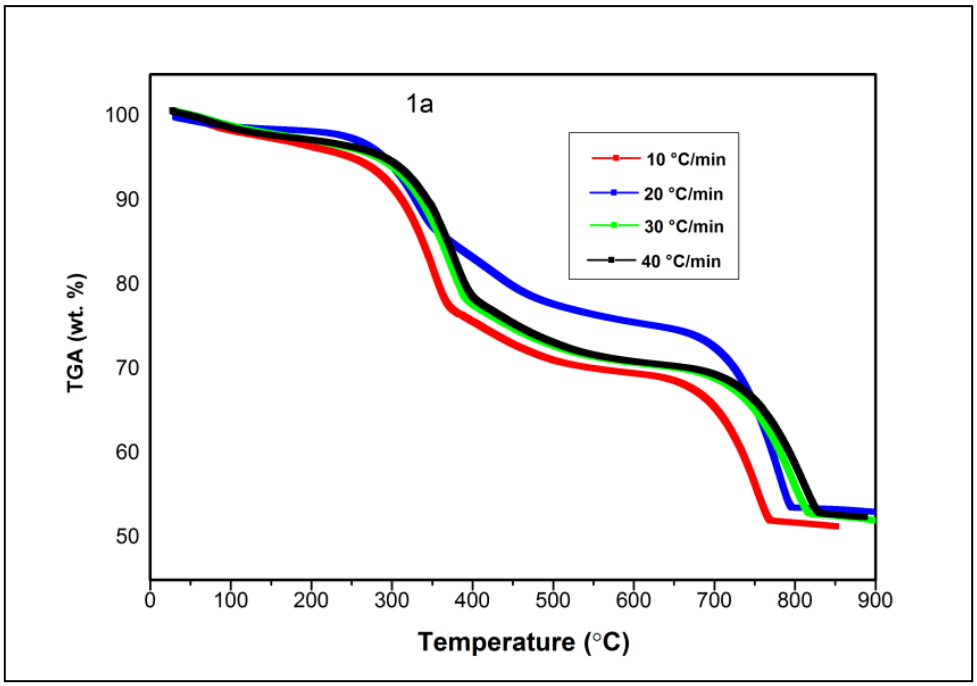

Figure-3.1 TG curves of deinking sludge (A) under nitrogen atmosphere with different heating rates

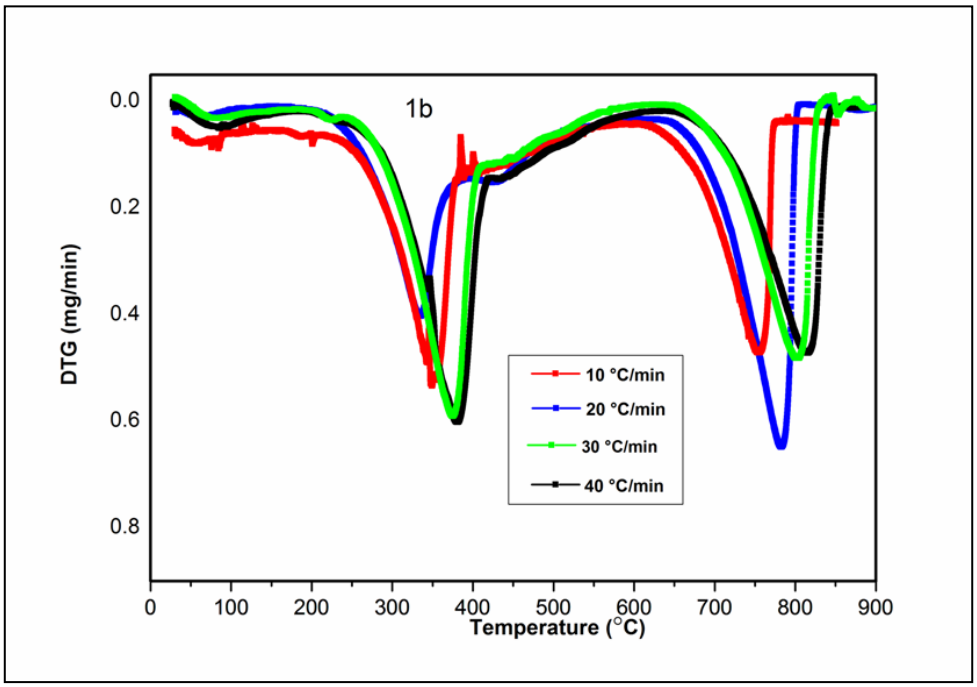

Figure-3.2 DTG curves of deinking sludge (A) under nitrogen atmosphere with different heating rates

Table-3.4. Thermal degradation of deinking sludge (A) under nitrogen atmosphere

Reaction zones	Heating rates (°C/min)	Water evolved (%)	Degradation temperature (°C)			Residue at 900 °C (%)
			Initial	Final	Maximum	
I	10	3.7	29	147	102	-
	20	2.4	29	146	102	-
	30	3.1	28	150	99	-
	40	3.4	28	149	100	-
II	10	-	147	390	301	-
	20	-	146	348	298	-
	30	-	150	400	347	-
	40	-	149	410	348	-
III	10	-	390	549	-	-
	20	-	348	552	-	-
	30	-	400	599	-	-
	40	-	410	598	-	-
IV	10	-	549	900	701	46.59
	20	-	552	900	754	46.30
	30	-	599	900	771	45.72
	40	-	598	900	780	48.64

During pyrolysis of deinking sludge (A) four heating rates namely 10, 20, 30 and 40 °C/min are applied. From the TG-DTG curves, for 10 °C/min heating rate, it is evident that the pyrolysis profile of this sample shows mainly three-region apart from moisture removal region. First stage represents the evaporation of superficial water. Second stage started at 147 °C and ended at around 390 °C. The maximum temperature of the peak in this stage occurred at 301 °C. Third stage showed slight peak. Fourth degradation stage has onset temperature at 549 °C and endset temperature at 900 °C with 701 °C as maximum peak temperature (Table-3.4). Second stage represents the de-volatilization of organic materials like hemicelluloses and celluloses. However, lignin decomposes at slowest rate at a wide temperature from ambient to 900 °C (Xie and Ma 2013). Fourth stage represents mainly the decomposition of calcium carbonate along

with other minerals. From the DTG curve, it can be observed that as the heating rate is increased, the peaks started shifting towards forward position or higher temperature. In other words, increase in heating rate delayed the thermal decomposition process. With increase in heating rate, the material reaches the same temperature in lesser time and thereby shifts the peaks to higher temperature. Moreover, Song et al. (2015) have stated that with increased heating rate, same temperature is reached in shorter time and makes the reaction stronger. The sample is not heated homogeneously, and some reactions could not occur. Thus, temperature lag effect results in shifting of peaks to higher temperature.

3.4.1.2.2. Combustion

The TG-DTG profiles of the combustion of deinking sludge (A) under air atmosphere are shown in Figure-3.3 to Figure-3.4 and thermal degradation behaviour is documented in Table-3.5.

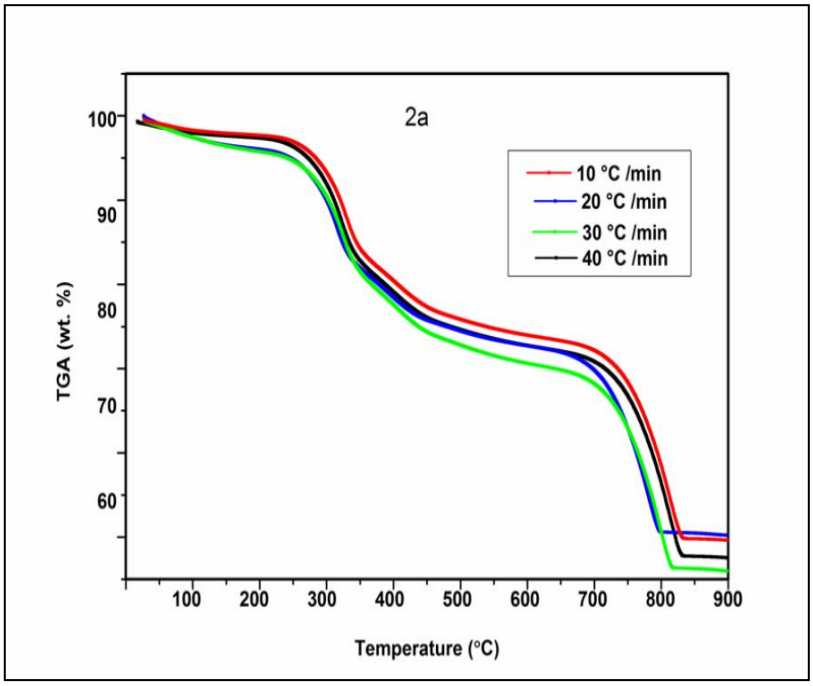

Figure-3.3 TG curves of deinking sludge (A) under air atmosphere with different heating rates

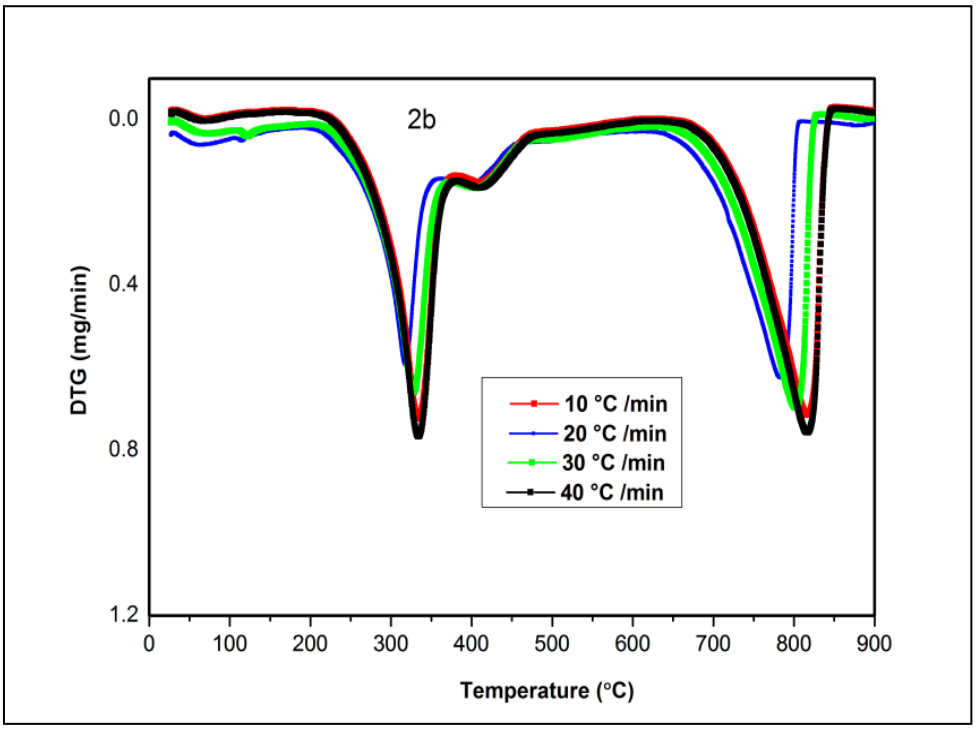

Figure-3.4 DTG curves of deinking sludge (A) under air atmosphere with different heating rates

Table-3.5. Thermal degradation of deinking sludge (A) under air atmosphere

Reaction zones	Heating rates (°C/min)	Water evolved (%)	Degradation temperature (°C)			Residue at 900 °C (%)
			Initial	Final	Maximum	
I	10	2.4	28	148	101	-
	20	3.2	27	148	102	-
	30	2.8	27	148	99	-
	40	1.4	29	150	97	-
II	10	-	148	331	263	-
	20	-	148	350	297	-
	30	-	148	348	297	-
	40	-	150	354	299	-
III	10	-	331	501	-	-
	20	-	350	553	-	-
	30	-	348	600	-	-
	40	-	354	597	-	-
IV	10	-	501	900	703	43.28
	20	-	553	900	748	43.10
	30	-	600	900	756	43.10
	40	-	597	900	761	43.09

In combustion also four heating rates namely 10, 20, 30 and 40 °C/min are applied to evaluate the effects of heating rate. It can be seen that the DTG curve shows mainly three degradation regions apart from moisture loss stage. First region is the superficial water loss stage. Second region started at 148 °C and ended at 331 °C with 263 °C as maximum peak temperature for 10 °C/min heating rate. This represents the combustion of volatiles like hemicellulose and cellulose. Third region is observed from 331°C to 501°C. This mainly represents the decomposition of lignin along with cellulose. Fourth region has onset temperature at 501°C and endset temperature at 900°C. This region represents the decomposition of calcium carbonate along with other minerals and few fixed carbons. From the DTG curve, it can be observed that in this case also the peaks are moving towards higher temperature with increase in heating rate.

The reason behind this phenomenon is same as discussed in section 3.4.1.2.1**.** Moreover, it can be observed that the peak height is increased in air atmosphere as compared to the corresponding peak height in nitrogen atmosphere. Hence, air atmosphere increases the reactivity of the deinking sludge, as peak height is directly proportional to the reactivity (Vamvuka et al. 2009). Moreover, sharper peaks and relatively smooth profile is observed in air atmosphere.

3.4.1.3. Kinetics

First order Arrhenius law can be used to describe the kinetics of the decomposition reaction

$$dx/dT = A/\beta \exp(-E/RT)(1-x) \quad (5)$$

Referring to the above equation several researchers *viz.* Coats and Redfern; Piloyan and Novikova; Reich and Stivala; Horowitz and Metzger models have modified rate expressions. The modified rate expressions are presented in Table-3.6 for calculating the kinetic parameters.

Table-3.6. Different models with their rate expressions for determination of kinetic parameters

Models	*Rate equations for determination of kinetic parameters
Coats - Redfern model (Coats et al. 1964; Gangavati et al. 2005)	$\ln [-\ln (1-x) / T^2] = \ln [AR / \beta E (1- (2RT / E)] – (E / RT)$ for n = 1.0 $\ln [-\ln \{1-(1-x)^{1-n} \}/ (1-n)T^2] = \ln [AR / \beta E (1- (2 RT/ E)] – (E / RT)$ for $n \neq 1.0$
Piloyan - Novikova model (Piloyan et al. 1966; Gangavati et al. 2005)	$\ln (\omega/ T^2) = \ln [(AR/\beta E)] – (E/RT)$
Horowitz -Metzger model (Horowitz et al. 1963; Gangavati et al. 2005)	$\ln [\ln (1- \omega)] = (E / (RT_p^2)$, when n = 1, $\ln [1- (1- \omega)^{1-n} / (1-n)] = (E\theta/ (RT_p^2)$ When $n \neq 1$, where $\theta = T- T_p$, T_p is the peak temperature as taken from the DTG curve
Reich and Stivala (Reich and Stivala 1983; Gangavati et al. 2005)	$\ln \left[\frac{1-(1-w_i)^{1-n}}{1-(1-w_{i+1})^{1+n}} \left(\frac{T_{i+1}}{T_i}\right)^2 \right] = \frac{E}{R} \left(\frac{1}{T_i} - \frac{1}{T_{i+1}}\right)$
*ω= decomposed fraction of solid at time t; E= activation energy (kJ /kg); A= pre-exponential factor in the Arrhenius equation (mg^{1-n} min^{-1}); n= order of reaction; R = universal gas constant (kJ/mol); x = fractional conversion $(W_0 – W_t) / (W_0 - W_\infty)$; W_t = weight of biomass at any time, (mg); W_∞ = weight of biomass at the completion of degradation (mg)	

Table-3.7. Determination of R^2 by different models under nitrogen atmosphere

Zones	Heating rates (°C/ min)	Models			
		Coats - Redfern model	Piloyan - Novikova model	Reich -Stivala model	Horowitz - Metzger model
		R^2	R^2	R^2	R^2
II	10	0.9610	0.9538	0.8550	0.9528
	20	0.9553	0.9504	0.8331	0.9195
	30	0.9578	0.9366	0.8489	0.9542
	40	0.9855	0.9792	0.9744	0.9331
III	10	0.9799	0.9594	0.9004	-
	20	0.9888	0.9494	0.9860	-
	30	0.9898	0.9730	0.9268	-
	40	0.9879	0.9788	0.8804	-
IV	10	0.9688	0.9020	0.7075	0.8991
	20	0.9986	0.9820	0.9418	0.9467
	30	0.9873	0.9768	0.9767	0.9690
	40	0.9877	0.9866	0.8715	0.8621

Table-3.8. Determination of R^2 by different models under air atmosphere

Zones	Heating rates (°C/min)	Models			
		Coats - Redfern model	Piloyan - Novikova model	Reich -Stivala model	Horowitz -Metzger model
		R^2	R^2	R^2	R^2
II	10	0.9709	0.7819	0.7334	0.9456
	20	0.9990	0.6284	0.8253	0.9967
	30	0.9901	0.6762	0.6824	0.9294
	40	0.9911	0.7367	0.9710	0.9218
III	10	0.9897	0.7142	0.9759	-
	20	0.9911	0.6907	0.9715	-
	30	0.9943	0.7019	0.9892	-
	40	0.9949	0.7812	0.9988	-
IV	10	0.9799	0.4085	0.6733	0.8346
	20	0.9963	0.8563	0.8472	0.8570
	30	0.9920	0.9886	0.6092	0.9231
	40	0.9993	0.6465	0.5714	0.9069

TG-DTG curves were fitted in the models given by (Coats and Redfern; Piloyan and Novikova; Reich and Stivala; Horowitz and Metzger) in nitrogen and air atmospheres and regression coefficient (R^2) was obtained in Table-3.7 and Table-3.8 respectively. It was found that Coats and Redfern model was best suited for the pyrolysis of deinking sludge. Hence, the kinetic parameters were calculated using Coats and Redfern model.

Table 3.9. Determination of Kinetic parameters under nitrogen and air atmospheres by Coats – Redfern model

Reaction zones	Kinetic parameters	Nitrogen Atmosphere				Air atmosphere			
		Heating rates (°C/min)				Heating rates (°C/min)			
		10	20	30	40	10	20	30	40
II	n	1.25	1.25	2.0	1.25	1.0	2.0	0.25	0.25
	E	110.02	113.56	123.35	106.82	92.53	117.79	140.08	138.73
	A	7.85 x 10^2	2.03 x 10^3	2.52 x 10^3	2.59 x 10^3	2.56× 10^4	2.07× 10^3	1.27× 10^3	1.52× 10^3
	R^2	0.9610	0.9553	0.9578	0.9855	0.9709	0.9990	0.9901	0.9911
III	n	1.0	1.25	2.0	1.25	1.0	1.0	1.0	1.0
	E	133.35	118.01	133.76	112.86	284.76	291.20	364.56	268.74
	A	1.40× 10^3	2.73 x 10^3	4.56 x 10^3	3.84 x 10^3	1.12× 10^6	7.69× 10^8	3.03× 10^9	3.74× 10^6
	R^2	0.9799	0.9888	0.9898	0.9879	0.9897	0.9911	0.9943	0.9949
IV	n	1.25	1.25	2.0	1.0	0.05	2.0	0.25	0.25
	E	124.64	121.44	132.85	133.25	102.78	105.05	151.91	152.28
	A	3.63 x 10^3	4.13 x 10^3	4.18 x 10^3	5.88 x 10^3	1.63× 10^3	8.56× 10^2	3.67× 10^3	5.16× 10^3
	R^2	0.9688	0.9986	0.9873	0.9877	0.9799	0.9863	0.9820	0.9993
Entire reaction zone	n	1.25	1.25	1.25	2.0	1.0	2.0	0.25	0.05
	E	115.21	109.03	115.24	117.72	262.52	117.7	152.74	151.46
	A	1.14 x 10^3	1.49 x 10^3	3.55 x 10^3	2.32 x 10^3	1.58× 10^5	2.06× 10^3	5.33× 10^3	5.88× 10^3
	R^2	0.9846	0.9516	0.9831	0.9826	0.9548	0.9987	0.9956	0.9948
Note: Units of A was taken as (min^{-1}) for n=1 and (mg^{1-n} min^{-1}) for any other values of n; E (kJ/mol^{-1})									

Table-3.9 shows the kinetic parameters of deinking sludge. The kinetic parameters were calculated by an integral approximation method (Coats and Redfern model) which gave best results as R^2 came out to be 0.9993 that is closest to one in air atmosphere at 40 °C/min heating rate which validates that experimental results were well fitting in reaction mechanism. Using integral approximation method the range of reaction order in both nitrogen and air atmosphere came out to be 1.0 to 2.0 and 0.05 to 2.0 respectively. Moreover the range of activation energy (E) in both nitrogen and air atmospheres was 106.82 to 133.76 kJ/mol and 92.53 to 364.56 kJ/mol respectively. Nevertheless the range of pre-exponential factor in nitrogen and air atmospheres was 7.85 x 10^2 min^{-1} to 5.88 x 10^3 min^{-1} and 8.56 x 10^2 min^{-1} to 3.03 x 10^9 min^{-1}

respectively. Activation energy (E) came more in air atmosphere than in nitrogen atmosphere. The pre-exponential factor came better in second and entire reaction zone under air atmosphere as compare to nitrogen atmosphere. The advantage of finding such results lies in the fact that these often help in practical applications like designing of systems and simulation models (Singh et al. 2013).

3.4.2. Section B- Co-processing of deinking sludge (B) with fuels

3.4.2.1. Characterization of raw materials

Table-3.10 Proximate analysis of raw materials (Dry basis)

Parameters (%)	Deinking sludge	Coal	Rice husk
Volatile matter	51.44	48.06	66.07
Ash	44.91	19.06	20.40
Fixed carbon	3.65	32.88	13.53

Table-3.11 Ultimate analysis of raw materials (Dry basis)

Parameters (%)	Deinking sludge	Coal	Rice husk
C	24.90	52.92	45.80
H	3.45	5.28	6.45
N	0.28	1.16	0.80
S	0.31	0.62	0.04
O	26.15	20.96	26.51

The proximate and ultimate analyses of deinking sludge (B), coal and rice husk are presented in Table-3.10 to Table-3.11. It can be seen from the Table-3.10 that deinking sludge shows high ash content along with low fixed carbon content as compared to coal. Moreover, deinking sludge also shows higher values for volatile matter as well as oxygen content. Volatile matter and oxygen content are the important elements for the initiation of ignition. Thus, blending of coal with deinking sludge can improve the ignition characteristics. In addition, they contain low amount of sulphur. Hence, the SOx emissions will not be a cause of concern for these fuels during their thermal degradation. Moreover, the rice husk contains more volatile matter and lower ash content as compared to deinking sludge. Also the rice husk as well as deinking sludge shows lower values for nitrogen and sulphur indicating clean combustion.

3.4.2.2. Thermal decomposition characteristics

In this section, the thermal decomposition characteristics of raw materials and their blends have been presented.

3.4.2.2.1. Pyrolysis

In this section, the pyrolysis of raw materials and their blends is focused

.

3.4.2.2.1.1 Pyrolysis of coal, deinking sludge (B) and rice husk

This section presents the thermal degradation of raw materials in nitrogen atmosphere.

Table-3.12 Thermal degradation of coal, deinking sludge and rice husk under nitrogen atmosphere

Sample Code	Zones	Temperature intervals (°C)			Total degradation (%)	Residue (%) at 1000 °C
		Initial temperature	Max. peak temperature	Final temperature		
Coal (C)	II	126	200	572	4.57	-
	III	572	889	1000	76.08	22.19
Deinking sludge (DS)	II	149	300	600	20.99	-
	III	600	743	804	24.70	51.62
Rice husk (RH)	II	204	317	561	78.94	12.63

The pyrolysis behavior of coal, deinking sludge and their blends has been presented from Figure 3.5 to Figure 3.7.

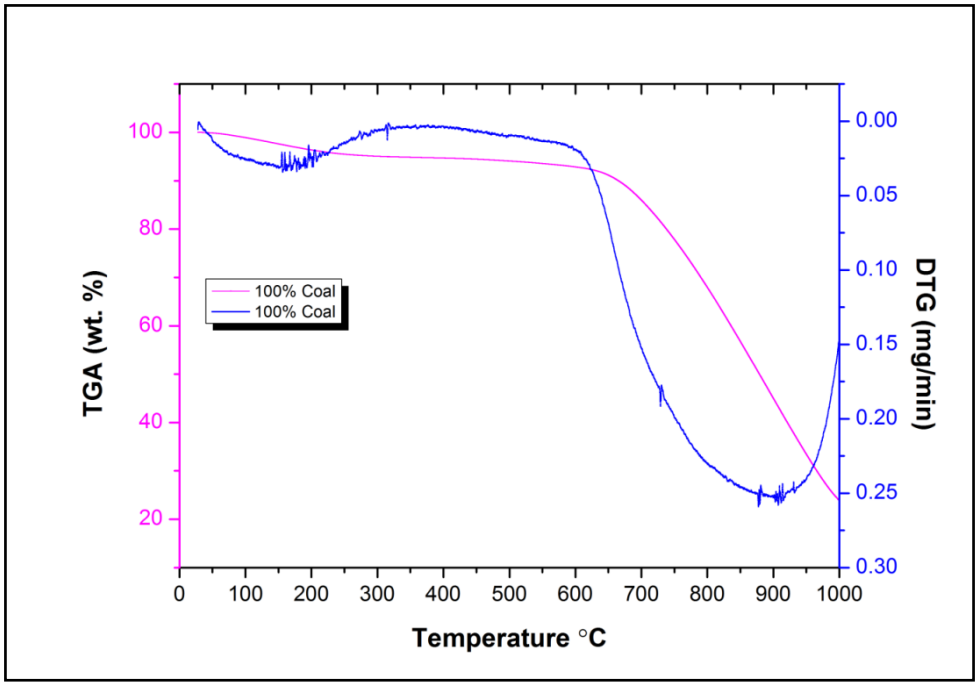

Figure-3.5 TG and DTG curves of coal in nitrogen atmosphere

The heating rate applied is 10 °C/min. From the DTG curve presented in Figure-3.5, it can be said that the pyrolysis of the coal depicts a two-region profile apart from moisture loss. In the first stage, occurring from 126 °C to 572 °C, mass loss along with some de-volatilization takes place. In this stage, the maximum weight loss occurs at 200 °C where total degradation of 4.7 wt% occurred. The mass loss indicates the evaporation of water. According to Yanfen and Xiaoqian (2010), in the mass loss stage of the coal, disruption of hydrogen bonds, vaporization and transport of non-covalently bonded molecular phase takes place. Second stage ranges from 572 °C to 1000 °C with maximum weight loss at 889 °C. This zone shows heavy degradation of 76.08 wt%. From the DTG curve, it can be observed that the profile is not getting flat indicating unburnt carbon left in the residue. This occurs because of the low reactive char component of coal. Hence, it can be argued that if the coal is blended with biomass material, then high reactive char components of biomass can increase the reactivity of the coal and thus facilitate the complete decomposition process. Hence study of the co-processing of the coal and biomass can yield improved results. Same trend is also observed by Vamvuka and Sfakiotakis (2011).

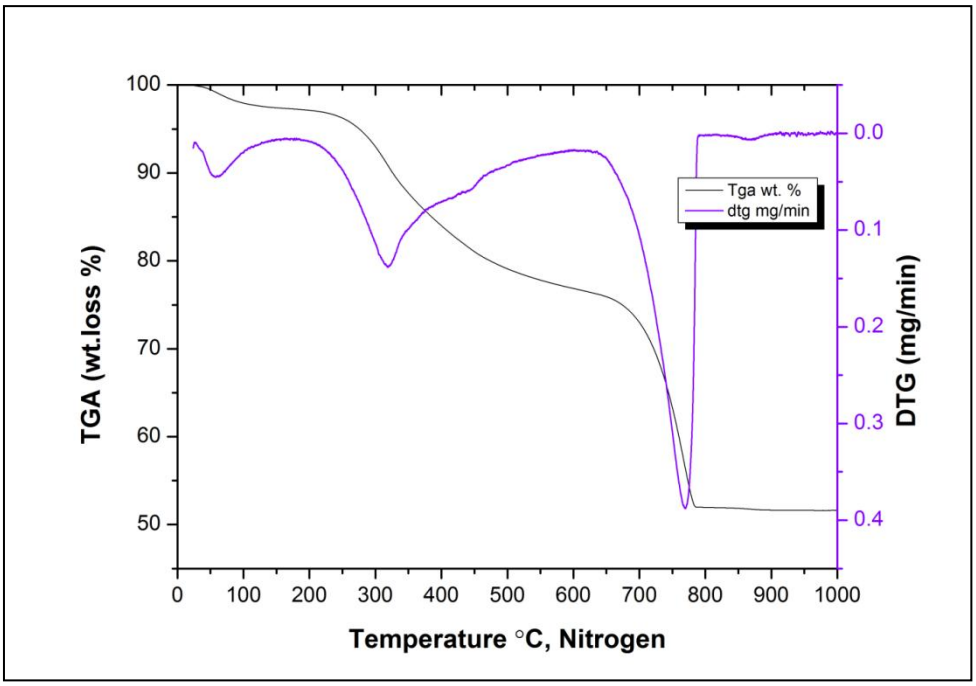

Figure-3.6 TG and DTG curves of deinking sludge in nitrogen atmosphere

The TG-DTG curves of the pyrolysis of deinking sludge at 10 °C/min heating rate have been presented in Figure 3.6. From the DTG curve, it can be observed that the deinking sludge is showing mainly two-region profile apart from moisture loss. The first stage that occurred from 149 °C to 600 °C with a maximum weight loss at 300 °C represents the decomposition of volatiles like hemicelluloses and celluloses. Hemicellulose decomposes earlier than cellulose. This is due to the difference in their structure. Hemicellulose has branched chain structure whereas cellulose has long chain structure without any branches. Therefore, hemicellulose decomposes easily relative to the cellulose. Moreover, lignin decomposes at the slowest rate in overall range of temperature from 100 °C to 900 °C (Xie and Ma 2013, Yanfen et al. 2007). In this stage total degradation of 20.99 wt% occurred. The second stage occurred form 600 °C to 804 °C with maximum peak temperature occurring at 743 °C. This stage depicts total degradation of 24.70 wt%. In this stage, mainly decomposition of calcium carbonate along with some other minerals takes place.

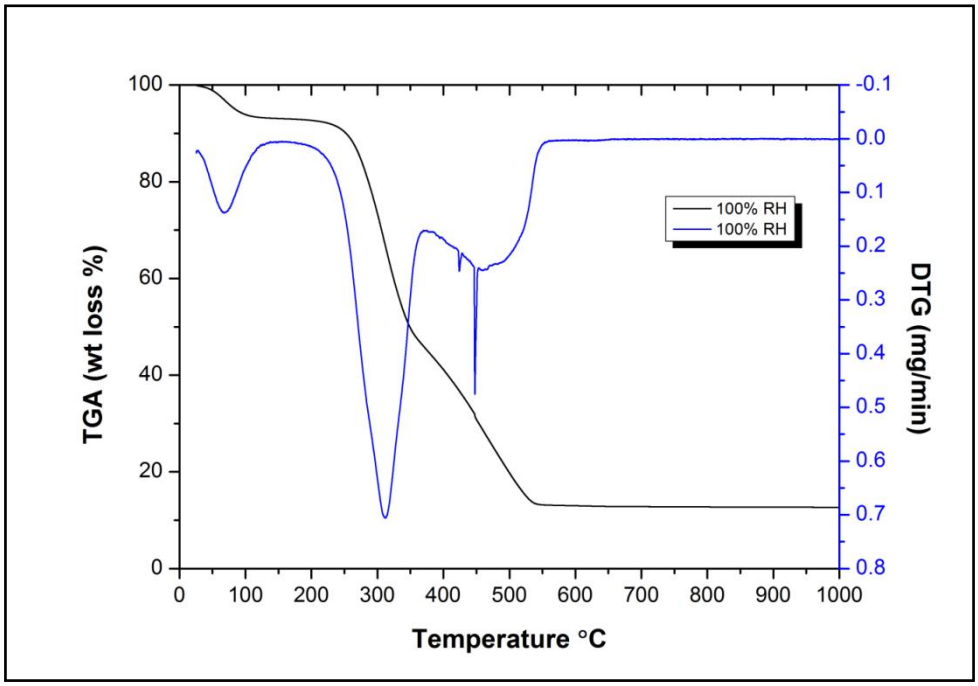

Figure-3.7 TG and DTG curves of rice husk (RH) in nitrogen atmosphere

The pyrolysis process of rice husk is displayed in Figure-3.7 and is documented in Table-3.12. It presents a small peak indicating mass loss in first stage. It represents removal of superficial water absorbed or external water bounded by surface tension. Slight de-volatilization may also have occurred. Second stage occurs from 204 °C to 561 °C. Total degradation of 78.94 wt% is observed in this stage. It depicts a big peak indicating heavy and rapid de-volatilization along with decomposition of inorganic matters. In this stage decomposition of hemicelluloses, cellulose and lignin occur. Mansaray and Ghaly (1998) have also observed similar trend. After this stage 12.63 % residue remains. The thermal behaviour of lignocellulosic substances are highly depends on their chemical composition. Therefore, thermal behaviour varies between varieties.

3.4.2.2.1.2 Co-pyrolysis of coal and deinking sludge (B)

Table-3.13 Thermal degradation of blends of coal and deinking sludge under nitrogen atmosphere

Sample Code	Zones	Temperature intervals (°C)			Total degradation (%)	Residue (%) at 1000 °C
		Initial temperature	Max. peak temperature	Final temperature		
90C10DS	II	224	351	552	6.71	-
	III	552	816	850	51.98	37.32
80C20DS	II	222	351	552	7.03	-
	III	552	848	874	50.43	39.32-
60C40DS	II	226	345	571	10.31	-
	III	571	823	860	45.43	41.4
50C50DS	II	227	286	562	10.46	-
	III	562	816	850	43.57	43.22

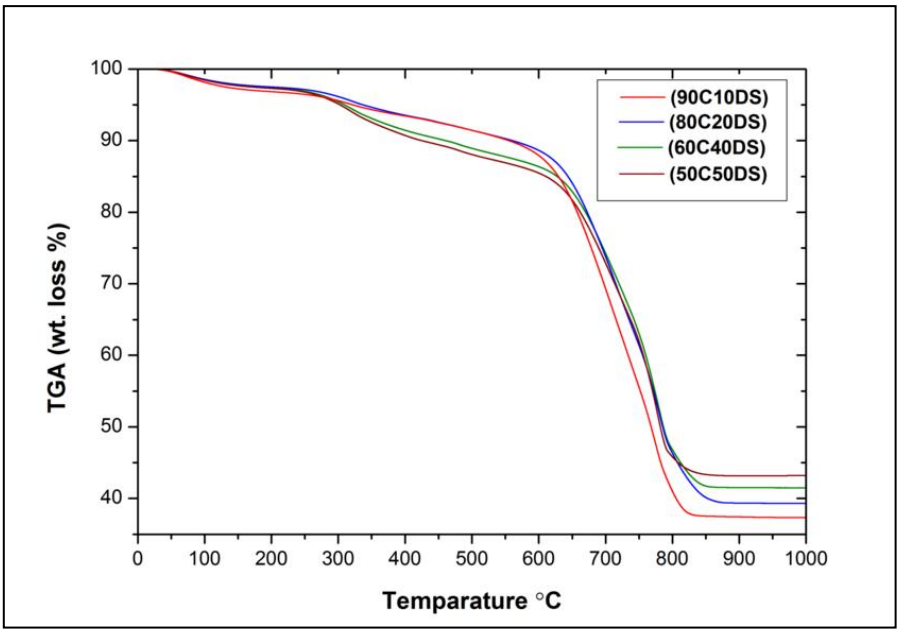

Figure-3.8 TG curves of blends of coal (C) with deinking sludge (DS) in nitrogen atmosphere

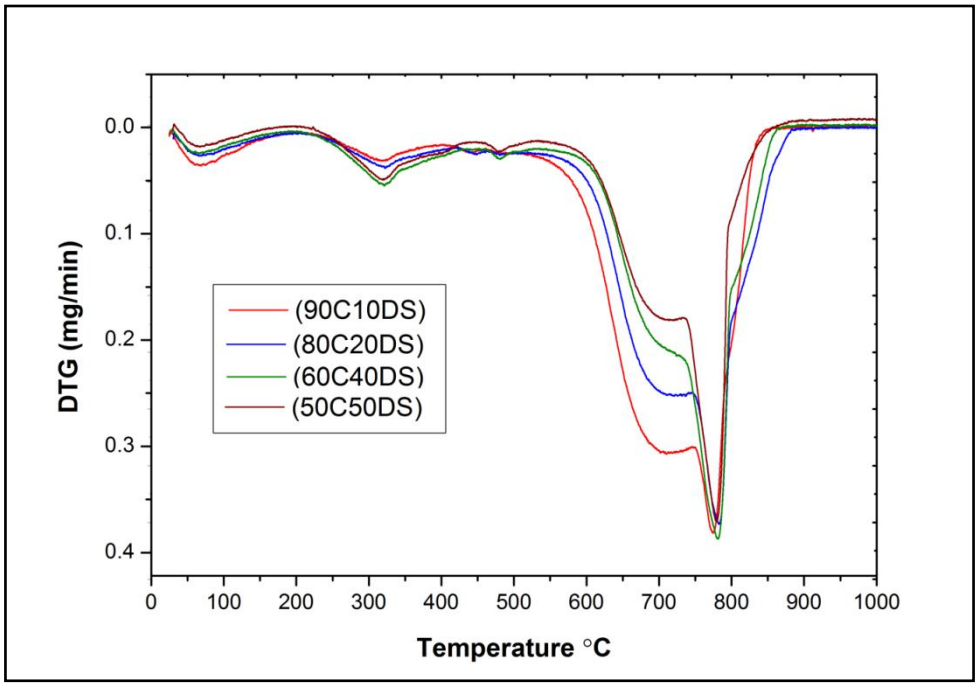

Figure-3.9 DTG curves of blends of coal (C) with deinking sludge (DS) in nitrogen atmosphere

On comparing the DTG curves of coal and deinking sludge under nitrogen atmosphere, it is evident that the peak height corresponding to coal is smaller than the peak height corresponding to deinking sludge. If peak height is directly proportional to reactivity and the temperature corresponding to peak height is inversely proportional to reactivity as mentioned by Vamvuka et al. (2009), then it can be inferred that the deinking sludge is more reactive than the coal. Moreover, unlike coal the profile of deinking sludge showed a flat region after 804°C indicating residue and thus completion of the process. Furthermore, the release of volatile matter occurred earlier than coal. Hence, deinking sludge presents better de-volatilization characteristics as compared to coal.

The pyrolysis of the blends of coal and deinking sludge has been presented from Figure-3.8 to Figure-3.9 at 10 °C/min heating rate. It can be said that the profiles of blends lies between coal and deinking sludge. The blend having 90% coal and 10% deinking sludge behaves similar to that of coal whereas the profile approaches to that of the deinking sludge as the proportion of the deinking sludge is increased. The DTG curves of blends show a three-region profile. The second stage corresponds to the light de-volatilization of the organic matter present in the blends. It started at around 224 °C and ended at about 552 °C for all combinations of blends. The total degradation in this stage increases as the proportion the deinking sludge is increased. The onset temperatures of different blends in the third stage are obtained at around 552 °C whereas the endset temperatures are noted at around 850 °C (Table-3.13). The peak shifts to a lower temperature after blending as compared to coal indicating increase in the reactivity because of the addition of deinking sludge. This is also validated by comparing the peak heights of the blends as compared to the coal. Moreover, unlike coal the blending with the deinking sludge results in completion of process as the curves become flat after 850 °C leaving behind the residue.

3.4.2.2.1.3 Co-pyrolysis of rice husk and deinking sludge (B)

Table-3.14 Thermal degradation of blends of rice husk and deinking sludge under nitrogen atmosphere

Sample Code	Zones	Temperature intervals (°C)			Total degradation (%)	Residue (%) at 1000 °C
		Initial temperature	Max. peak temperature	Final temperature		
90RH10DS	II	196	317	573	76.71	-
	III	573	653	703	1.18	16.37
80RH20DS	II	201	344	576	75.17	-
	III	576	654	707	2.16	14.63
60RH40DS	II	204	340	550	48.64	-
	III	550	701	761	12.25	34.13
50RH50DS	II	206	338	523	42.03	-
	III	523	700	768	15.81	38.86

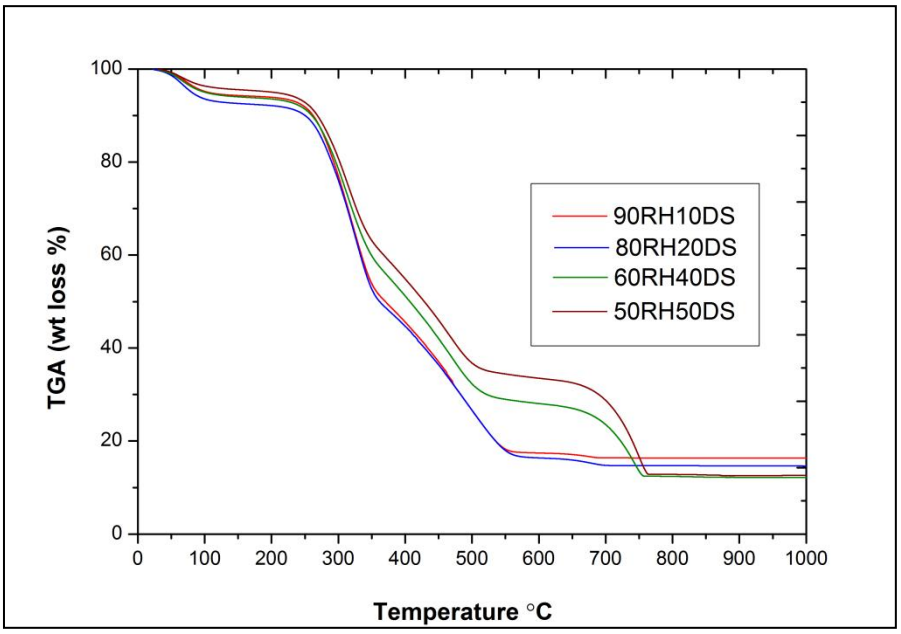

Figure-3.10 TG curves of blends of rice husk (RH) with deinking sludge (DS) in nitrogen atmosphere

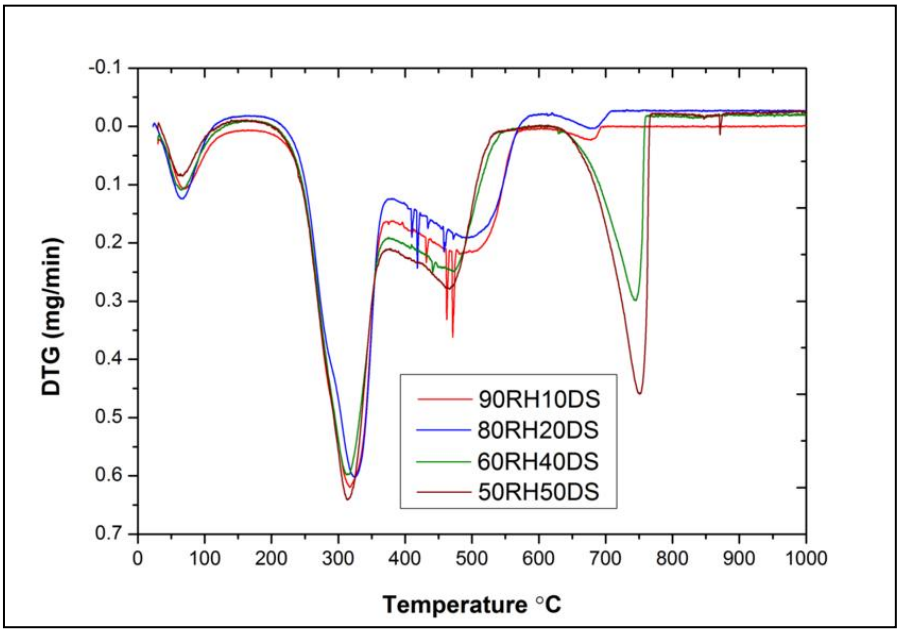

Figure-3.11 DTG curves of blends of rice husk (RH) with deinking sludge (DS) in nitrogen atmosphere

The pyrolysis of blends containing different proportions of rice husk and deinking sludge has been documented in Table-3.14. The TG-DTG curves have been presented in Figure-3.10 and Figure-3.11. From the DTG profile in nitrogen atmosphere of the blend containing 90 wt% rice husk and 10 wt% deinking sludge, it can be said that DTG shows a three region profile. Apart from moisture removal in first stage, second region is characterized by bulk de-volatilization of organic or lignocellulosic (hemicelluloses, cellulose and lignin) materials. In this stage, 76.71-wt% total degradation is observed. The blend containing 90 wt% rice husk behaves somewhat like rice husk. Therefore, the third region starting from 573 °C and ending at 703 °C shows a small peak that increases as the deinking sludge is increased. Third region depicts the decomposition of inorganic matter. Thus, as the amount of deinking sludge is increased the profile approaches similar to that of deinking sludge.

3.4.2.2.2. Combustion

In this section, the combustion behaviour of raw materials and their blends has been investigated.

3.4.2.2.2.1 Combustion of coal, deinking sludge (B) and rice husk

This section highlights the degradation behaviour of raw materials in air atmosphere. The degradation behaviour of coal, deinking sludge and rice husk is documented in Table-3.15.

Table-3.15 Thermal degradation of coal, deinking sludge and rice husk in the presence of air atmosphere

Sample Code	Zones	Temperature intervals (°C)			Total degradation (%)	Residue (%) at 1000 °C
		Initial temperature	Max. peak temperature	Final temperature		
Coal (C)	II	123	250	446	2.82	-
	III	446	731	745	75.66	19.06
Deinking sludge (DS)	II	151	300	600	21.12	-
	III	600	744	799	24.55	51.63
Rice husk (RH)	II	200	249	484	0.47	12.85

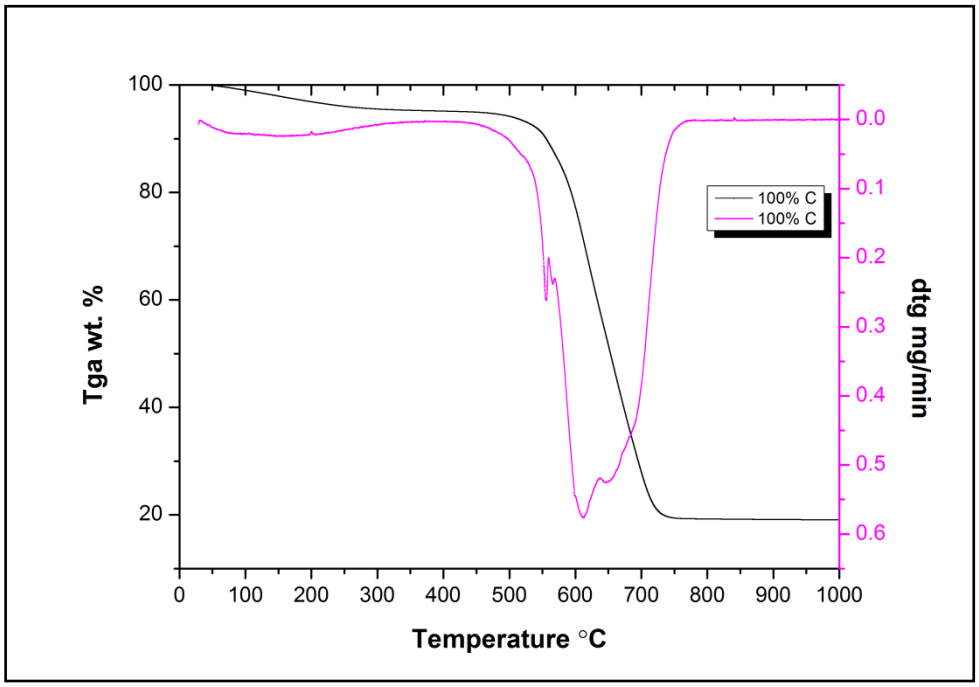

Figure-3.12 TG and DTG curves of coal in air atmosphere

The burning profile of coal at 10 °C/min heating rate has been shown in Figure-3.12. From the DTG curve, it can be observed that the coal shows a bimodal peak. The reason behind this is the presence of various compounds with different reactivity (Vamvuka et al. 2009). Moreover, the profile shows a little decomposition from 123 °C to 446 °C with maximum weight loss at 250 °C in second stage. This stage shows some de-volatilization. Third stage starts at 446 °C until 745 °C with maximum peak temperature at 731 °C. Here heavy de-volatilization along with decomposition of minerals takes place. Total degradation of 75.66 wt% is noted in this stage. After this about 19 wt% residue is left (Table-3.15). The combustion profile becomes flat shaped after 745 °C which is absent in the pyrolysis profile of the coal. Moreover, the position of the peak shifts towards lower temperature in combustion as compared to the pyrolysis. In addition, the combustion produces higher peak as compared to peak observed in pyrolysis. Hence, it can be interpreted that the oxygen enhances degradation process. Moreover, increase in the peak height indicates increase in the reactivity of the fuel. According to Yanfen and Xiaoqian (2010) oxygen reduces force of diffusion layer causing volatiles to release quickly.

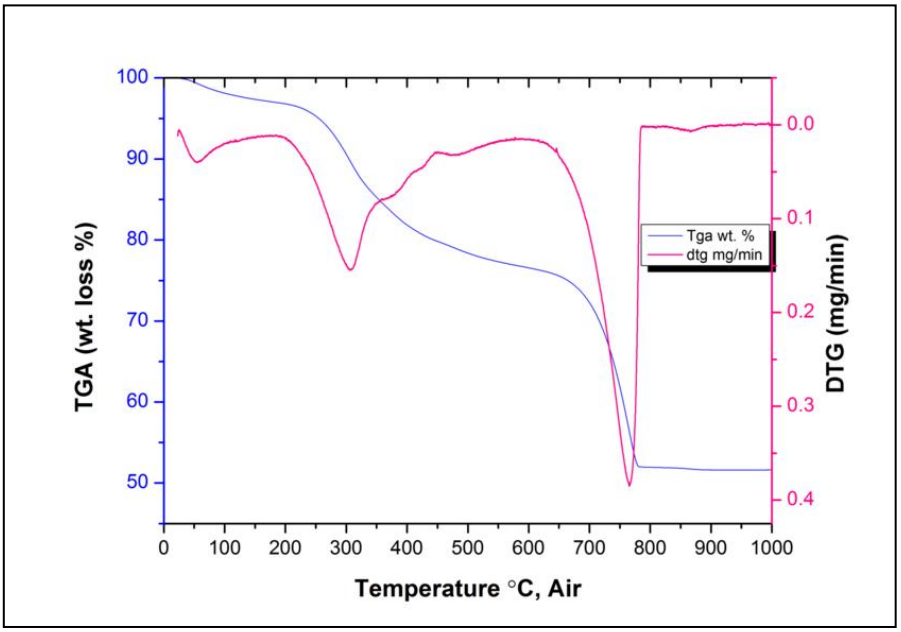

Figure-3.13 TG and DTG curves of deinking sludge in air atmosphere

Figure-3.13 shows the DTG curve in air atmosphere of the deinking sludge at 10 °C/min heating rate. This profile also shows mainly two regions apart from moisture removal stage. Second stage ranges from 151 °C to 600 °C with a maximum peak temperature at 300 °C. In this stage 21.12 wt% total degradation is observed. Third stage ranges from 600 °C to 799 °C

with maximum peak temperature at 744 °C. Total degradation in this stage is found as 24.55 wt%. Second stage shows the decomposition of volatiles like hemicelluloses and celluloses with hemicelluloses decomposing earlier than cellulose due to the difference in their structures. The lignin decomposes at slowest rate from ambient to 900 °C. Third stage shows heavy decomposition of volatiles along with decomposition of calcium carbonate and other minerals. On comparing the DTG profiles of pyrolysis and combustion of the deinking sludge it can be inferred that the position of the peaks is almost same but the combustion produces higher peak as comprared to the pyrolysis indicating increase in the reactivity of the deinking sludge in air atmosphere. Moreover, there is no significant change is observed in the shape of the DTG profiles of deinking sludge (B) in combustion as compared to nitrogen atmosphere.

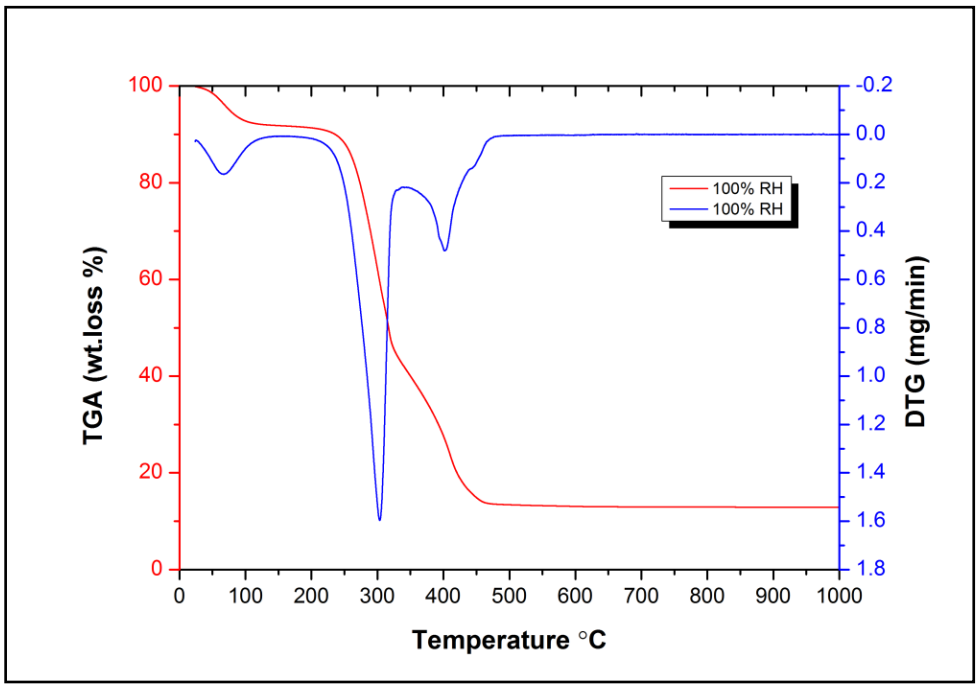

Figure-3.14 TG and DTG curves of rice husk in air atmosphere

Combustion profile of rice husk is shown in Figure-3.14 and degradation zones have been documented in Table-3.15. Heating rate of 10 °C/min is applied in air atmosphere. From the DTG profile of rice husk in Figure-3.14, it can be observed that like pyrolysis, here also two region profile is seen. First stage occurred with mass loss along with slight decomposition of organic compounds. After this second reaction zone is characterized by bulk de-volatilization accompanied by decomposition of inorganic matter. In this stage, hemicellulose decomposes first because it has amorphous branched chain structure that resulted in its bad thermal stability.

Cellulose has higher decomposition temperature range compared to hemicelluloses. The reason behind this phenomenon is that cellulose has long chain structure of D-glucose bonded by glycosidic linkages that results in its better thermal stability than hemicelluloses. However, lignin decomposes at slowest rate as compared to above lignocellulosic materials. Lignin decomposes at a wide range of temperature. It consists of polysaccharides with phenyl propane monomers bonded by ether bonds and carbon-carbon bonds and this is the reason that lignin has very good thermal stability and is hard to decompose (Xie and Ma 2013). After this stage, 12.85 % residue is left. Moreover, if the pyrolysis and combustion profiles of rice husk is compared then it can be observed that the peak height increases in the air atmosphere and the peak shifter towards lower temperature indicating an increased reactivity of rice husk in air atmosphere.

3.4.2.2.2.2 Co-combustion of coal and deinking sludge (B)

Table-3.16 Thermal degradation of blends of coal and deinking sludge under air atmosphere

Sample Code	Zones	Temperature intervals (°C)			Total degradation (%)	Residue (%) at 1000 °C
		Initial Temperature	Max. peak Temperature	Final Temperature		
90C10DS	II	148	315	449	3.69	-
	III	449	687	745	55.82	38.03
80C20DS	II	146	303	453	4.83	-
	III	453	698	745	51.67	40.87
50C50DS	II	150	252	449	8.76	-
	III	449	689	765	46.84	41.54

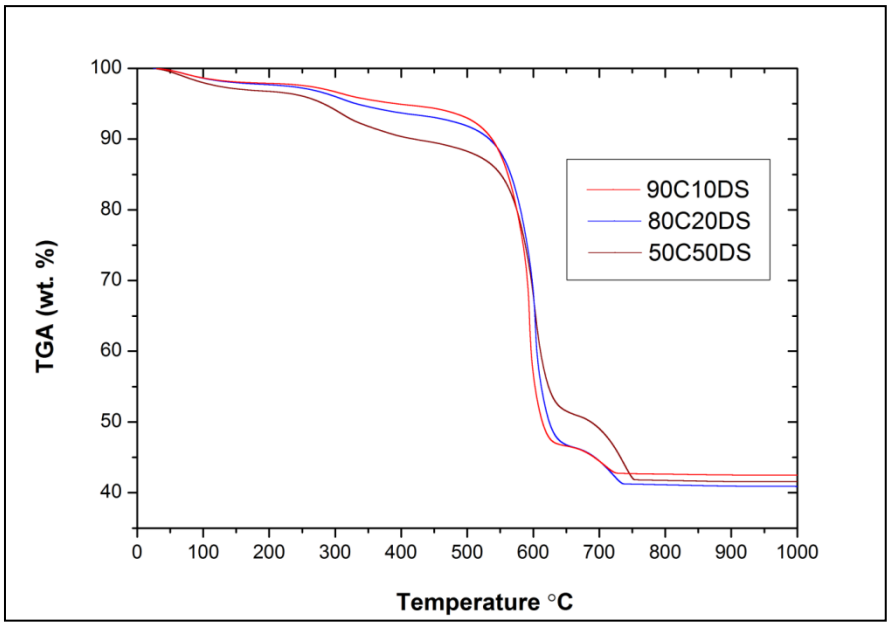

Figure-3.15 TG curves of blends of coal with deinking sludge in air atmosphere

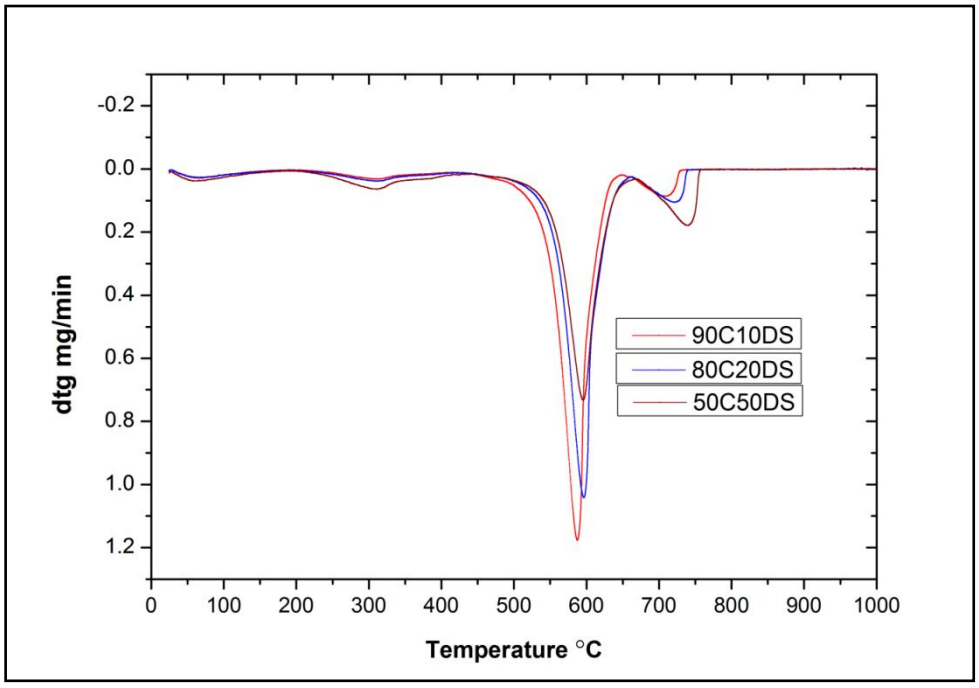

Figure-3.16 DTG curves of blends of coal with deinking sludge in air atmosphere

Figure-3.15 and Figure-3.16 show the TG and DTG curves of blends of coal and deinking sludge in air atmosphere at 10 °C/min heating rate. From the DTG curve of the blends it can be observed that as the proportion of deinking sludge is increased the profiles approaches to that of the deinking sludge. Moreover, the profiles of various sludge additions mainly show three-

stages. First stage is characterized with moisture removal. Second stage is observed from about 148 °C to around 449 °C for different proportions of deinking sludge. However for blends having 10-20 wt% deinking sludge proportions shows maximum peak temperature at around 315 °C whereas the maximum peak temperature for 50 wt% deinking sludge addition is observed at 252 °C indicating that shifting of peaks towards lower temperature with increase in sludge proportion. In addition, it can be seen that the peak height is increasing with increase in the deinking sludge proportion. According to Vamvuka et al. (2009), the peak height is directly proportional to the reactivity whereas the temperature at which the peak occurs is inversely proportional to the reactivity. Hence, it is evident from above observations that with increase in the sludge content increase in the reactivity occurs. Moreover in the second stage release of volatiles is noted which increases as the proportion of the deinking sludge is increased. However, bulk decomposition is observed in third stage where heavy de-volatilization accompanied with decomposition of mineral matter takes place. In this stage also, the peak corresponding to the 50 wt% deinking sludge shows largest area indicating increase in de-volatilization with increase in sludge content.

3.4.2.2.2.3 Co-combustion of rice husk and deinking sludge (B)

Table-3.17 Thermal degradation of blends of rice husk and deinking sludge under air atmosphere

Sample Code	Zones	Temperature intervals (°C)			Total degradation (%)	Residue (%) at 1000 °C
		Initial Temperature	Max. peak Temperature	Final Temperature		
90RH10DS	II	201	252	476	74.79	-
	III	476	601	694	1.73	17.26
80RH20DS	II	201	245	472	73.01	-
	III	472	598	696	2.65	15.75
60RH40DS	II	199	250	478	40.12	-
	III	478	700	756	12.47	42.13
50RH50DS	II	199	247	499	33.58	-
	III	499	701	755	19.19	43.32

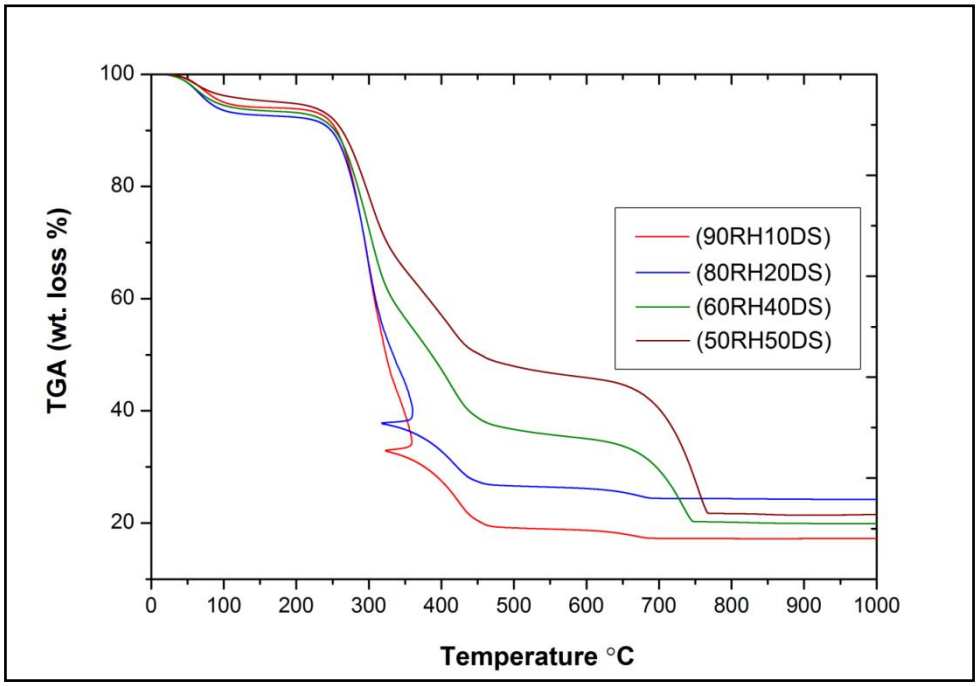

Figure-3.17 TG curves of blends of rice husk with deinking sludge in air atmosphere

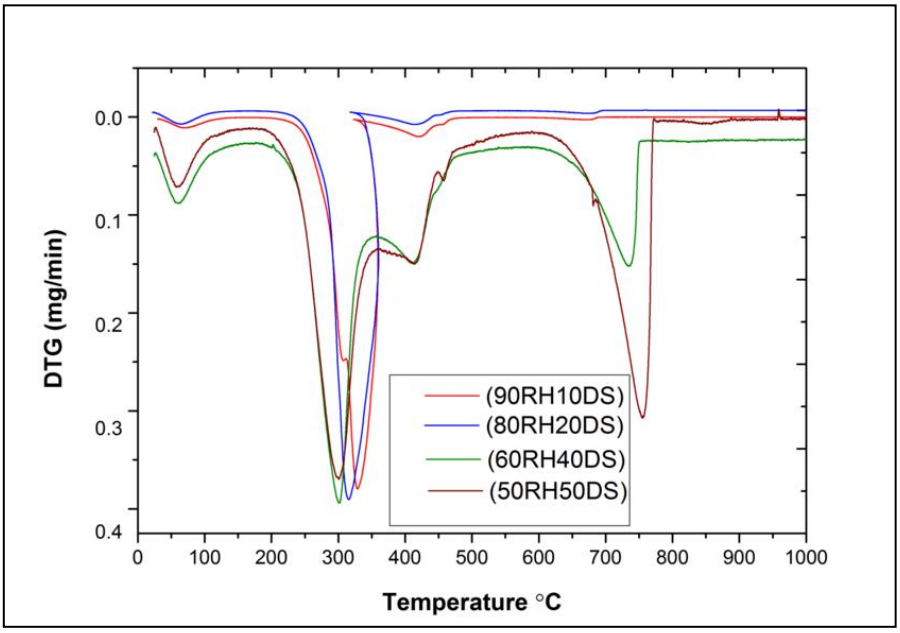

Figure-3.18 DTG curves of blends of rice husk with deinking sludge in air atmosphere

The combustion behaviour of various blends of rice husk and deinking sludge is presented by the TG-DTG curves shown in Figure-3.17 and Figure-3.18 and documented in Table-3.17. Like pyrolysis, the combustion profiles of the blends also lie between individual rice husk and deinking sludge profile. As the amount of deinking sludge is added to the blend, the profile reaches to that of the deinking sludge. Mainly three regions can be observed from the profile. First region depicts the mass loss. Second region depicts the heavy de-volatilization and third region presents the decomposition of inorganic compounds along with residue left. It can be seen that as the quantity of deinking sludge is increased the peak representing the de-volatilization becomes larger indicating increase in release of volatiles. With 90-80 wt% rice husk a small peak is observed after the major peak indicating almost whole process is completed in the second region. However, with 60-50 wt% deinking sludge, the peak shifts towards higher temperature and increases in size.

3.4.2.3. Kinetics

The kinetic model of thermal analyses of deinking sludge, coal and rice husk as well as their blends can be represented by the scheme described in section 3.2.7. Several researchers have modified the following rate expression

$$dx/dT = A/B \exp(-E/RT)(1-x) \quad (6)$$

Where $B = dT/dt$ (°C/min)

t=Time (min)

A=Pre-exponential factor ($mg^{1-n}\ min^{-1}$)

E=Activation energy (kJ/mol)

R=Gas constant

T=Temperature (°C)

x = fractional conversion of A at time t

Referring to the equation (6), several researchers (Coats and Redfern 1964; Horowitz and Metzger 1963; Piloyan et al. 1966; Reich and Stivala 1983) have presented models with modified rate expressions shown in Table-3.6. The data obtained from the TG-DTG analysis coupled with the reaction mechanism best describing the process are useful for calculating the kinetic parameters like activation energy and frequency factors for Arrhenius type rate expressions. The best suited model for the calculation of kinetic parameters is chosen by finding the regression coefficient (R^2).

Table-3.18 Determination of R^2 of coal, deinking sludge and their blends by different models under nitrogen atmosphere

Codes	Zones	Coats - Redfern model	Piloyan - Novikova model	Reich -Stivala model	Horowitz - Metzger model
		R^2	R^2	R^2	R^2
100C	II	0.99698	0.99169	0.95749	0.78188
	III	0.9805	0.97714	0.81544	0.95819
90C10DS	II	0.99624	0.8180	0.97183	0.98212
	III	0.96362	0.9266	0.83601	0.92288
80C20DS	II	0.99747	0.8358	0.96895	0.96776
	III	0.98176	0.96142	0.84931	0.9830
60C40DS	II	0.99882	0.86717	0.98863	0.92521
	III	0.96736	0.86929	0.81160	0.98657
50C50DS	II	0.99907	0.89258	0.98822	0.91876
	III	0.96406	0.91734	0.82385	0.9601
100DS	II	0.98099	0.80809	0.98404	0.90973
	III	0.9068	0.64728	0.77133	0.88376

Table-3.19 Determination of kinetic parameters of coal, deinking sludge and their blends by Coats and Redfern model under nitrogen atmosphere

Codes	Zones	n	E	A	R^2
100C	II	2.0	11.75	2.02×10^7	0.99698
	III	-	64.16	4.39×10^{10}	0.9805
90C10DS	II	1.25	14.03	6.65×10^6	0.99624
	III	-	46.53	2.25×10^9	0.96362
80C20DS	II	1.25	14.38	7.21×10^6	0.99747
	III	-	55.24	7.49×10^9	0.98176
60C40DS	II	1.25	15.65	1.08×10^7	0.99882
	III	-	39.23	7.09×10^8	0.96736
50C50DS	II	1.25	15.90	1.19×10^7	0.99907
	III	-	37.36	5.54×10^8	0.96406
100DS	II	0.25	21.69	3.68×10^8	0.98099
	III	-	36.63	2.85×10^5	0.9068

Table-3.20 Determination of R^2 of coal, deinking sludge and their blends by different models under air atmosphere

Codes	Zones	Coats - Redfern model	Piloyan - Novikova model	Reich -Stivala model	Horowitz - Metzger model
		R^2	R^2	R^2	R^2
100C	II	0.99993	0.98118	0.94029	0.80129
	III	0.98198	0.93077	0.77468	0.97696
90C10DS	II	0.98595	0.96804	0.81945	0.97143
	III	0.90732	0.84871	0.89201	0.89442
80C20DS	II	0.98945	0.6166	0.85584	0.97352
	III	0.94128	0.85937	0.88988	0.91367
50C50DS	II	0.98747	0.67145	0.90188	0.96817
	III	0.92152	0.84102	0.90638	0.9145
100DS	II	0.9888	0.76188	0.95493	0.86433
	III	0.92783	0.67677	0.7227	0.90711

Table-3.21 Determination of kinetic parameters of coal, deinking sludge and their blends by Coats and Redfern model under air atmosphere

Codes	Zones	n	E	A	R^2
100C	II	2.0	11.31	1.60×10^7	0.99993
	III	-	62.52	4.40×10^{10}	0.98198
90C10DS	II	0.5	12.84	1.35×10^7	0.98595
	III	-	145.78	1.59×10^{17}	0.90732
80C20DS	II	1.25	12.19	3.99×10^6	0.98945
	III	-	66.77	1.36×10^{11}	0.94128
50C50DS	II	1.25	12.93	5.52×10^6	0.98747
	III	-	56.48	2.19×10^{10}	0.92152
100DS	II	0.25	21.68	3.95×10^8	0.9888
	III	-	40.15	8.37×10^9	0.92783

Table-3.18 and Table-3.20 shows the values of R^2 obtained by different models. It is evident that among all models, the Coats and Redfern model presents best fit and thus seems best suited for the determination of kinetic parameters in both pyrolysis and combustion process. Hence, the activation energy E and pre-exponential function have been calculated by Coats and Redfern model.

Table-3.19 shows the kinetic parameters of different zones for coal, deinking sludge and their blends in N_2 atmosphere. From the Table-3.19, it is evident that the activation energy (E) for various deinking sludge replacement of coal is obtained between the individual coal as well as individual deinking sludge for all the zones. The E value for coal in second and third reaction zones are obtained as 11.75 kJ/mol and 64.16 kJ/mol whereas for the deinking sludge the E values in second and third reaction zones are 21.69 kJ/mol and 36.63 kJ/mol respectively. As the deinking sludge is increased in the blend, the activation energy (E) approaches towards the activation energy value obtained with individual deinking sludge. The results are in accordance with Yanfen and Xiaoqian (2010). However, some deviation in the data is observed that could be attributed to the heat transfer limitations. This observation is very useful for the co-pyrolysis of coal and deinking sludge. Moreover it can also be seen that the activation energy (E) is higher for deinking sludge in de-volatilization stage as compared to coal whereas in the III reaction zone the coal showed higher activation energy (E) compared to deinking sludge. Hence, it can be inferred that blending of deinking sludge with coal can enhance the main de-volatilization stage (Zone II) and thus can improve the ignition characteristics. Similar trend is also observed in the kinetic parameters for the coal, deinking sludge and their blends during combustion. However, it can be found in combustion that the value of activation energy (E) for the coal, deinking sludge and their blends are higher than their corresponding values of E in their respective zones in pyrolysis (Table-3.21).

Table-3.22 Determination of R^2 of rice husk and its blend with deinking sludge by different models under nitrogen atmosphere

Codes	Zones	Coats - Redfern model	Piloyan - Novikova model	Reich -Stivala model	Horowitz - Metzger model
		R^2	R^2	R^2	R^2
100RH	II	0.94015	0.78459	0.92645	0.90624
	III	0.99592	0.99958	0.96109	0.9588
90RH10DS	II	0.98246	0.78383	0.93273	0.90265
	III	0.9991	0.76843	0.88011	0.83101
80RH20DS	II	0.97234	0.80465	0.94293	0.88553
	III	0.99843	0.90501	0.94712	0.94893
60RH40DS	II	0.9944	0.82296	0.95929	0.88366
	III	0.89737	0.71747	0.65836	0.77268
50RH50DS	II	0.99544	0.85338	0.95815	0.88894
	III	0.81672	0.68343	0.58568	0.72694

Table-3.23 Determination of kinetic parameters of rice husk and its blend with deinking sludge by Coats and Redfern model under nitrogen atmosphere

Codes	Zones	n	E	A	R^2
100RH	II	1.25	32.45	1.39×10^9	0.94015
	III	-	30.30	1.56×10^9	0.99592
90RH10DS	II	1.25	30.48	7.65×10^8	0.98246
	III	-	77.35	1.68×10^{12}	0.9991
80RH20DS	II	0.5	32.84	3.27×10^9	0.97234
	III	-	81.31	1.29×10^{13}	0.99843
60RH40DS	II	1.25	24.47	1.61×10^8	0.9944
	III	-	41.00	2.46×10^9	0.89737
50RH50DS	II	1.25	23.98	1.35×10^8	0.99544
	III	-	36.61	1.12×10^9	0.81672

Table-3.24 Determination of R^2 of rice husk and its blend with deinking sludge by different models under air atmosphere

Codes	Zones	Coats - Redfern model	Piloyan - Novikova model	Reich -Stivala model	Horowitz - Metzger model
		R^2	R^2	R^2	R^2
100RH	II	0.98153	0.81915	0.92935	0.92861
90RH10DS	II	0.97116	0.75015	0.92364	0.8305
	III	0.99857	0.99967	0.77155	0.75198
80RH20DS	II	0.97176	0.71463	0.91377	0.81915
	III	0.99954	0.99975	0.75533	0.77885
60RH40DS	II	0.92589	0.8437	0.95785	0.90256
	III	0.98928	0.66523	0.60363	0.69903
50RH50DS	II	0.99472	0.8303	0.9648	0.88708
	III	0.99943	0.81431	0.6029	0.72081

Table-3.25 Determination of kinetic parameters of rice husk and its blend with deinking sludge by Coats and Redfern model under air atmosphere

Codes	Zones	n	E	A	R^2
100RH	II	2.0	58.45	5.95×10^{12}	0.98153
90RH10DS	II	1.5	23.47	3.02×10^{8}	0.97116
	III	-	20.99	1.21×10^{9}	0.99857
80RH20DS	II	0.25	32.02	6.25×10^{9}	0.97176
	III	-	32.02	1.58×10^{10}	0.99954
60RH40DS	II	2.0	25.58	1.56×10^{9}	0.92589
	III	-	22.25	2.12×10^{9}	0.98928
50RH50DS	II	1.25	22.61	1.01×10^{8}	0.99472
	III	-	16.46	2.66×10^{7}	0.99943

Table-3.22 and Table-3.24 shows the values of regression coefficient (R^2) obtained by applying different models. It can be found that the Coats and Redfern model seems most suitable for the determination of kinetic parameters as it produces R^2 closest to unity in most of the cases as compared to other models. Hence, the kinetic parameters of different zones of rice husk and its blends with deinking sludge in pyrolysis as well as combustion processes have been calculated using Coats and Redfern model.

Table-3.23 and Table-3.25 show the kinetic parameters namely activation energy (E) and pre-exponential factor (A) of rice husk and its blends with deinking sludge under nitrogen and air atmospheres respectively. From the results of Table-3.23, it can be observed that the activation energy (E) value decreases as the amount of deinking sludge is increased in the blend in II zone. However, some deviation in the data is observed that could be attributed to the heat transfer limitations. This zone corresponds to the main de-volatilizaiton zone. Furthermore, the regression coefficients of these values show high accuracy in the results. Similar accuracy is also observed for combustion. For zone III, the E value of blend initially increases up to 20% deinking sludge replacement but after that it decreases (Table-3.23). However, the blend has higher E value than rice husk in III zone irrespective of quantity. This indicates that deinking sludge requires higher burnout temperature as compared to rice husk. However, the activation energy decreases with increase in the amount of deinking sludge in the blends except at 10 % deinking sludge replacement in case of combustion as evident from Table-3.25. Concisely, it can be said that the interaction of deinking sludge and rice husk improves the thermal decomposition of their blends at higher temperature.

3.5 Conclusions

In this chapter, effect of heating rates on deinking sludge (Sample A) in pyrolysis and combustion processes has been conducted in first part whereas the possibility of co-processing of deinking sludge (Sample B) with coal and rice husk is investigated under pyrolysis and combustion. The following conclusions can be drawn from the study:

1. Increase in the heating rate causes delay in thermal decomposition process of deinking sludge as the pyrolysis or combustion profile starts moving towards higher temperature.
2. Deinking sludge has higher reactivity than coal. Thus, use of deinking sludge with coal in Pyrolysis or combustion system may improve the performance.

3. Combustion enhances the thermal degradation process and increases the reactivity of coal, deinking sludge and their blends.
4. Deinking sludge enhances the de-volatilization stage and thus can improve the ignition characteristics of coal
5. Blending of coal upto 20% with deinking sludge gives the similar combustion profile as of coal. Thus deinking sludge can be used with coal in existing combustion system without any major modification except ash handling system.
6. The reactivity of blends of rice husk and deinking sludge decreases with increase in the amount of deinking sludge in pyrolysis.
7. Deinking sludge requires higher burnout temperature as compared to rice husk in pyrolysis.
8. The value of activation energy (E) of rice husk decreases after deinking sludge is blended.
9. Blending of rice husk upto 20% with deinking sludge give almost similar pyrolysis profile as of individual rice husk.
10. The results obtained after the thermal processing and co-processing of deinking sludge, coal as well as rice husk with their respective blends can be used for the effective design of thermal processing systems.
11. Hence, deinking sludge can be used as an alternative fuel for power production and thus can address the problem of its disposal.

CHAPTER 4

UTILIZATION OF DEINKING SLUDGE IN FIRED CLAY BRICKS

4.1. Introduction

There is an increasing demand for sustainable and energy efficient building products. Moreover, solid waste like deinking sludge needs proper management. Hence, deinking sludge is used in fired burnt clay bricks that will increase the insulation capacity of the brick and contribute in energy conservation. Moreover, it will also address the problem of disposal of deinking sludge. Initially characterization of deinking sludge is carried out using various techniques and then it is mixed with clay and water in different proportions. All the brick specimens made from different proportions are fired at 900 °C, 950 °C and 1000 °C. After this, SEM and XRD of fired brick specimens at optimum temperature have been carried out. Then various properties have been evaluated and optimum temperature along with a suitable deinking sludge replacement proportion is determined.

4.2. Literature review

4.2.1. Clay

Clay is a fine-grained soil minerals with traces of metal oxides and organic matters according to AIPEA (Association International Pour Etude des Argiles) and CMS (Clay Mineral Society) nomenclature committees. It is plastic at appropriate amount of water whereas it becomes hard, brittle and non-plastic upon drying and firing. Apart from phyllosilicates it might contain materials that induce plasticity and hardens during firing or drying (Guggenheim and Martin 1995). The type of application of clay mainly depends on its chemical and physical properties. Along with silica, alumina and water it also contains iron, alkali metals and alkaline earth metals. Most clay minerals are composed of two structural units in their atomic lattices. (Nayak and Singh 2007). Clay is natural resource that is formed over a long period by gradual chemical weathering of rocks. It is a traditional material for the production of fired clay bricks (Kanthe and Chavan 2012).

4.2.2. Porous fired clay bricks

Due to the environmental regulations, there is a growing demand for the production of porous fired clay bricks because it reduces the thermal conductivity and thus lowers the heat loss through the walls. Porous fired clay bricks can be manufactured by incorporating pore-forming agents into the bricks. There are mainly two types of pore forming agents- organic pore formers and inorganic pore formers (Demir et al. 2005).

4.2.2.1. Organic pore formers

Organic pore forming agents are abundant in quantity. Because of their abundance, they are not expensive. They are easily and locally available. Hence, they are widely used in the brick industry. They are cheaper than inorganic pore formers. In addition, they give oversupply of heat in firing furnace. They include recycled paper processing residues, kraft pulp residues, cigarette butts from tobacco industry, bagasse, wheat straw, corn cob, several seeds, rice husk, rice husk ash, resinous wood fibres from wood industry, sawdust, coal and coke, tea and coffee industry wastes and various industrial organic wastes (Bories et al. 2014, Demir et al. 2005).

4.2.2.2. Inorganic pore formers

Inorganic pore formers are also referred as mineral type pore formers. These types of pore forming agents break down during firing stage and generate carbon dioxide leaving behind the pores. Carbon dioxide mainly produced as a result of decomposition of calcium carbonate. The properties of final product as brick highly depends on the type of pore former added as well as its quantity. Inorganic pore formers are costlier than organic pore formers. Also inorganic pore formers may increase the amount of water required to maintain the plasticity. They include perlite, vermiculite, pumice, diatomite, phosphogypsum, waste glass, marble residues, granite powder and many more. However organic pore formers are widely used in brick industries (Bories et al. 2014, Demir et al. 2005).

4.2.3. Deinking sludge

The sludge produced from the recycle paper industries is called deinking sludge. This generally posses ink particles, sizing agents, coatings, fillers, fines, fibres etc (Mendez et al. 2009). It contains both organic and inorganic materials (Garcia et al. 2008). However according to Catalogue of European Residues (CER) cellulose and paper residues are non-hazardous (Garcia et al. 2008). It is generally land filled but because of decreasing land filing sites and strict

environmental regulations, its disposal is becoming a problem (Vamvuka et al. 2009). Hence it should be used in applications like construction of building materials.

4.2.4. Characterization techniques

The deinking sludge and the clay were analysed prior to their use. For the characterisation of raw materials, techniques namely XRF, SEM, TGA and XRD were used.

4.2.4.1. Chemical analysis

The chemical composition of clay and deinking sludge is determined by XRF technique. Nayak and Singh (2007) have found silica, calcium and alumina in major quantities in clay. However, Demir et al. (2008) have also found iron in significant amount. Iron oxide is responsible for imparting redness to the fired clay bricks (Johari et al. 2010). Johari et al. (2010) also found fluxing components (K_2O, Na_2O and CaO) less than 3 wt. % in their clay. Recycle paper mill waste contains heavy metals like copper (Cu), manganese (Mn), strontium (Sr) and Zirconium (Zr) in traces (below 0.1%). With such a low concentration the possibility of leaching of heavy metals can be ruled out (Arshad et al. 2014, Raut et al. 2013 and Rajput et al. 2012). It does not possess a major threat and hence is considered as non- hazardous waste. Therefore Catalogue of European Residues (CER) classified wastes from cellulose as well as paper manufacturing as non dangerous (Garcia et al. 2008). Moreover Sutcu et al. (2014) found the loss of ignition of clay as well as paper sludge after heating at 1000 °C as 7.5% and 53.8% respectively.

4.2.4.2. SEM analysis

Scanning electron microscope (SEM) applies a focused beam of electrons to create signals on the surface of solid specimen. These signals give detailed information about the specimen including external morphology and chemical composition. Recycle paper mill residue is fibrous in nature (Raut et al. 2013). It contains mainly cellulose fibres and $CaCO_3$ (Sutcu and Akkurt 2009). Moreover some inorganic materials like SiO_2, MgO as well as Al_2O_3 are also found on the fibre surfaces besides other inorganic elements in small amount. It has porous structure with irregular pores. This porous and fibrous nature holds the water and prevents it to move towards the surface (Rajput et al. 2012, Raut et al. 2012).

4.2.4.3. XRD analysis

X-ray diffraction (XRD) is a non-destructive technique which provides information of the chemical composition as well as crystallographic structure of specimen. It is a technique mainly used for phase identification of a crystalline substance and gives the information at unit cell dimensions. The principle of XRD is constructive interference of crystalline specimen and monochromatic X-rays. These X-rays are produced by cathode ray tube. The incident rays on the specimen create constructive interference that satisfies the Bragg's law. Bragg's law relates the wavelength of radiation with diffraction angle as well as lattice spacing in the specimen. These X-rays are processed and counted after being detected. All diffraction directions of the lattice are attained by scanning the specimen through a range of 2θ angles. Minerals are identified by converting diffraction peaks to d-spacing since each mineral has a set of unique d-spacing.

Johari et al. (2010) has found mainly two minerals namely kaolinite and quartz in the clay. However, on the other hand, Raut et al. (2013) observed amorphous nature of the recycle paper mill residue.

4.2.4.4. Thermogravimetric analysis (TGA)

TGA is a technique in which the mass loss of a substance is monitored as a function of time or temperature. The substance is subjected to controlled temperature that increases according to the heating rate required. In other words, it measures the weight of the substance during heating or cooling. The results are generally presented in the form of curve depicting the mass loss against temperature.

Raut et al. (2013) carried out the TG analysis of recycle paper mill residue. They found that superficial water was removed between temperatures 30 °C and 280 °C. Then the second loss occurred beyond 280 °C when the material was thermally sintered. The third loss occurred beyond 300 °C depicting the combustion of solid organic material. Rajput et al. (2012) obtained similar results. However according to Sutcu and Akkurt (2009) mass loss observed beyond 700 °C may be due to decomposition of carbonates.

4.2.5. Brick analysis and properties

Fired clay bricks exhibits certain properties which decides their strength and durability. Hence measurement of these properties is imperative.

4.2.5.1. Physical properties

The literatures on physical properties of fired clay bricks are given in subsequent paragraphs:

4.2.5.1.1. Physical appearance

The colour of the fired clay brick after sintering process turns dark red. The reason behind this appreance is the presence of Fe_2O_3 content in the clay (Johari et al. 2010). But the colour fades and the brick gets lighter shades with increase in the amount of waste material like paper processing residues. Presence of calcium is the reason behind the colour of the brick getting lighter (Sutcu et al. 2014, Sutcu and Akkurt 2009).

4.2.5.1.2. Mass loss

According to Bories et al. (2014), mass loss in the brick specimen is determined by calculating the difference between the mass after firing stage and drying stage expressed in terms of percentage according to following formula:

$$\text{Mass loss (\%)} = [(W_d - W_f)/ (W_d)] * 100$$

Where W_d = weight of the oven dried sample (g)

W_f = weight of the fired sample (g)

Mass loss % increases with increase in the proportion of the pore-forming agents. These pore formers creates voids during firing process by dehydroxylation and carbonate decomposition. The creation of voids leads to the reduction of mass. However mass loss % must not be more than 15% in order to have good serviceability (Bories et al. 2014).

4.2.5.2. Properties of burnt clay brick specimens

The literatures on mechanical properties of fired clay bricks are given in subsequent paragraphs:

4.2.5.2.1. Compressive strength

Compressive strength is an important parameter that determines the durability and serviceability of the brick. Increase in residues like paper processing residues facilitates the formation of porosity that indeed reduces the density. Reduction in density lowers the compressive strength (Bories et al. 2014, Sutcu and Akkurt 2009). Hence, compressive strength is inversely proportional to the fibrous materials (Raut et al. 2013). However compressive

strength increases with increase in firing temperature. Increase in compressive strength occurs because of the increment in density as well as reduction in porosity. However firing time has no significant effect on the compressive strength (Karaman et al. 2006). According to Turkish and corresponding European standards (TS EN 771-1) the minimum compressive required for bricks is 7 MPa (Sutcu and Akkurt 2009). Moreover according to British standard BS 6073 Part 2: 2008, a brick must possess a minimum compressive strength of 7 N/mm^2 or 7 MPa (Ismail et al. 2010).

4.2.5.2.2. Water absorption

The capacity of the water to be absorbed and stored in the structure of the brick is called water absorption. Water absorption increases with increase in the pore forming agent like paper waste (Demir et al. 2005, Sutcu and Akkurt 2009, Sutcu et al. 2014). Water absorbing capability of cellulosic wastes like deinking sludge can be attributed to cellulose fibres (Ismail et al. 2010). Water absorption is directly related to the amount and size of porosity generated into the brick (Phonphuak 2013). Moreover it also depends on clay, mode of production and firing temperature (Karaman et al. 2006). Water absorption improves the thermal insulation of the brick. However excessive water absorption can affect the durability of the brick (Bories et al. 2014).

4.2.5.2.3. Efflorescence

Efflorescence is the deposit of salts on the surface of the brick. The magnitude of efflorescence is reported as nil, slight, moderate, heavy or serious according to codal standard IS 3495 (Part 3):1992. Nil efflorescence corresponds to the bricks having no observable deposit whereas slight efflorescence is a thin deposit of salts less than 10% of the exposed area. When this percent increases from 10% then the efflorescence lies in the category of moderate whereas when the efflorescence is observed on more than 50% of the area then it comes under the heavy efflorescence. However when heavy deposit of salts occurs with the powdering of the surfaces then the efflorescence is called serious efflorescence.

4.2.5.2.4. Density

Density is defined as the mass per unit volume of a specimen. The density of the brick specimen decreases with increase in the content of residues (Demir et al. 2005, Sutcu and Akkurt 2009). The possible cause of decrease in the density is the light weight of the additives.

This can be advantageous in high-rise construction by saving significant cost through reduced weight (Ismail et al. 2010).

4.2.5.2.5. Apparent porosity

The apparent porosity is the ratio of the volume of the open pores in the specimen to its exterior volume expressed in percentage (ASTM C20-00 2015). It influences strength, durability as well as the general qualities of the brick specimen. The size and amount of pores depend on the type of pore former, additives or impurities, firing temperature, clay and amount of water (Fernandes et al. 2009). Porosity can be generated using pore forming agents. With increase in the proportion of pore formers in the clay- sludge mixture the porosity increases (Demir et al. 2005). However porosity decreases with increment in firing temperature. This occurs due to the diffusion of particles into the structure (Johari et al. 2010). Moreover porosity improves the water absorption and thermal insulation capability of the brick specimen (Sutcu and Akkurt 2009).

4.2.5.2.6. Firing shrinkage

The firing shrinkage in the structure or material is observed when the particles of the material are fused with one another and thus shrinkage occurs. Bories et al. (2014) determined the firing shrinkage by measuring the length of specimen before and after firing and expressing the reduction in terms of percentage. They prescribed the following formula

Firing shrinkage (%) = [1- (Length of fired specimen/ length of oven dry specimen)] x 100

The increment in shrinkage increases the drying stress that makes the brick more susceptible to cracking (Demir et al. 2008). Brick must have shrinkage less than 8% for good performance. This is required as an excessive shrinkage can create tension and breakage of the product (Bories et al. 2014).

4.2.5.2.7. Thermal conductivity

Thermal conductivity is the ability of a material to conduct heat. A material with lower thermal conductivity passes heat slowly than the material having higher thermal conductivity. Hence, lower the thermal conductivity lower will be the heat loss. Moreover because of environmental regulations there is an increasing need for higher energy efficient buildings (Bories et al. 2014). This can be achieved by increasing the insulation capacity of the building. The insulation

capacity of the building can be increased by lowering the thermal conductivity of the brick. The thermal conductivity can be reduced by incorporating pore-forming materials. During firing stage the organic content of pore formers burns off leaving behind the micrometer scale pores or air pockets that reduces thermal conductivity of the brick (Sutcu et al. 2014, Phonkphuak et al. 2013). The reduction in thermal conductivity increases the energy saving potential of the building. Hence, thermal conductivity is closely related to the porosity (Sutcu and Akkurt 2009). Thermal conductivity decreases with decrease in density and increase in porosity (Phonkphuak et al. 2013).

4.3. Materials and methods

In this section the account of various materials used and the experimental procedure of various characterization techniques as well as the measurement of different properties has been presented.

4.3.1. Materials

4.3.1.1. Deinking sludge

Deinking sludge used as a pore former was obtained from one of the recycle paper industry in Punjab, India. This sludge was received in grey colour. Raw deinking sludge is shown in Figure-4.1.

Figure-4.1 Raw deinking sludge

4.3.1.2. Clay

Clay was obtained from a local area in Roorkee, Uttrakhand (India). Figure-4.2 shows photograph of the clay procured.

Figure-4.2 Raw clay

4.3.1.3. Water

Portable water was used throughout the experimental procedure.

4.3.2. Characterization of raw materials and burnt clay brick specimens

4.3.2.1. Particle size analysis

Particle size analysis was carried out by using Horiba's laser scattering diffraction particle size distribution analyzer Partica LA-950. This instrument is available at CSIR-Central Buliding Research Institute, Roorkee, India.

4.3.2.2. X-ray fluorescence (XRF) analysis

The chemical composition of Clay and deinking sludge was determined by using X-ray fluorescence (XRF) (Model no: Bruker S4 Pioneer spectrometer) and presented in Table-4.2 and Table-4.3 respectively.

4.3.2.3. X-ray diffractometer (XRD) analysis

XRD analysis of deinking sludge, clay and fired clay brick specimens were performed. XRD analysis was performed using Bruker AXS D8 Advance diffractrometer (Germany) with scanning rate of 1 °C/min. Nickel filtered CuKα radiation was used as target with 1.54060 Å wavelength. It was operated at 40 kV and 30 mA, in the angular range (2θ) of 5° to 70°. Finely powdered samples were placed in the cavity of the holder made of poly methyl methacrylate. DIFFRAC Plus XRD Commander software was used to obtain wide-angle x-ray scattering (WAXS) patterns of the samples and analysis was done on DIFFRAC Plus (Version 8.0) software.

4.3.2.4. Scanning electron microscopy (SEM) analysis

For visualizing the surface morphology of raw materials and fired clay brick specimen, SEM images were captured. Scanning Electron Microscopy image analyzer (Model no.: QUANTA 200F FEI) was used for this purpose. Samples were coated with gold by sputter coater for a clear visibility of the surface morphology. SEM images were taken with an accelerated voltage of 15 kV.

4.3.2.5. Thermogravimetric analysis (TGA)

Thermogravimetric Analyzer SII Seiko Instrument EXSTAR (Model : TG/ DTA 6300, Tokyo, Japan) with balance sensitivity of 0.1 µg and balance accuracy better than 0.02 % available at the Institute Instrumentation Centre (IIC) of Indian Institute of Technology Roorkee, India was used for performing the Thermogravimetric analysis (TGA). The present study was carried out under nitrogen atmosphere with the application of 10 °C/min heating rate. The setup was heated from ambient to 1000 $^{\circ}$C. The purge gas flow rate of 200 mL/min was taken throughout the experiment. For plotting of TG-DTG curves, OriginPro (8.6) software was used.

4.3.3. Methods

4.3.3.1. Preparation of brick specimens

Deinking sludge and clay were initially dried in oven for 2 h at 45 °C. The samples were powdered by mortar and pestle and sieved through 600 micron sieve size. Clay was taken in which water was added for preparing control brick specimens (0% deinking sludge content). Hand-mixing was done for 30 min with calculated amount of water. No lump formation was observed in the mixture. Mould made of brass was coated with lubricating oil to prevent any possible leakage. After this, mixture was poured into the mould of size 75x50x33 mm^3. Then again clay was taken and 5% by wt of deinking sludge was sprinkled on it and hand-mixing was done. Calculated amount of water was added to the mixture and poured into the mould after handmixing. Similar procedure was followed for 10%, 15%, 20%, 25% and 30% by wt of deinking sludge mixed with clay. The brick specimens were kept for 24 h at room temperature followed by 45 °C and then 100 °C for 2 h in an oven. Dried specimens were fired in a laboratory-type electrical furnace until 900 °C at the rate of 2 °C/min until 200 °C, 4 °C/min until 400 °C and 5 °C/min until 900 °C. The furnace had maximum firing temperature capacity of 1200 °C. The above procedure was again followed for 950 °C and 1000 °C firing

temperatures. In each set of experiment, three specimens were casted. The above experimental procedure is depicted in Figure-4.3 and the mix proportion is mentioned in Table-4.1.

Table-4.1 Mass of raw materials and amount of water as required per brick specimen for different proportions of clay-deinking sludge mixtures

S.No	Ratio of Clay : deinking sludge mixtures	Clay	Sludge	Total mass of raw material	Water added
	(wt%)	(g)	(g)	(g)	(mL)
1	100 : 0	1500	0	1500	330
2	95: 5	1425	75	1500	358.5
3	90 : 10	1350	150	1500	387
4	85 : 15	1275	225	1500	415.5
5	80 : 20	1200	300	1500	444
6	75 : 25	1125	375	1500	472.5
7	70 : 30	1050	450	1500	501

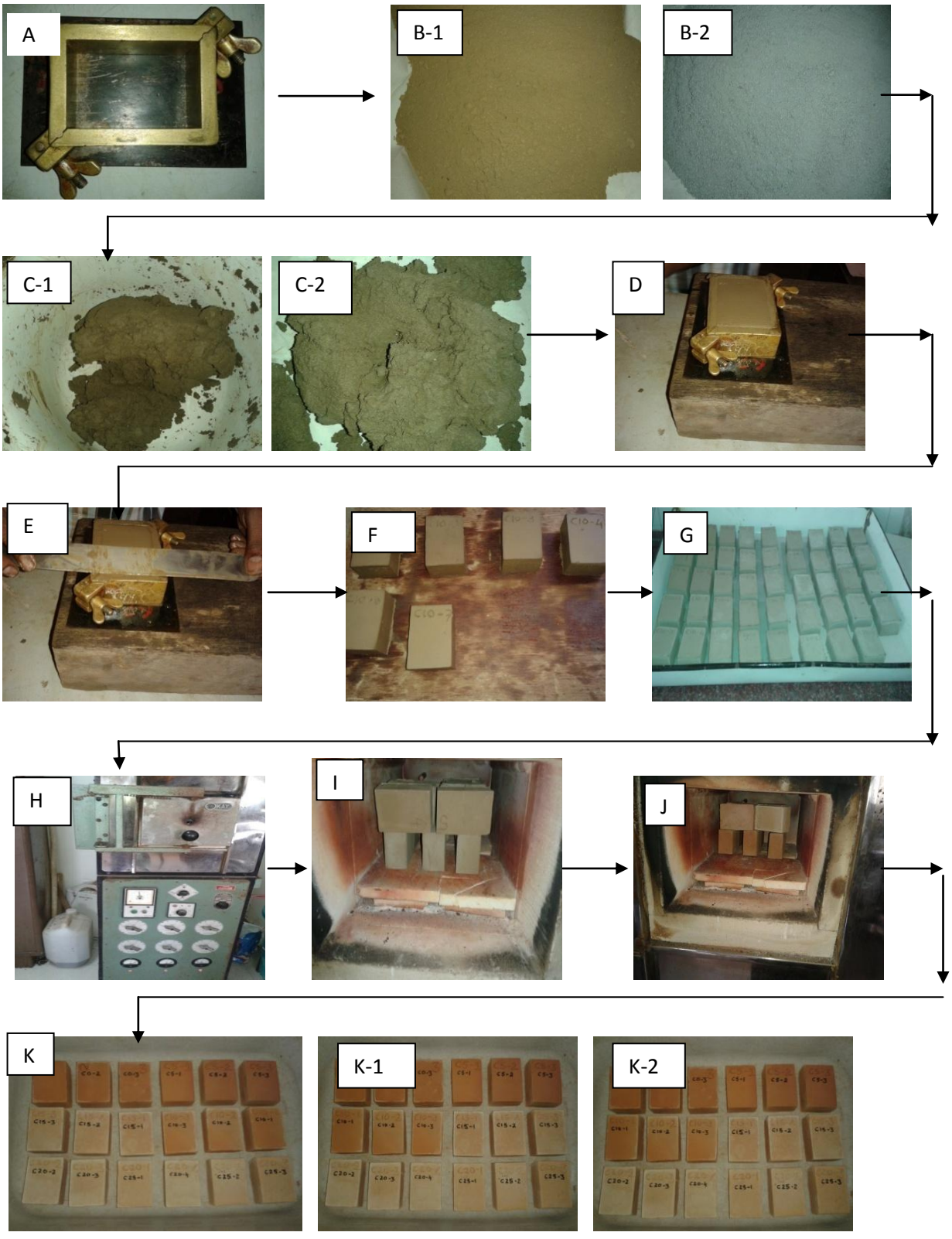

Figure-4.3 Experimental sequences for making brick specimens made by clay and deinking sludge (Annexure-2).

4.3.3.2. Test methods

Various test methods of burnt clay brick specimens have been described in subsequent paragraphs

4.3.3.2.1. Appearance

Visual appearance was noted before and after firing of the brick specimens.

4.3.3.2.2. Compressive strength, water absorption and efflorescence

Compressive strength, water absorption and efflorescence of fired burnt clay brick specimens were determined using IS 3495 (Part 1-4):1992. The compressive strength of brick specimens was determined using Universal Testing machine (Model: UH-1000kN, SHIMADZU corporation, Kyoto, Japan) having maximum capacity of 1000 kN. Three samples of each composition were subjected to a compressive strength test and the average strength was recorded.

4.3.3.2.3. Apparent porosity

Apparent porosity was determined by ASTM C20-00 (2015). In this test water is boiled for 2 h. Then specimen was immersed in water for 12 h. Then weight of the specimen was measured. Dry weight (D_{dry}) of the specimen, suspended weight (W_{sus}) of specimen while suspended in water and saturated weight (W_{sat}) of each specimen after being saturated with water were determined. Then apparent porosity was determined by following formula:

$$P\% = [(W_{sat}-D_{dry})/W_{sat}-W_{sus}] \times 100$$

4.3.3.2.4. Firing shrinkage

The firing shrinkage of the fired clay brick specimens was determined by following formula:

Linear shrinkage (%) = $[(L_{od}– L_f)/ (L_{od})] \times 100$

Where L_{od} = Length of oven dried specimen

L_f = Length of fired specimen

The mould used to find the firing shrinkage conforms to the IS 12979: 1990 and is presented in Figure-4.4.

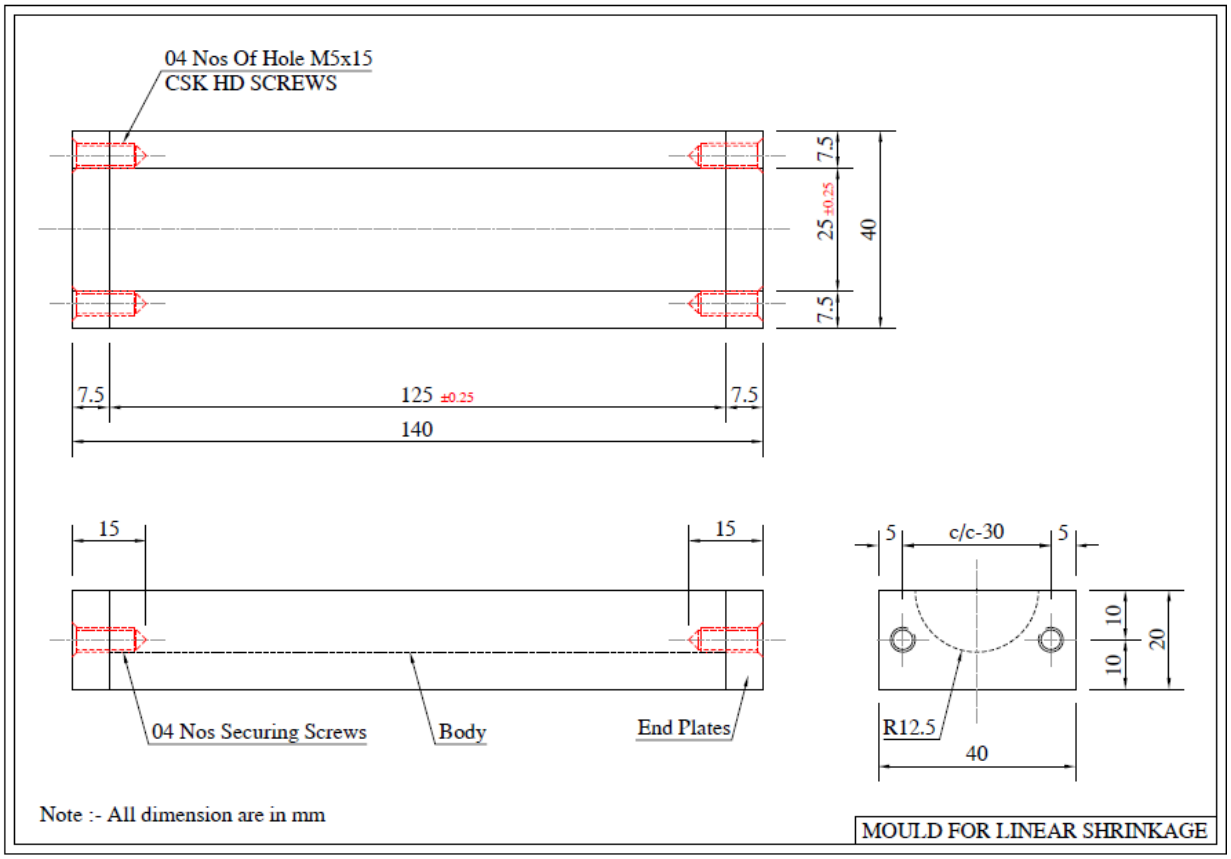

Figure-4.4 Mould for the determination of firing shrinkage

4.3.3.2.5. Thermal conductivity

The thermal conductivity of specimens was measured by Thermal Properties Analyzer (Model : KD2 Pro, Decagon Devices Inc., USA). It was measured at ambient temperature. It uses transient line heat source method to measure the thermal conductivity. It conforms to ASTM 5334 and IEEE 442 standards. It uses different types of sensors for the measurement of different properties. Thermal conductivity of solids is measured by TR-1 sensor. It is 10 cm long and 2.4 mm in diameter. It is single needle sensor primarily designed for porous materials, soil or other granular materials. Thermal conductivity was measured by inserting the probe (TR-1 sensor) into the fired burnt clay brick specimens by drilling a hole into the specimens. The measured value was immediately shown on the display of the instrument once measurement was finished. The obtained value was the thermal conductivity of the brick specimens.

4.4. Results and discussion

4.4.1. Chemical analysis

The chemical analysis of clay and deinking sludge has been found by XRF studies and presented in Table-4.2 and Table-4.3 respectively. It is evident from the results that the main constituents of clay are silicon dioxide (SiO_2), Aluminium Oxide (Al_2O_3) and Ferric Oxide (Fe_2O_3). The red colour of the fired clay brick is imparted because of the presence of the Ferric Oxide (Fe_2O_3). It is also observed that the chemical composition of deinking sludge mainly contains calcium oxide (CaO) and silicon dioxide (SiO_2). Aluminium oxide (Al_2O_3) is also found in the deinking sludge in significant amount but lesser then the amount found in clay. Loss of ignition of clay and deinking sludge is characterized by TGA (Thermo-gravimetric analysis). The loss of ignition value of clay and deinking sludge after heating upto 900 °C are found as 7.62% and 57.62% respectively as shown in Figure-4.5 and Figure-4.6. This indicates that clay contains lesser carbonaceous matter whereas deinking sludge contains higher organic matter.

Table-4.2 Chemical composition of clay

Parameters	Al_2O_3	SiO_2	CaO	MgO	K_2O	Fe_2O_3	TiO_2	SO_3	P_2O_5	ZrO_2	LOI
Clay	15.34	51.62	2.10	3.19	6.19	16.71	1.82	0.33	1.92	0.16	7.62

Table-4.3 Chemical composition of deinking sludge

Parameters	Al_2O_3	SiO_2	CaO	MgO	K_2O	Fe_2O_3	TiO_2	SO_3	P_2O_5	ZrO_2	LOI
Deinking sludge	10.40	25.44	51.42	6.69	0.21	1.76	1.10	1.62	0.18	0.03	57.62

4.4.2. TG analysis of raw materials

The thermogravimetric analysis (TGA) of clay and deinking sludge is presented as follows

4.4.2.1. TG analysis of raw clay

The thermal behaviour of the clay has been studied by thermogravimetric analysis and is presented in Figure-4.5. Heating rate of 10 °C/min is applied under nitrogen atmosphere with flow rate of 200 ml/min and sample is heated gradually from ambient to 1000 °C. From the curve, it can be observed that the first stage which is showing the removal of water in the pores, started at 27 °C and ended at 200 °C. The second stage showed the removal of chemically combined water along with burning of organic matter of the clay. This reaction is called dehydroxylation where part of clay (the hydroxyl groups) is destroyed. The second stage started at 200 °C and ended at 500 °C with 3.17% mass loss. The third stage started at 500 °C and ended a 1000 °C with 1.99% mass loss. This stage represents the decomposition of carbonates along with the formation of oxides as well as carbon dioxide.

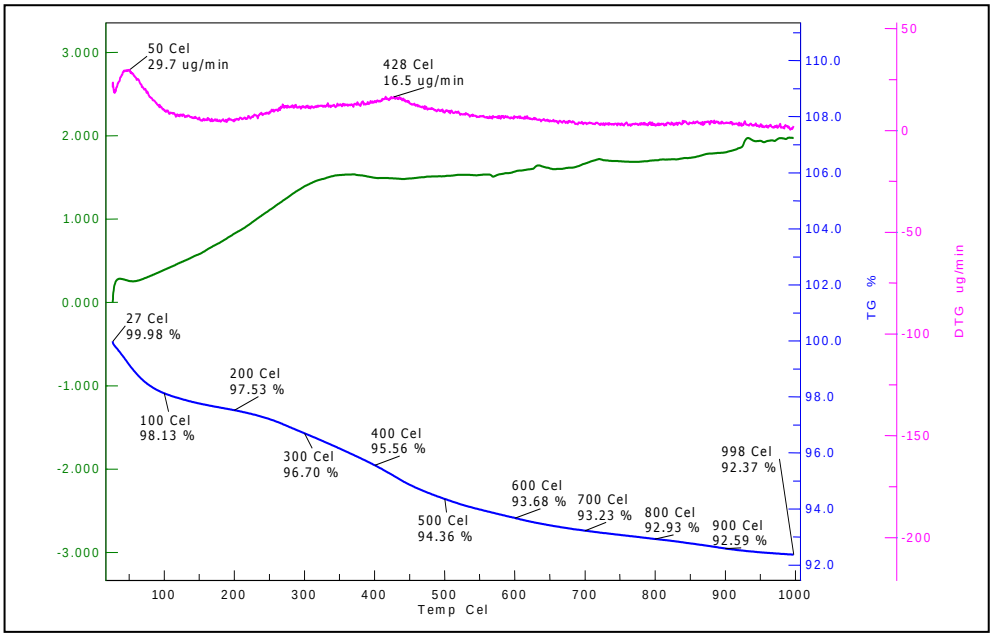

Figure-4.5 TGA profile of raw clay

4.4.2.2. TG analysis of raw deinking sludge

The thermal behaviour of deinking sludge has been studied by TGA and is shown in Figure-4.6. Heating rate of 10 °C/min and the air flow rate of 200 ml/min under nitrogen atmosphere is applied in this study. Sample is heated from ambient to 900 °C. From the curve, it appears that first stage starts at 30 °C and ends at 200 °C. In this stage removal of superficial water molecules takes place. About 4.98% loss in mass is observed in the first stage. Second stage ranges from 200 °C to 500 °C with 29.55% mass loss. In this stage, devolatilization takes place. It represents the decomposition of hemicellulose and cellulose. Third stage ranges from 500 °C to 900 °C with a mass loss of 23%. In this stage, decomposition of calcium carbonate and combustion of few fixed carbons occurred.

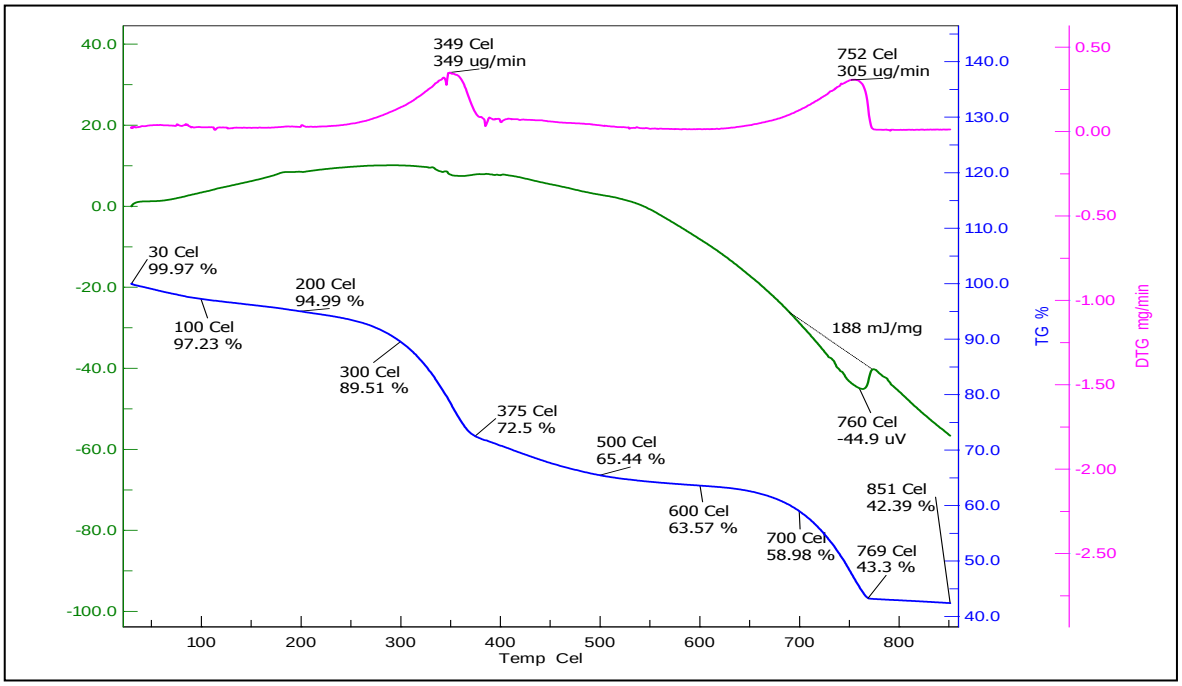

Figure-4.6 TG profile of deinking sludge

4.4.3. Particle size distribution of clay

The particle size distribution of clay is presented in Figure-4.7. The different size of the clay particles distribution has been given in Table 4.4. The physical properties of clay have been given in Table 4.5. The liquid limit (LL) and plastic limit (PL) of clay are 22.70% and 16.40% respectively. The clay comprising of clay minerals, slits and sand amounting to 13.15%,

75.18% and 11.04% respectively. It is evident from the physical properties and particle size distribution that the clay is good for brick making.

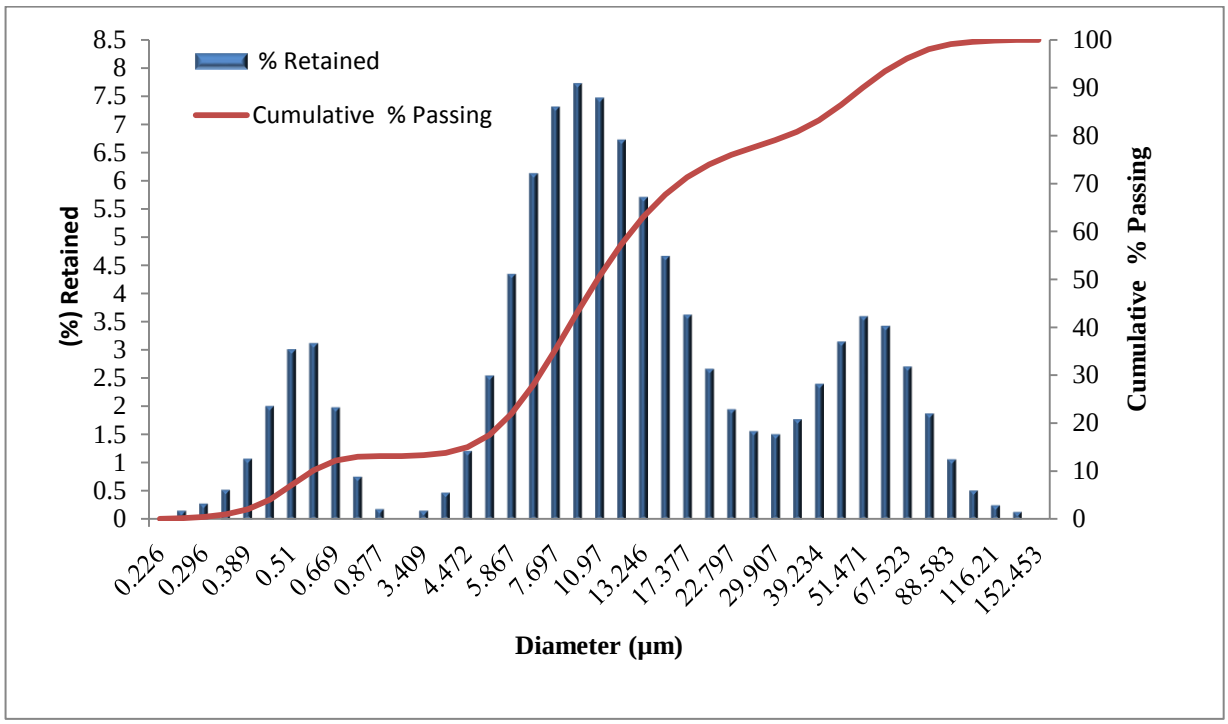

Figure-4.7 Particle size distribution of clay

Table-4.4 Particle size distribution of clay

Particle size (µm)	0.2-1.0	1.0-10	10-50	50-100
% distribution	13.15	37.35	39.50	10.00

Table-4.5 Physical properties of clay

Parameters	Clay
Liquid limit (%)	22.70
Plastic limit (%)	16.40
Plasticity index (%)	6.30
Sand size particle sieve (%)	11.04
Silt size particle sieve (%)	75.18
Clay size particle sieve (%)	13.15

4.4.4. Heating profile of brick specimens

The temperature profile of the furnace during firing the brick specimens made with deinking sludge and clay is given in Figure-4.8. The heating profile for the specimens has been based on standard heating procedures for the burnt clay brick specimens. Initially, the bricks have been fired at the rate of 2 °C/minute upto 200 °C and further it was fired at the rate of 4 °C/minute upto 400 °C and further the rate was kept 5 °C/minute until firing temperature then the brick specimens were put on the constant maximum temperature for next 120 minutes. The brick specimens were allowed to cool on naturally in furnace. A typical heating and cooling of brick specimens has been shown in Figure-4.8.

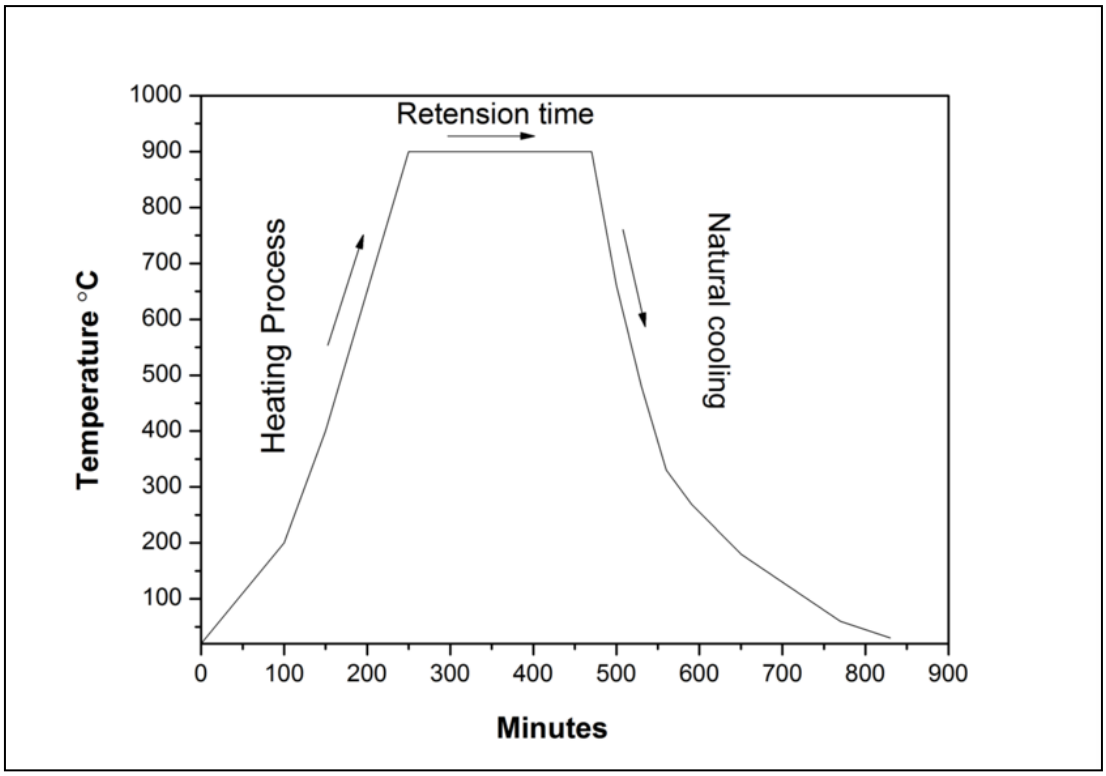

Figure-4.8 The heating profile of brick specimens made of deinking sludge and clay.

4.4.5. SEM of raw materials

This section presents the scanning electron microscopy (SEM) analysis of raw materials

4.4.5.1. SEM analysis of clay

The micro structural analysis of the clay is carried out by Scanning electron microscope (SEM) analysis and is represented in Figure-4.9. From the SEM image that is taken at 500X magnification, it can be inferred that it contained mainly silicon dioxide. Moreover, from the SEM image it appears that clay has compact structure and not fibrous or porous like deinking sludge. Furthermore, the structure seems more in layered form as shown in Figure-4.9.

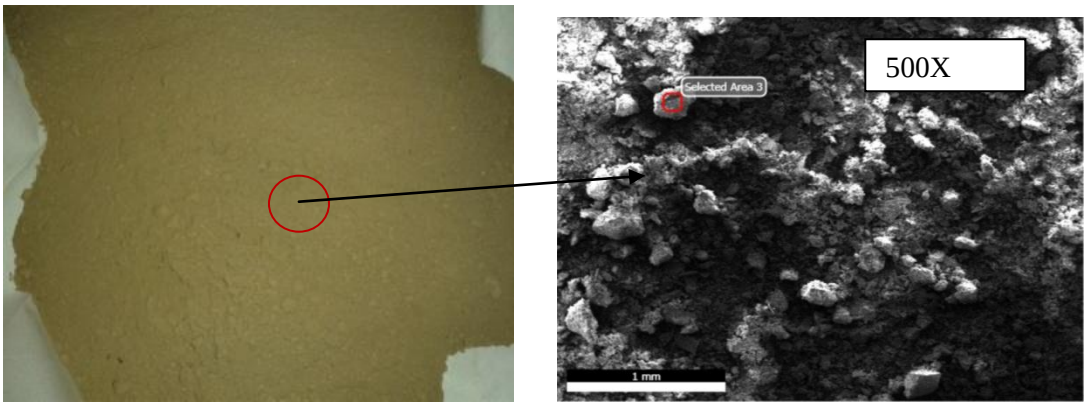

Figure-4.9 SEM image of raw clay.

4.4.5.2. SEM analysis of deinking sludge

The micro structural study of deinking sludge is carried out by SEM analysis. Figure-4.10 shows the SEM image of deinking sludge at 5000X magnification. From the images, it seems that the structure of deinking sludge is highly porous and fibrous. In addition, the pores appear irregular in shapes. These pores are responsible for holding the water molecules within them and hence increase the water absorption capability of the matrix. This capability indeed increases the thermal insulation of the structure if incorporated into the brick. Moreover, these fibrous structures give lightweight character to the brick.

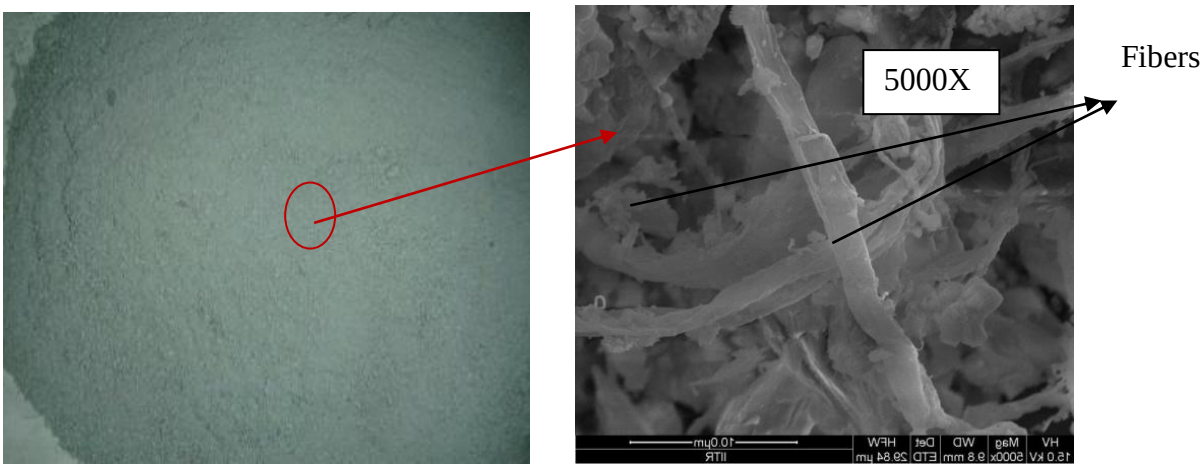

Figure-4.10 SEM Image Analysis of raw deinking sludge

4.4.6. X-ray diffraction analysis (XRD) of raw materials

The X-ray diffraction analysis of raw materials is presented as follows

4.4.6.1. XRD analysis of clay

The X-ray diffraction pattern to analyze the crystalline phase of the clay has been presented in Figure-4.11. The XRD pattern shows the presence of quartz, muscovite/illite and kaolinite.

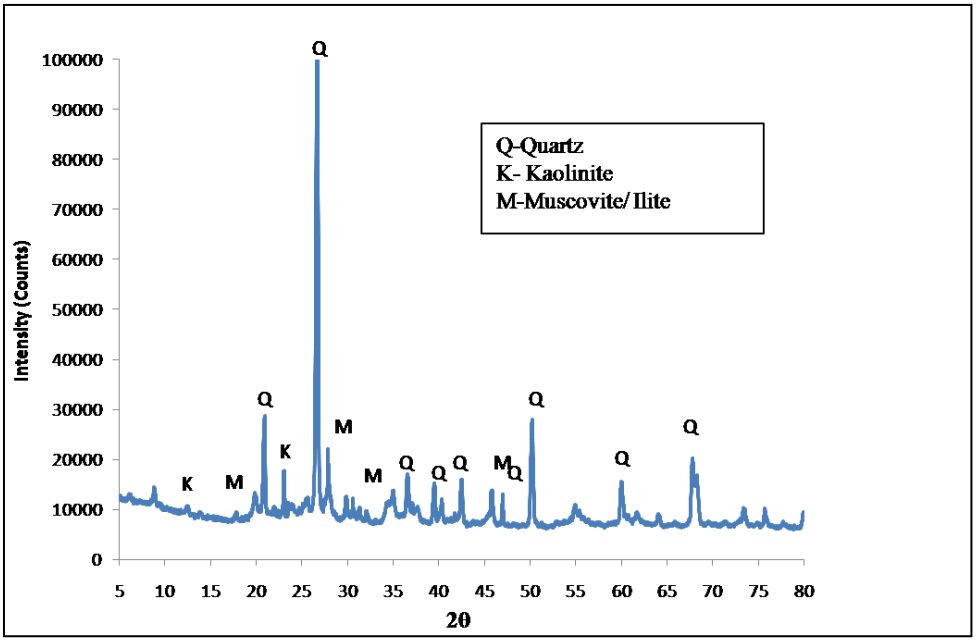

Figure-4.11 XRD analysis of clay

4.4.6.2. XRD analysis of deinking sludge

The crystallinity as well as phase analyses of deinking sludge has been carried out using XRD analysis and is presented in Figure-4.12. From the Figure-4.12, it is evident that the XRD analysis of deinking sludge contains calcite and weak peaks of cellulose and kaolinite. Calcium mainly exists in the form of calcite ($CaCO_3$) in the deinking sludge. Hence, it can be inferred that deinking sludge contains significant amount of calcium which is also evident from the chemical analysis of deinking sludge.

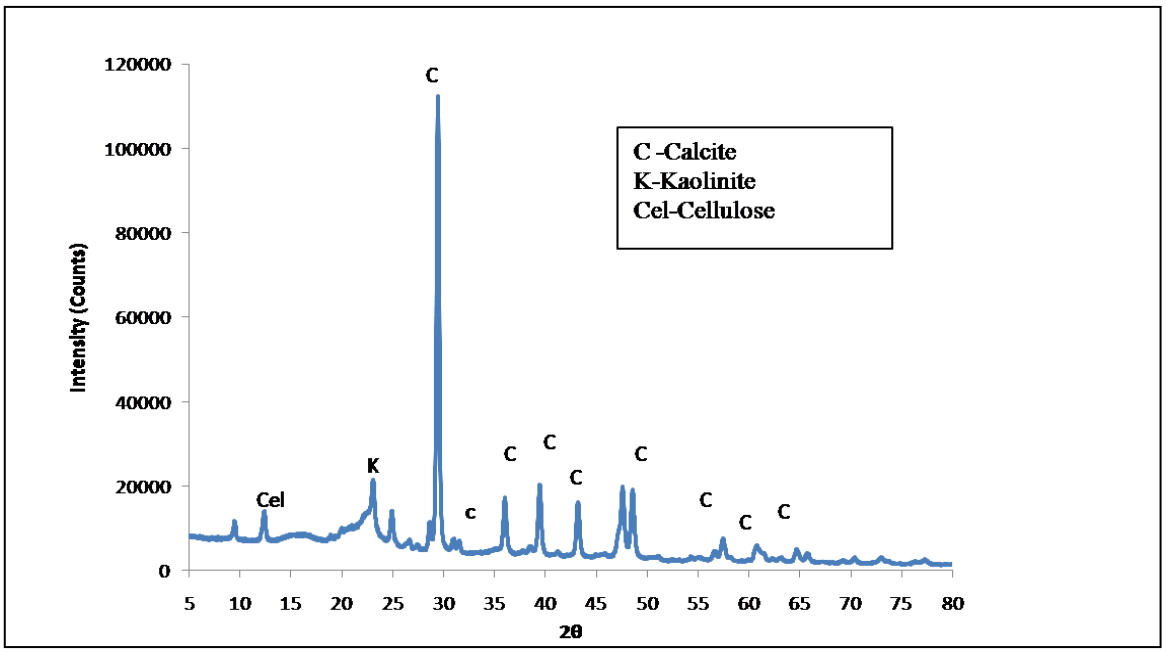

Figure-4.12 XRD analysis of raw deinking sludge

4.4.7. Physical appearance

The physical appearance of brick specimens before and after firing at 900 °C has been shown in Figure-4.13. It is evident from the results that as the content of deinking sludge is increased into the mix proportion, the colour of the brick changed from dark red to light red and then finally cream colour and buff colour. Moreover, from Table-4.6, it is evident that the brick specimen retains dark red colour until 5% by wt of the deinking sludge replacement. Then colour of the brick specimen changes to light brikish red and remains the same until 15% by wt deinking sludge replacement. Then at 20% by wt deinking sludge substitution the colour of the brick specimen changes to cream colour and finally to buff colour after 20% by wt deinking

sludge addition. The reason for reduction in redness is the decrease in Fe_2O_3 content since deinking sludge contains Fe_2O_3 in lesser amount relative to the clay. Hence, with increase in the amount of deinking sludge the amount of Fe_2O_3 decreases. Moreover, according to Sutcu and Akkurt (2009), the increment in CaO content with increase in the percentage of residue is another cause of reduction in redness.

Same trend is also observed with 950 °C and 1000 °C firing temperature. After being fired at these temperatures, brick specimen acquires same colour with same deinking sludge proportion as evident from Table-4.6 to Table-4.8. Hence, it can be inferred that the physical appearance of the brick specimen remains same at a particular proportion of the deinking sludge in the above range of temperatures tested as can be observed from the Table-4.6 to Table-4.8.

(a) (b)

Figure-4.13 Visual appearance of brick specimens before and after firing with different dosage of deinking sludge

4.4.8. Mass loss

The mass loss of brick specimens with deinking sludge after firing is given in Table-4.6 to Table-4.8 for firing temperatures of 900 °C, 950 °C and 1000 °C respectively. It is found that the mass loss increases with increasing amount of deinking sludge in mix. The % mass loss is in the order of 5.04%, 7.15%, 9.00%, 11.30%, 13.80%, 16.50% and 18.05% for the 0%, 5%, 10%, 15%, 20%, 25% and 30% replacement of clay with deinking sludge respectively for 900 °C. The trend of mass loss is same for the firing temperatures of 950 °C and 1000 °C as shown in Figure-4.14. The % mass loss is obtained as 5.12%, 7.23%, 9.11%, 11.54%, 14.00%, 16.60% and 18.25% for the 0%, 5%, 10%, 15%, 20%, 25% and 30% substitution of clay with deinking sludge respectively for 950 °C. Further with 1000 °C firing temperature, the % mass loss is found to be 5.17%, 7.26%, 9.20%, 11.60%, 14.10%, 16.68% and 18.12% for 0%, 5%, 10%,

15%, 20%, 25% and 30% respectively. From the above results, it appears that the mass loss% increases with increase in the replacement of clay by deinking sludge for firing temperatures of 900 °C, 950 °C and 1000 °C. In addition, it seems that mass loss increases with increase in the firing temperature for the same amount of sludge content.

Deinking sludge is a waste material that facilitates the formation of pores. The pores are formed when the sludge fibres burns off leaving the voids behind them. This creation of pores reduces the mass of the brick and ultimately lowers the density. But on the other hand, the formation of pores proves to be advantageous as they facilitate the increment in water absorption capability and hold the moisture into the structure. This ultimately leads to the reduction of thermal conductivity which finally lowers the heat loss through the walls of the buildings. However excessive mass loss can turn detrimental as it may affect the serviceability of the brick. It has been found that the mass loss % of fired clay bricks must not exceed 15% ((Bories et al. 2014, Karaman et al. 2006).

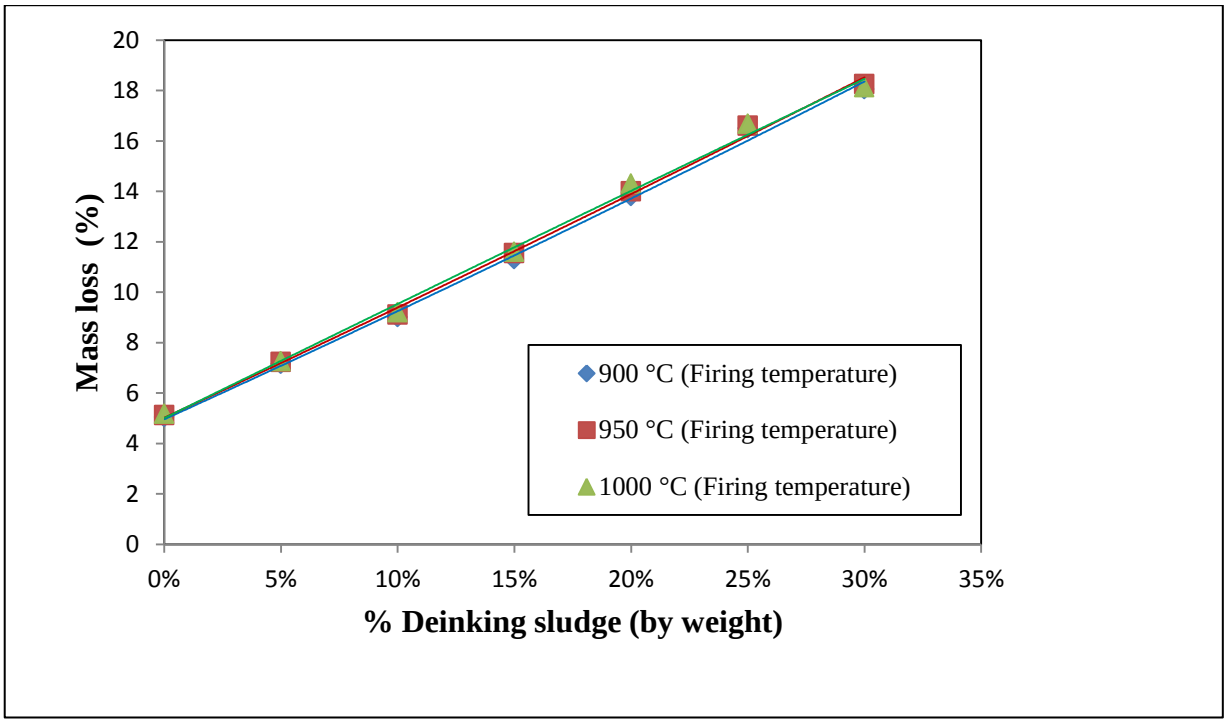

Figure-4.14 Mass loss vs % replacement of clay by deinking sludge (by weight)

4.4.9. Properties of burnt clay brick specimens

In this section property of burnt clay brick specimens have been described. The following tables show various properties at 900 °C, 950 °C and 1000 °C.

Table-4.6 Properties of burnt clay brick specimens with different dosage of deinking sludge proportion (Firing temperature at 900 °C)

Mix proportion	Mass Loss	Appearance		Water Absorption	Density	Shrinkage	Compressive Strength	Thermal Conductivity	Apparent porosity
		Before Firing	After Firing						
(%)	(%)			(%)	(kg/m^3)	(%)	(MPa)	(W/mK)	(%)
0	5.04	Greyish Brown	Brikish Red	12.80	1770.66	2.67	21.80	0.534	33.61
5	7.15	Greyish Brown	Brikish Red	15.08	1640.33	2.78	17.25	0.464	36.16
10	9.00	Greyish Brown	Light Brikish Red	17.25	1616.26	2.84	13.84	0.394	38.29
15	11.30	Greyish Brown	Light Brikish Red	19.12	1462.35	2.90	9.50	0.357	40.20
20	13.80	Greyish Brown	Cream Colour	20.80	1372.38	2.95	7.19	0.319	41.58
25	16.50	Greyish Brown	Buff colour	24.83	1266.29	2.98	5.21	0.281	45.61
30	18.05	Greyish Brown	Buff colour	28.64	1218.75	3.01	4.68	0.242	49.42

Table-4.7 Properties of burnt clay brick specimens with different dosage of deinking sludge proportion (Firing temperature at 950 °C)

Mix proportion	Mass Loss	Appearance		Water Absorption	Density	Shrinkage	Compressive Strength	Thermal conductivity	Apparent porosity
		Before Firing	After Firing						
(%)	(%)			(%)	(kg/m^3)	(%)	(MPa)	(W/mK)	(%)
0	5.12	Greyish Brown	Brikish Red	12.34	1820.67	2.74	22.55	0.531	33.12
5	7.23	Greyish Brown	Brikish Red	14.64	1699.19	2.83	18.11	0.458	35.05
10	9.11	Greyish Brown	Light Brikish Red	16.62	1665.84	2.89	14.84	0.395	36.65
15	11.54	Greyish Brown	Light Brikish Red	18.77	1553.48	2.95	10.39	0.350	39.05
20	14.00	Greyish Brown	Cream Colour	20.85	1489.84	3.00	8.15	0.310	42.10
25	16.60	Greyish Brown	Buff colour	24.26	1357.08	3.04	7.16	0.276	44.83
30	18.25	Greyish Brown	Buff colour	28.57	1301.48	3.06	5.82	0.245	49.05

Table-4.8 Properties of burnt clay brick specimens with different dosage of deinking sludge proportion (Firing temperature at 1000 °C)

Mix proportion	Mass Loss	Appearance		Water Absorption	Density	Shrinkage	Compressive Strength	Thermal conductivity	Apparent porosity
		Before Firing	After Firing						
(%)	(%)			(%)	(kg/m^3)	(%)	(MPa)	(W/mK)	(%)
0	5.17	Greyish Brown	Brikish Red	12.36	1823.99	2.75	22.70	0.525	32.84
5	7.26	Greyish Brown	Brikish Red	14.95	1748.63	2.83	18.32	0.455	34.98
10	9.20	Greyish Brown	Light Brikish Red	16.80	1670.81	2.90	15.04	0.390	37.53
15	11.60	Greyish Brown	Light Brikish Red	18.90	1592.07	2.95	10.43	0.345	39.03
20	14.10	Greyish Brown	Cream Colour	21.05	1498.38	3.01	8.10	0.305	42.95
25	16.68	Greyish Brown	Buff colour	25.18	1362.04	3.03	7.45	0.271	44.78
30	18.12	Greyish Brown	Buff colour	28.92	1308.81	3.07	6.07	0.240	48.28

4.4.9.1. Compressive strength

Compressive strength is defined as the ratio of load per unit area. The compressive strength of brick specimens with different dosage of deinking sludge at firing temperatures of 900 °C, 950 °C and 1000 °C is presented in Table-4.6 to Table-4.8 respectively. The compressive strength of control (0% deinking sludge) burnt clay brick specimen is 21.80 MPa, 22.55 MPa and 22.70 MPa for 900 °C, 950 °C and 1000 °C respectively. The compressive strength at 950 °C and 1000 °C is found to be more than 900 °C because of formation of mullites taking place at firing temperature of 950 °C. From the Table-4.6 it can be observed that with increase in the clay

replacement with deinking sludge, there appears reduction in the compressive strength. Compressive strength is found to be 21.80 MPa with 0% sludge addition whereas with 30% sludge addition it reduces to 4.68 MPa. Similar trend is also observed with firing temperatures of 950 °C and 1000 °C. However, the compressive strength increases with increase in firing temperature keeping the quantity of the clay replacement with deinking sludge constant as evident from the Figure-4.15. However, there is a slight difference between the compressive strengths of 950 °C and 1000 °C. At 900 °C firing temperature, with 5% deinking sludge substitution, compressive strength of 17.25 MPa is observed. It increases to 18.11 MPa and 18.32 MPa at firing temperatures of 950 °C and 1000 °C with same deinking sludge substitution. Similar trend is observed with all other proportions of deinking sludge.

However the deinking sludge shall be used particularly for partition wall etc. up to 15% replacement. According to the codal provision IS 1077:1992, the compressive strength shall not be less than 10 MPa for brick designation of class of 10. From Table-4.6, it can be observed that the deinking sludge replacement of 15% gives compressive strength below 10 MPa at firing temperature of 900 °C. However, at 950 °C and 1000 °C temperature, deinking sludge addition of up to 15% satisfies the above criteria as can be observed from Table-4.7 and Table-4.8.

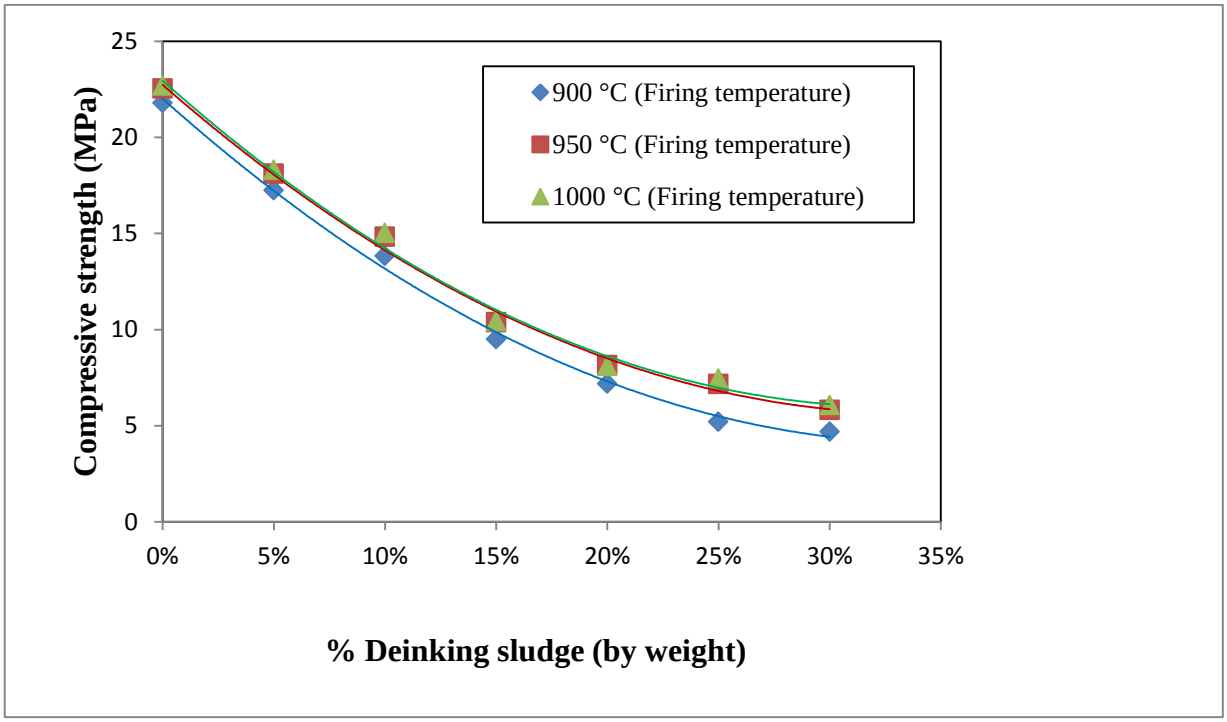

Figure-4.15 Compressive strength of burnt clay brick specimens with different dosage of deinking sludge

4.4.9.2. Water absorption

The water absorption of brick specimens with different proportions of deinking sludge at 900 °C, 950 °C and 1000 °C has been determined according to IS 3495 (Part 2):1992 and is presented in Table-4.6 to Table-4.8. The water absorption of brick specimens is found from 12.80% to 28.64% for deinking sludge dosage from 0% and 30% respectively at 900 °C. From the Figure-4.16, it can be analysed that with increase in the sludge content from 0% to 30%, the water absorption also increases. This implies that more the sludge content more will be the water absorption capacity. Hence, it can be said that the water absorption is directly proportional to the amount of deinking sludge present in the brick specimen.

The deinking sludge shall be utilized effectively in brick work particularly for partition wall etc. up to 15% replacement. According to the codal provision IS 1077:1992 the maximum water absorption shall not exceed 20% for brick designation of class of 12.5 and below. It can be observed from the Table-4.6 that the deinking sludge addition of up to 15% results in water absorption below 20%. Hence deinking sludge addition of up to 15% is suitable. Similar results have been observed with the firing temperatures of 950 °C and 1000 °C.

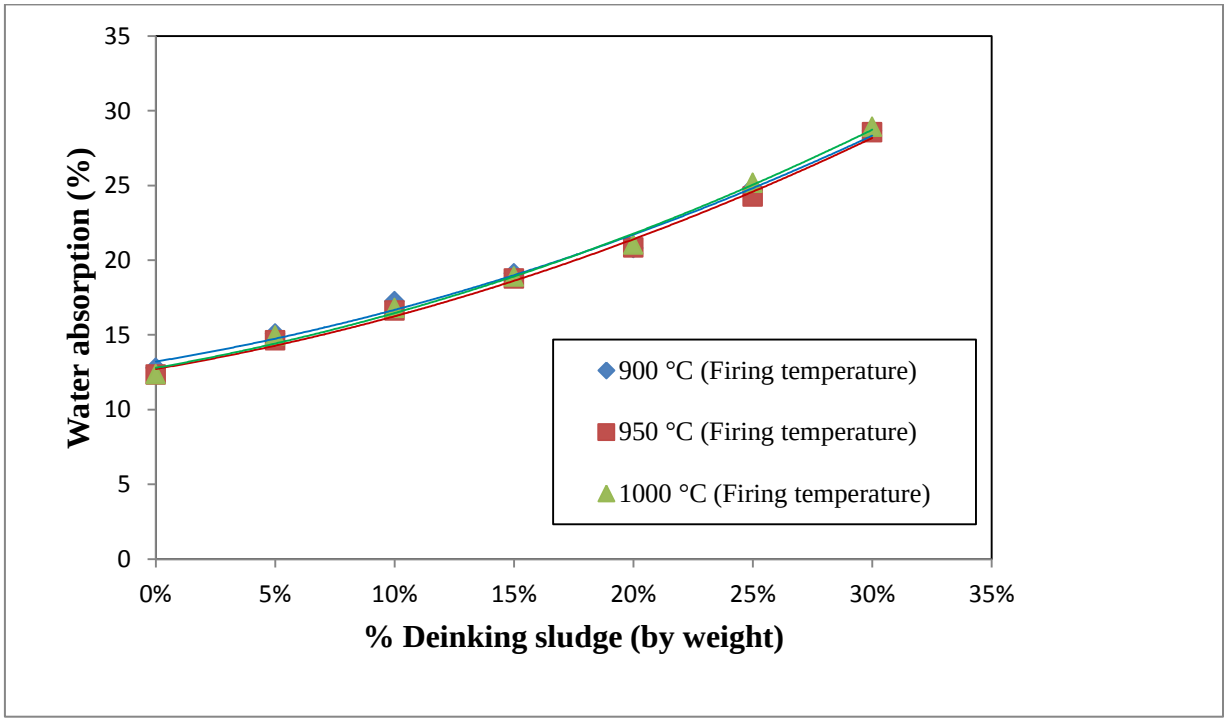

Figure-4.16 Water absorption of burnt clay brick specimens with different dosage of deinking sludge

4.4.9.3. Efflorescence

The brick specimen corresponding to 0%, 5%, 10%, 15%, 20%, 25% and 30% deinking sludge replacement after firing at temperatures 900 °C, 950 °C and 1000 °C show efflorescence moderately and satisfies codal provision as per IS 3495 (Part 3): 1992 and IS 1077 : 1992.

4.4.9.4. Density

The density of control (0% deinking sludge) burnt clay brick specimens for firing temperatures of 950 °C and 1000 °C is found 1820.67 kg/m^3 and 1823.99 kg/m^3 respectively whereas the density of the brick specimen for the firing temperature of 900 °C is only 1770.66 kg/m^3. This is because of formation of mullites at 950 °C and above. The densities of burnt clay brick specimens for temperatures of 900 °C, 950 °C and 1000 °C have been shown in Table-4.6 to Table-4.8. From the Table-4.6, it can be found that with increase in the clay replacement with deinking sludge, there appears reduction in the density. Density is found to be 1640.33 kg/m^3 with 5% sludge addition whereas with 30% sludge addition it reduces to 1218.75 kg/m^3. Similar trend is also observed with firing temperatures of 950 °C and 1000 °C as represented in the Figure-4.17.

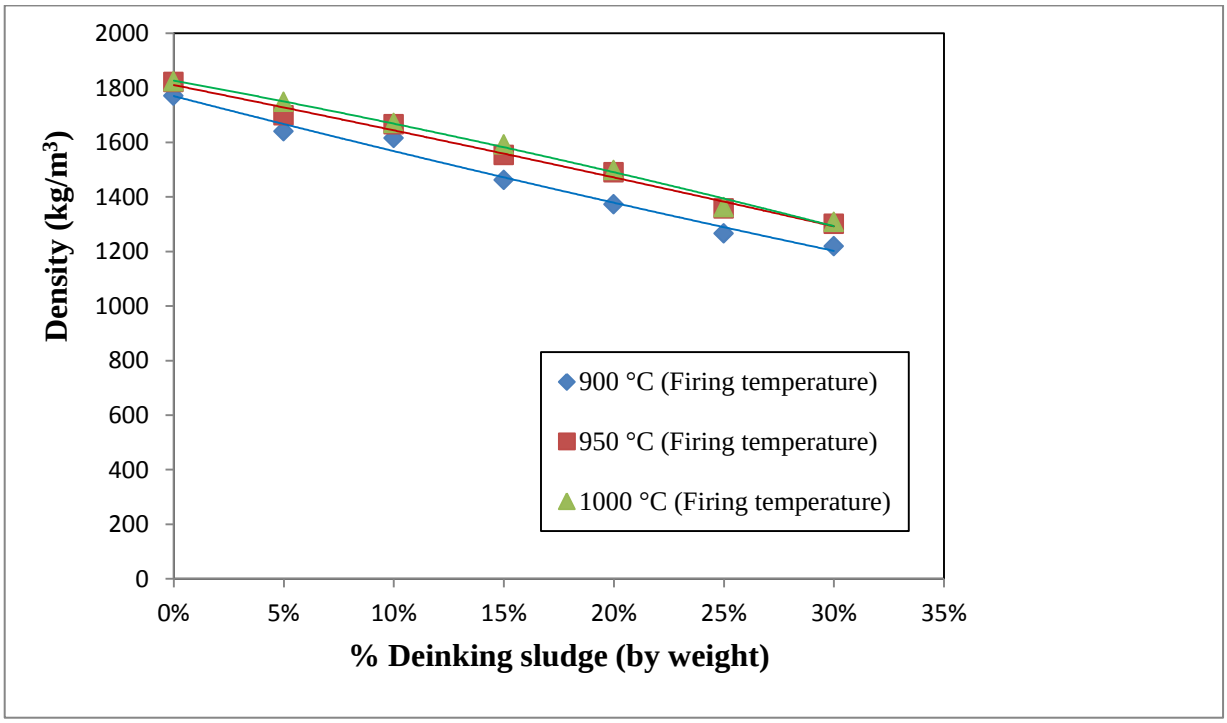

Figure-4.17 Density of burnt clay brick specimens with different dosage of deinking sludge

4.4.9.5. Apparent porosity

The apparent porosity of burnt clay brick specimens with different proportions of deinking sludge at 900 °C, 950 °C and 1000 °C has been determined according to ASTM C20-00 (2015) standard and is presented from Table-4.6 to Table-4.8. As evident from the Table-4.6, that the apparent porosity is found as 33.61% with control burnt clay brick specimen whereas it goes on increasing to 49.42% with 30% deinking sludge substitution. Hence, apparent porosity increases with increase in the deinking sludge dosages in burnt clay brick specimens. With 950 °C and 1000 °C firing temperatures, the apparent porosities of control burnt clay brick specimens are found as 33.12% and 32.84% respectively. In addition, the apparent porosity also increases with increase in the deinking sludge replacement for 950 °C and 1000 °C as evident from Figure-4.18. The reason behind this is that deinking sludge burns off during firing stage leaving behind the pores. Moreover, $CaCO_3$ also facilitates the formation of porosity to a little extent by decomposing into calcium oxide thereby releasing carbon dioxide. Hence, to some extent calcium facilitates porous structure and thus helps in reducing the thermal conductivity (Sutcu and Akkurt 2009). Moreover, if the apparent porosity is observed based on temperature keeping the deinking sludge replacement ratio constant, then it can be found that it decreases with increase in temperature. The reason behind decrement in apparent porosity with increase in temperature is the diffusion of particles into the structure (Johari et al. 2010). However, increase in porosity increases the insulation capacity of the brick (Demir et al. 2005). Insulation capacity can be increased by reducing the thermal conductivity. Thermal conductivity is reduced with increase in porosity because of the resistance offered by pore to the heat transfer (Sutcu and Akkurt 2009). However, excessive porosity can turn detrimental for the product, as the brick will contain too much holes that will make the brick fragile (Bories et al. 2014).

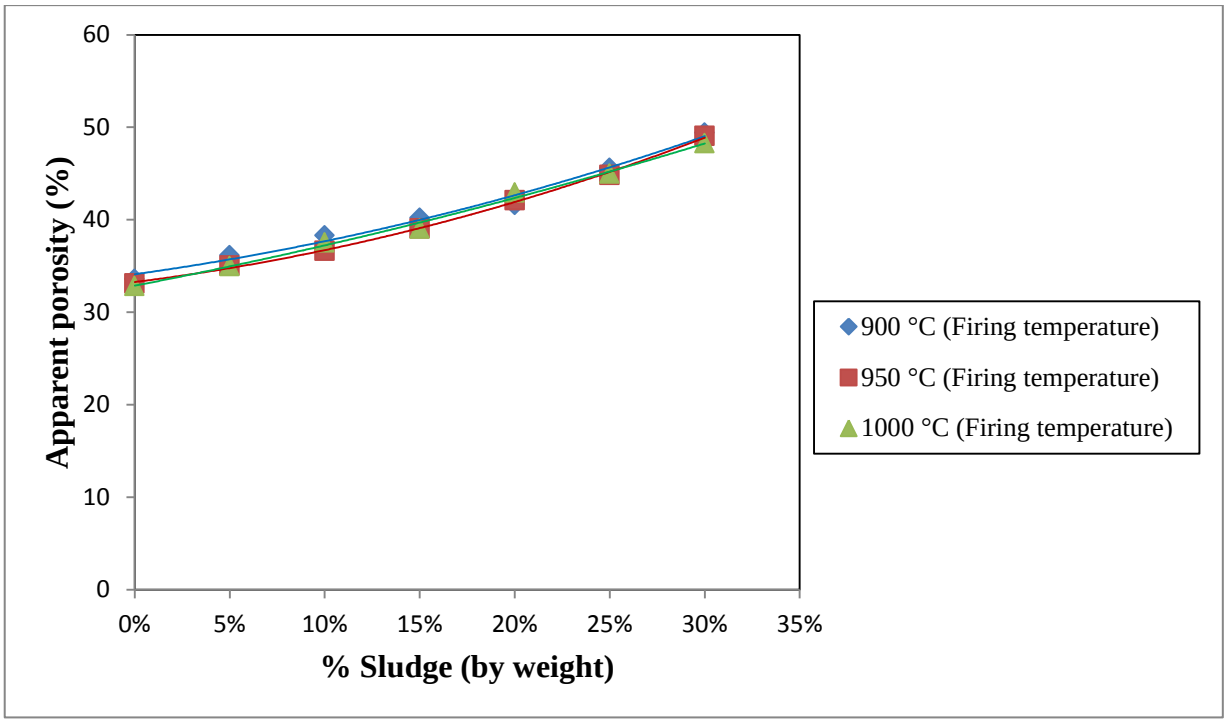

Figure-4.18 Apparent porosity of burnt clay brick specimens with different dosage of deinking sludge

4.4.9.6. Firing shrinkage

The firing shrinkage of brick specimens with different dosage of deinking sludge at firing temperatures of 900 °C, 950 °C and 1000 °C is presented in Table-4.6 to Table-4.8 respectively. The firing shrinkage of control burnt clay brick specimen is found to be 2.67%, 2.74% and 2.75% for 900 °C, 950 °C and 1000 °C respectively. From the Figure-4.19, it can be seen that the firing shrinkage increases at 950 °C and 1000 °C as compared to 900 °C for the same sludge replacement. However, from the Figure-4.19, it can also be observe that the firing shrinkage is almost equivalent at 950 °C and 1000 °C for the same amount of sludge. Moreover, it has been observed from the Figure-4.19, that with increase in the deinking sludge dosage from 5% to 30% by wt in the mixing proportion, the shrinkage increases from 2.78% to 3.01% at 900 °C. Similar trend is also found with 950 °C and 1000 °C.

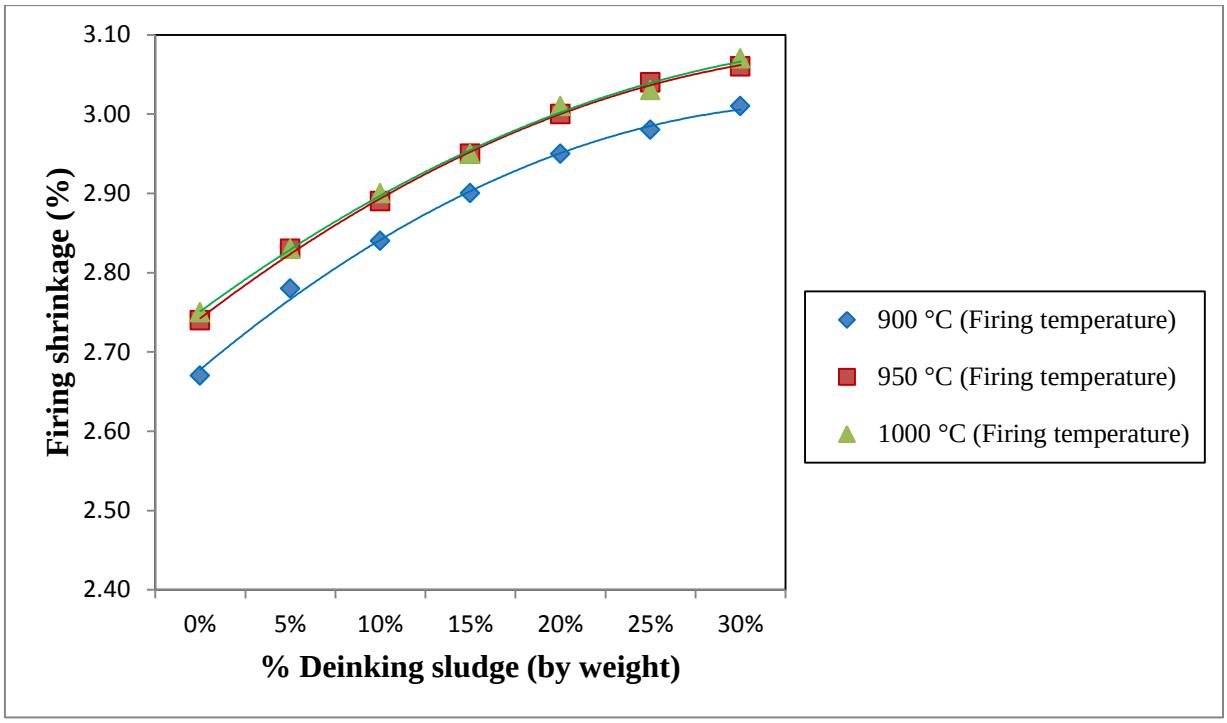

Figure-4.19 Firing shrinkage of burnt clay brick specimens with different dosage of deinking sludge

4.4.9.7. Thermal conductivity

The thermal conductivity of brick specimens with different proportions of deinking sludge replacement at 900 °C, 950 °C and 1000 °C has been determined by KD2 Pro thermal conductivity meter and is presented in Table-4.6 to Table-4.8 and shown in Figure-4.20. The thermal conductivity of control burnt clay brick specimens is found to be 0.534 W/mK, 0.531 W/mK and 0.525 W/mK for 900 °C, 950 °C and 1000 °C temperatures respectively. From Table-4.6, it can be observed that the thermal conductivity decreases with increase in the deinking sludge content in the burnt clay brick specimens. Same trend is also observed with 950 °C and 1000 °C as evident from the Figure-4.20. Decrease in thermal conductivity implies increment in thermal insulation of brick specimen. Increase in thermal insulation will ultimately decrease the heat loss through the walls and hence will make the building more energy saving. It can be concluded that deinking sludge replacement in the burnt clay bricks facilitates reduction in thermal conductivity and is encouraging for energy saving purposes. However, for obtaining higher thermal conductivity, the mechanical properties are to be compromised.

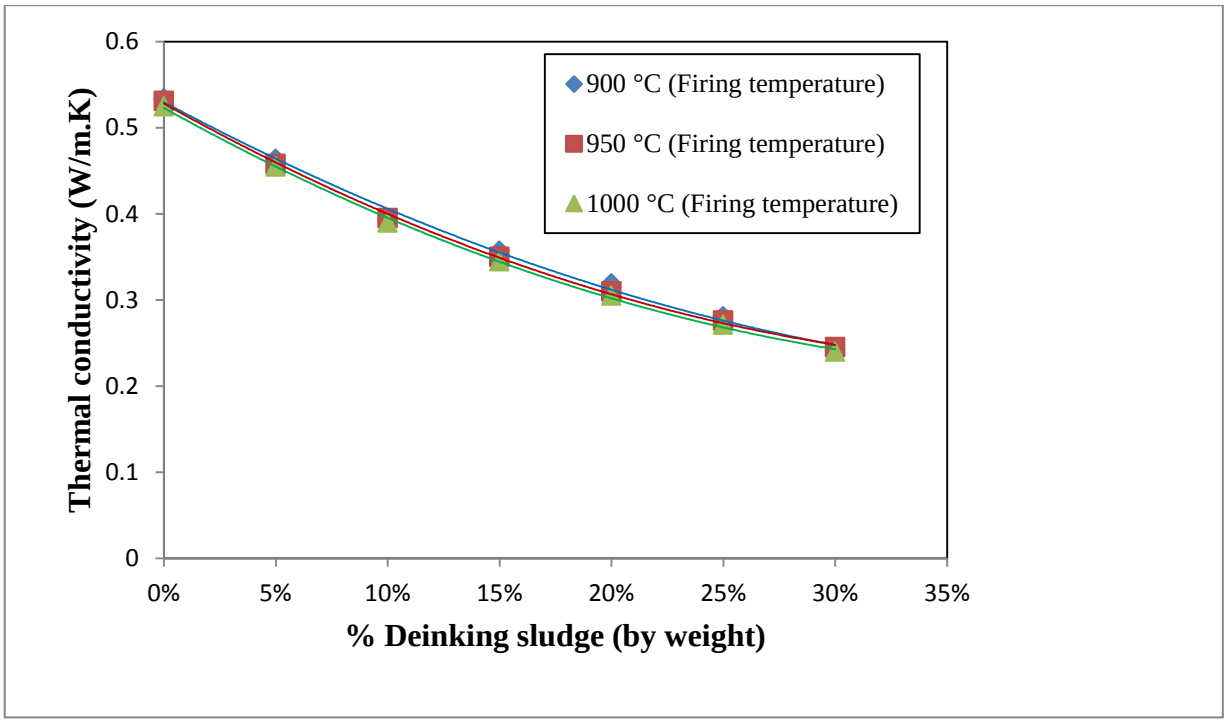

Figure-4.20 Thermal conductivity of burnt clay brick specimens with different dosage of deinking sludge

4.4.10. Effect of thermal conductivity and apparent porosity of burnt clay brick specimens

Thermal conductivity decreases with increase in the dosage of deinking sludge whereas apparent porosity increases with increase in the dosage of deinking sludge. The optimum value for % replacement of deinking sludge is found 15% as shown in Figure-4.21. At 15% replacement of deinking sludge, thermal conductivity and apparent porosity are obtained as 0.350 W/mK and 39.05% respectively. In addition the compressive strength and water absorption is found as 10.39% and 18.77% respectively for 15% replacement of deinking sludge at 950 °C temperature.

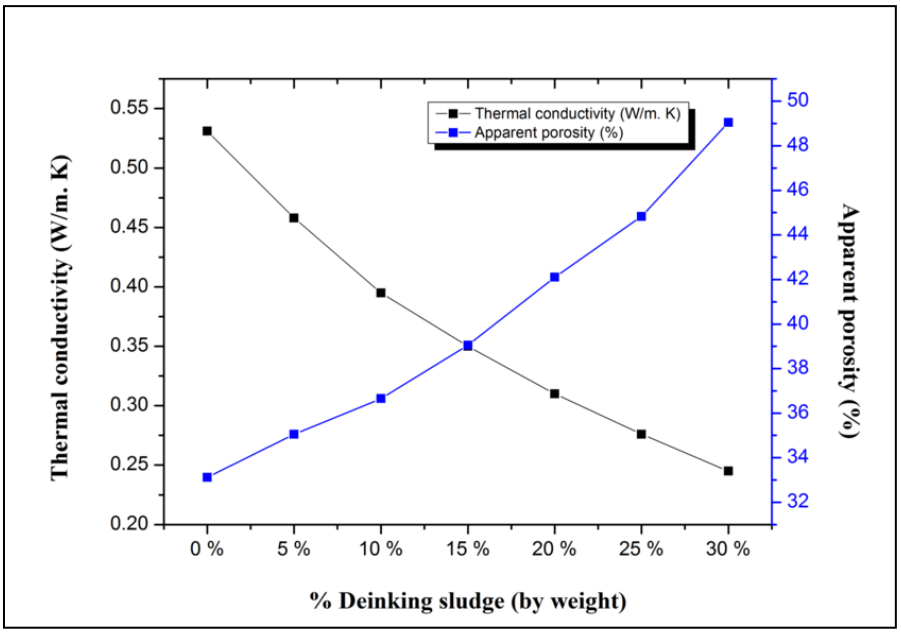

Figure-4.21 Effect of thermal conductivity and apparent porosity of burnt clay brick specimens with different dosage of sludge proportion at 950 °C firing temperature

4.4.11. SEM analysis

The scanning electron microscope (SEM) of burnt clay brick specimens with 0% to 30% deinking sludge dosage at optimum temperature of 950 °C has been presented in Figure-4.22. The SEM images has been presented at 100X, 2500X and 5000X magnification for control burnt clay specimen. The SEM images of other specimens have been presented at 5000X magnification. It can be observed from the Figure-4.22 that deinking sludge replacement facilitates the formation of pores in the structure. The deinking sludge burns during firing stage and leaves the pores behind. Moreover, these pores appear irregular in shape.

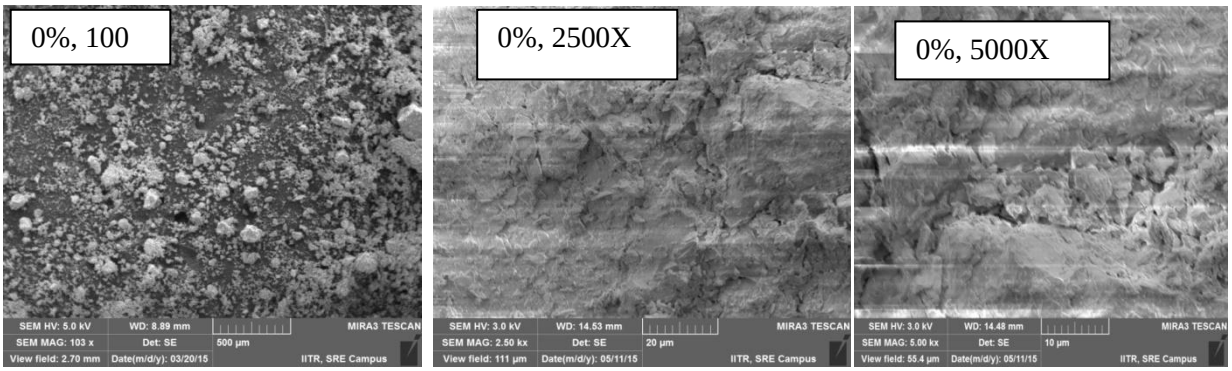

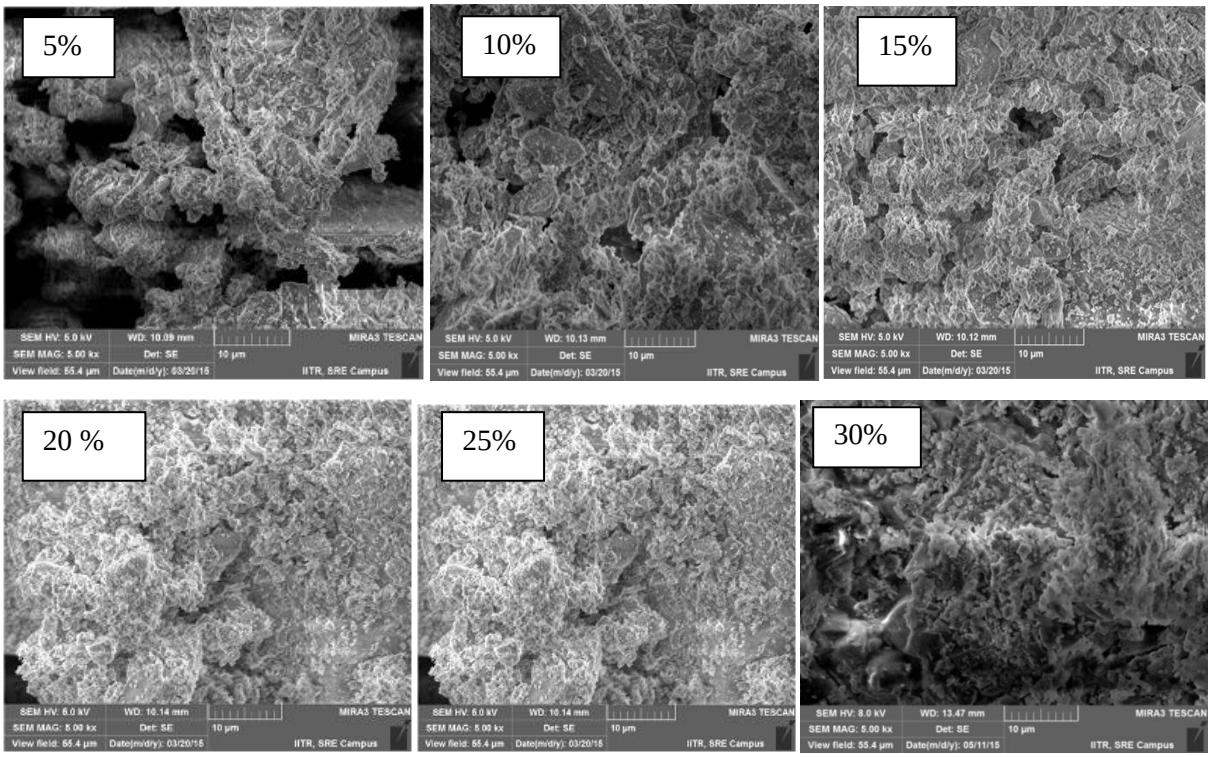

Figure-4.22 SEM images of burnt clay brick specimens fired at 950 °C

4.4.12. XRD analysis

The X-ray diffraction (XRD) of burnt clay brick specimens with 0% to 30% deinking sludge dosage at optimum temperature of 950 °C has been presented in Figure-4.23. From the Figure 4.23 it is evident that the formation of mullite and quartz are observed in the XRD patterns of the fired clay brick specimens at 950 °C. Moreover, proper crystallinity has been found in the brick specimen of firing temperature at 950 °C. Therefore, the firing temperature for the fired clay brick specimen with deinking sludge incorporated should be 950 °C.

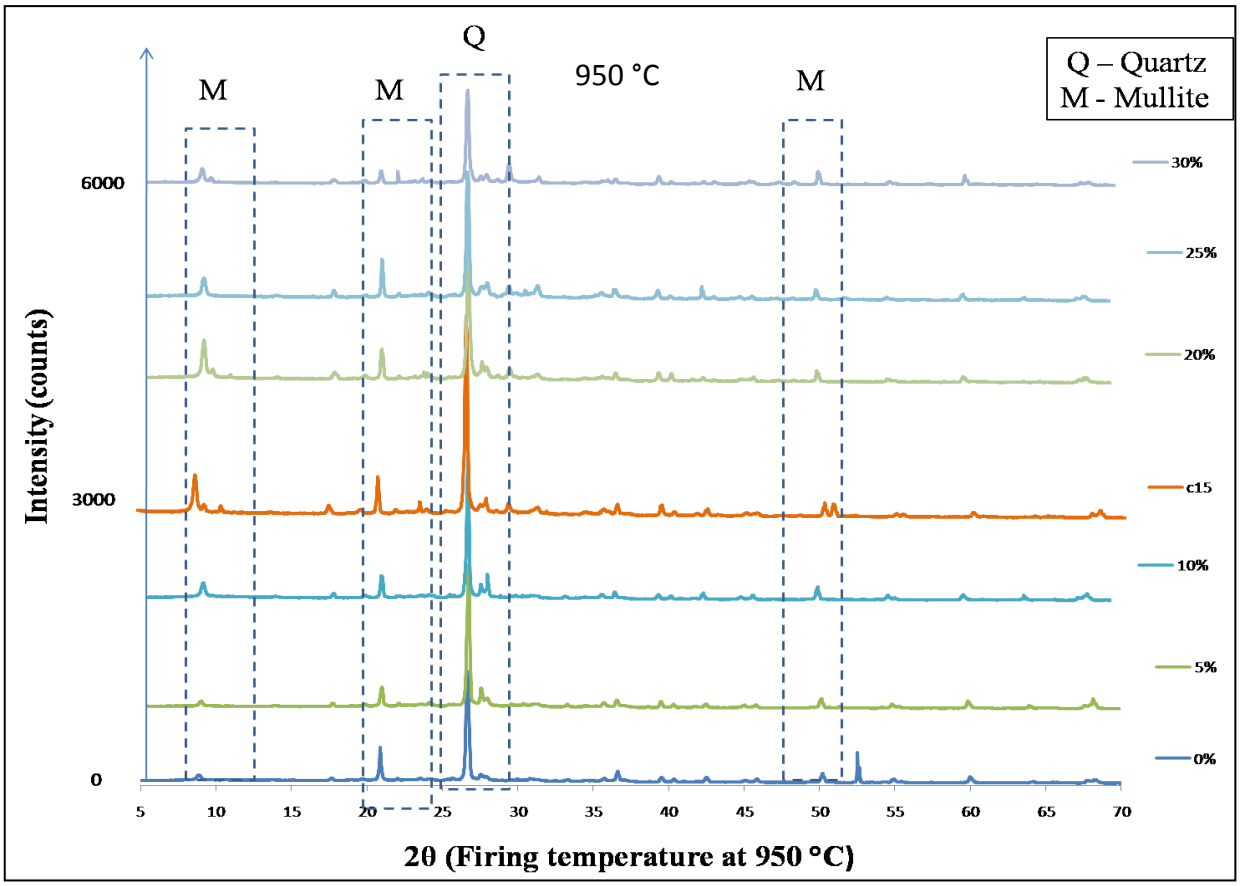

Figure-4.23 XRD patterns of burnt clay brick specimens fired at 950 °C

4.5. Conclusions

Based on the study carried out in this chapter, the following conclusions are obtained:

1. From the study, it is found that the optimum amount of deinking sludge addition in production of fired clay bricks is found to be 15%.

2. Furthermore, from the investigation on burnt clay brick specimens, it is found that the optimum firing temperature for deinking sludge and clay brick specimen is found to be 950 °C.

3. The compressive strength and water absorption for the fired clay brick at 950 °C with 15% deinking sludge addition are calculated as 10.39 MPa and 18.77% respectively. These values satisfy the codal standard IS 1077:1992. This comes under the brick class of class of 10 that is suitable for brick masonry work.

4. The thermal conductivity reduces with increase in the amount of deinking sludge in fired clay brick specimen whereas apparent porosity increases with increase in the percentage of deinking sludge.

5. The optimum value of thermal conductivity and apparent porosity is found at 15% deinking sludge addition. The values of thermal conductivity and apparent porosity is found as 0.350 W/mK and 39.05% respectively at 950 °C.

6. With decrease in the thermal conductivity, insulation capability of fired clay brick specimen increases which is favourable for energy saving purposes. Hence, application of these brick shall further reduce the energy requirement in the household unit.

7. Thus, deinking sludge replacement can be utilized effectively which will not only resolve the land disposal problem but it is a sustainable approach having these bricks as more energy efficient.

RECOMMENDATIONS

The present work makes the following recommendations:

- Detailed analysis of the study of mechanism of Ultrasound and UV irradiation treatment on various properties is necessary.

- In the present work focus is more on the time duration of the treatment given at particular energy intensity. However the results are not co-related with total energy input. It is recommended that the further study should be carried out on the basis of energy input.

- It is recommended that studies on combination of enzymatic deinking with UV-irradiation and US treatment and their environmental impacts should be investigated.

- Inherent mineral matter of these samples (deinking sludge, coal and rice husk) may appear as obstacle to overall thermal degradation process. Therefore, effect of demineralization of samples should be investigated.

- The thermal conversion of carbonaceous materials is highly complex in nature. Hence, the study of other models should be done for studying the kinetics of the thermal behaviour of deinking sludge, coal and rice husk with their respective blends.

- Mineralogical analysis of coal and rice husk should be investigated

- Effect of inorganic constituents in thermal conversion characteristic like reactivity, slagging, fouling and environmental impact of thermal conversion process should be investigated.

- Effect of mixed atmosphere of N_2: O_2 should be studied on deinking sludge, coal, rice husk and their blends.

- Ash properties and behaviour after thermal conversion processes should be investigated.

- Finite elemental analysis is suitable for determining solutions of heat transfer equations. Hence, FEM should be carried out to analyse the heat transfer phenomenon inside porous fired clay bricks.

- The studies on mechanical mixing of clay and deinking sludge may enhance the properties of burnt clay bricks.

- Addition of deinking sludge in cement concrete building products needs to be studied. This will enhance the compressive strength of the specimen.

REFERENCES

- ✓ About Lignite. (2015). Retrieved August 10, 2015, from https://www.lignite.com/about-lignite/
- ✓ Agnihotri, P. (2007). Deinking studies of ONP and its blends with other recycled papers. *Ph.D Thesis.* Indian Institute of Technology Roorkee, Roorkee.
- ✓ Arshad, M. S., and Pawade, P. Y. (2014). Reuse of natural waste material for making light weight bricks. *International Journal of Scientific and Technology research, 3*(6), 49-53.
- ✓ ASTM C20-00. (2015). Standard test methods for Apparent Porosity, Water Absorption, Apparent specific Gravity and Bulk Density of Burned Refectory Brick and Shapes by Boiling Water. *American Society for Testing and Materials*, West Conshohocken, PA 19428-2959, United States.
- ✓ ASTM D3172 (2013). Standard practice for proximate analysis of coal and coke. *American Society for Testing and Materials*, West Conshohocken, PA 19428-2959, United States.
- ✓ Battaglia, A., Calace, N., Nardi, E., Petronio, B. M., and Pietroletti, M. (2003). Paper mill sludge–soil mixture: kinetic and thermodynamic tests of cadmium and lead sorption capability. *Microchemical Journal*, *75*(2), 97-102.
- ✓ Bharadwaj, A., Wang, Y., Sridhar, S., and Arunachalam, V. S. (2004). Pyrolysis of rice husk. *Current Science*, *87*(7), 981-986.
- ✓ Bhardwaj, N. K., Bajpai, P., and Bajpai, P. K. (1997). Enhancement of strength and drainage of secondary fibres. *Appita Journal*, *50*(3), 230-232.
- ✓ Bhuiyan, M. N. A., Murakami, K., and Ota, M. (2008). On thermal stability and chemical kinetics of waste newspaper by thermogravimetric and pyrolysis analysis. *Journal of Environment and Engineering, 3*(1), 1-12.
- ✓ Bories, C., Borredon, M. E., Vedrenne, E., and Vilarem, G. (2014). Development of eco-friendly porous fired clay bricks using pore-forming agents: A review. *Journal of Environmental Management*, *143*, 186-196.
- ✓ Chinnaraj, S., Vijayakumar, T., Kumar, M. S., and Subrahmanyam, S. V. (2011). Carbon footprint reduction strategies and efforts by TNPL. *IPPTA Journal*, *23*(1), 147-150.
- ✓ Coats, A. W., and Redfern, J. P. (1964). Kinetic parameters from thermogravimetric data. *Nature, 201*(4914), 68-69.
- ✓ Demir, I., Baspınar, M. S., and Orhan, M. (2005). Utilization of kraft pulp production residues in clay brick production. *Building and Environment*, *40*(11), 1533-1537.

- ✓ Dixit, A. K., Jain, R. K., and Mathur, R. M. (2012). Innovations & Process Development for Efficient Operation of Chemical Recovery System In Paper Industry. *IPPTA Journal*, *24*(4), 119-123.
- ✓ Dixit, A. K., Thapliyal, B. P., Jain, R. K., and Mathur, R. M. (2010). Desilication of Bamboo and Straw Black Liquors. *IPPTA Journal*, *22*(3), 121-123.
- ✓ Dondi, M., Marsigli, M., and Fabbri, B. (1997). Recycling of industrial and urban wastes in brick production: a review. *Tile and Brick International*, *13*(3), 218-225.
- ✓ Fernandes, F. M., Lourenço, P. B., and Castro, F. (2010). Ancient clay bricks: manufacture and properties. Chapter 3 *Materials, Technologies and Practice in Historic Heritage Structures*. Springer science & Business Media B.V., 29-48.
- ✓ Fricker, A., Thompson, R., and Manning, A. (2007). Novel solutions to new problems in paper deinking. *Pigment & Resin Technology*, *36*(3), 141-152.
- ✓ Galan, I., Glasser, F. P., and Andrade, C. (2013). Calcium carbonate decomposition. *Journal of thermal analysis and calorimetry*, *111*(2), 1197-1202.
- ✓ Gangavati, P. B., Safi, M. J., Singh, A., Prasad, B., and Mishra, I. M. (2005). Pyrolysis and thermal oxidation kinetics of sugar mill press mud. *Thermochimica acta*, *428*(1), 63-70.
- ✓ García, R., de la Villa, R. V., Vegas, I., Frías, M., and de Rojas, M. S. (2008). The pozzolanic properties of paper sludge waste. *Construction and Building Materials*, *22*(7), 1484-1490.
- ✓ Guggenheim, S., and Martin, R. T. (1995). Definition of clay and clay mineral: joint report of the AIPEA nomenclature and CMS nomenclature committees. *Clays and clay minerals*, *43*(2), 255-256.
- ✓ Horowitz, H. H., and Metzger, G. (1963). A new analysis of thermogravimetric traces. *Analytical Chem*istry, *35*(10), 1464-1468.
- ✓ Ikonomou, G. D. and Lo, D. K. (1995). *U.S. Patent No.5,413,675.* Washington DC: U.S. Patent and Trademark Office.
- ✓ Imamoglu, S. (2006). Deinkability efficiency of waste office paper printed using a duplicating machine. *Journal of Applied Sciences*, *6*(9), 2006-2009.
- ✓ Indian paper industry at a glance. (2015). Retrieved April 23, 2015, from http://www.indianmirror.com/indian-industries/2015/paper-2015.html
- ✓ Indian Paper Industry. (2015). Retrieved April 23, 2015, from http://www.ipma.co.in/paper_industry_overview.asp
- ✓ IS 1077 (1992): Common burnt clay building bricks specifications. *Bureau of Indian Standards*, New Delhi, India.

- ✓ IS 12979 (1990): Mould for determination of linear shrinkage specification. *Bureau of Indian Standards*, New Delhi, India.
- ✓ IS 3495 (Part 1 - 4) (1992): Methods of tests of burnt clay building bricks. *Bureau of Indian Standards*, New Delhi, India.
- ✓ Ismail, M., Ismail, M. A., and Keok, L. S. (2010). Fabrication of bricks from paper sludge and palm oil fuel ash. *Concrete Research Letters*, *1(*2), 60-66.
- ✓ Jain, R. K., Thakur, V. V., Pandey, D., Adhikari, D. K., Dixit, A. K., and Mathur, R. M. (2011). Bioethanol from bagasse pith a lignocellulosic waste biomass from paper/sugar industry. *IPPTA Journal*, *23*(1), 169-173.
- ✓ Jeffries, T. W., Klungness, J. H., Sykes, M. S., and Rutledge-Cropsey, K. R. (1994). Comparison of enzyme-enhanced with conventional deinking of xerographic and laser-printed paper. *Tappi Journal*, *77*(4), 173-179.
- ✓ Jeffries, T. W., Sykes, M. S., Rutledge-Cropsey, K., Klungness, J. H., and Abubakr, S. (1995). Enhanced removal of toners from office waste papers by microbial cellulases. *Proceedings of the 6th International Conference on Biotechnology in the Pulp and Paper Industry: Advances in Applied and Fundamental Research*, Facultas-Universitatsverlag, Vienna, Austria, 141-144.
- ✓ Jiang, C., and Ma, J. (2000). De-inking of Waste Paper: Flotation. *Encyclopedia of Separation Science*, 2537-2544.
- ✓ Johari, I., Said, S., Hisham, B., Bakar, A., and Ahmad, Z. A. (2010). Effect of the change of firing temperature on microstructure and physical properties of clay bricks from Beruas (Malaysia). *Science of Sintering*, *42*(2), 245-254.
- ✓ Josefsson, A. (2010). Ultrasonic refining of chemical pulp fibres. *M.Sc. Thesis.* Chalmers University of Technology, Goteborg, Sweden.
- ✓ Kanthe, V. N., and Chavan, P. G. Solid Waste Used As Construction Material. *IOSR Journal of Engineering (IOSRJEN)*, ISSN 2250-3021.
- ✓ Karaman, S., Ersahin, S., and Gunal, H. (2006). Firing temperature and firing time influence on mechanical and physical properties of clay bricks. *Journal of scientific and industrial research*, *65*(2), 153.
- ✓ Kulkarni, S., Chauhan, N., Kumar, V. and Bansal, M. C. (2012). Characterization of deinking sludge from combined deinking technology. *IPPTA Journal*, *24* (3), 81-86.
- ✓ Kumar, A., Mohanta, K., Kumar, D., and Parkash, O. (2012). Properties and industrial applications of rice husk: A review. *IJETAE*, *2*(10), 86-90.

- ✓ Lee, C. K., Ibrahim, D., and Omar, I. C. (2013). Enzymatic deinking of various types of waste paper: efficiency and characteristics. *Process Biochemistry*, *48*(2), 299-305.
- ✓ Lee, C. K., Ibrahim, D., Ibrahim, C. O., and Daud, W. R. W. (2011). Enzymatic and chemical deinking of mixed office wastepaper and old newspaper: Paper quality and effluent characteristics. *BioResources*, *6*(4), 3859-3875.
- ✓ Lee, J. M., Kim, Y. J., Lee, W. J., and Kim, S. D. (1998). Coal-gasification kinetics derived from pyrolysis in a fluidized-bed reactor. *Energy*, *23*(6), 475-488.
- ✓ Lee, J. W., Houtman, C. J., Kim, H. Y., Choi, I. G., and Jeffries T. W. (2011). Scale –up study of oxalic acid pretreatment of agricultural lignocellulosic biomass for the production of bioethanol. *Bioresource Technology*, *102* (16), 7451-7456.
- ✓ Lee, J. W., and Jeffries, T. W. (2011). Efficiencies of acid catalysts in the hydrolysis of lignocellulosic biomass over a range of combined severity factors. *Bioresource Technology*, *102* (10), 5884-5890.
- ✓ Lehmann, K., Domsch, A., and Hawel, H. (1990). *U.S. Patent No.4,959,123.* Washington DC : U.S. Patent and Trademark Office.
- ✓ Liu, K., Ma, X. Q., and Xiao, H. M. (2010). Experimental and kinetic modeling of oxygen-enriched air combustion of paper mill sludge. *Waste management*, *30*(7), 1206-1211.
- ✓ Lou, R., Wu, S., Lv, G., and Yang, Q. (2012). Energy and resource utilization of deinking sludge pyrolysis. *Applied Energy*, *90*(1), 46-50.
- ✓ Manfredi, M., de Oliveira, R. C., da Silva, J. C., and Reyes, R. I. Q. (2013). Ultrasonic treatment of secondary fibers to improve paper properties. *Nordic Pulp & Paper Research Journal*, *28*(2), 297-301.
- ✓ Manning, A., and Thompson, R. (2002). The Influence of Ultrasound on Virgin Paper Fibres. *Progress in Paper Recycling*, *11*(4), 6-12.
- ✓ Mansaray, K. G., and Ghaly, A. E. (1998). Thermal degradation of rice husks in nitrogen atmosphere. *Bioresource Technol*ogy, *65*(1), 13-20.
- ✓ Market facts. (2014). Retrieved April 23, 2015, from http://india.paperex-expo.com/Exhibitors/Market-Facts.aspx
- ✓ Mason T. J. and Cordemans E. D. (1996). Ultrasonic intensification of chemical processing and related operations: a review. *Trans lChemE, 74*(Part A).
- ✓ Mathur, S., Kumar, S., and Rao, N. J. (2005). Xylanase Prebleaching of Chemical Pulps. *IPPTA Journal*, *17*(4), 35 – 47.

- ✓ Mehmannavaz, T., Ismail, M., Sumadi, S. R., and Samadi, S. M., (2014). Lightweight mortar incorporating various percentages of waste materials. *Jurnal Teknologi (Science and Engineering)*, *67* (3), 83-89.
- ✓ Méndez, A., Fidalgo, J. M., Guerrero, F., and Gascó, G. (2009). Characterization and pyrolysis behaviour of different paper mill waste materials. *Journal of Analytical and Applied Pyrolysis*, *86*(1), 66-73.
- ✓ Nayak, P. S., and Singh, B. K. (2007). Instrumental characterization of clay by XRF, XRD and FTIR. *Bulletin of Materials Science*, *30*(3), 235-238.
- ✓ Pala, H., Mota, M., and Gama, F. M. (2004). Enzymatic versus chemical deinking of non-impact ink printed paper. *Journal of Biotechnology*, *108*(1), 79-89.
- ✓ Pala, H., Mota, M., and Gama, F. M. (2006). Factors influencing MOW deinking: laboratory scale studies. *Enzyme and Microbial Technology*, *38*(1), 81-87.
- ✓ Pala, H., Mota, M., and Gama, F. M. (2007). Laboratory paper pulp deinking: an evaluation based on Image Analysis, ISO brightness and ERIC. *Appita Journal*, *60*(2), 129.
- ✓ Park, D. K., Kim, S. D., Lee, S. H., Lee, J. G. (2010). Co-pyrolysis characteristic of sawdust and coal blend in TGA and a fixed bed reactor. *Bioresource Technol*ogy, *101*, 6151-6156.
- ✓ Pathak, P. (2014). Enzymatic deinking of photocopier waste papers. *Ph.D Thesis.* Indian Institute of Technology Roorkee, Roorkee.
- ✓ Pathak, P., Bhardwaj, N. K., and Singh, A. K. (2010). Enzymatic deinking of office waste paper: an overview. *IPPTA Journal*, *22*(2), 83-88.
- ✓ Pathak, P., Bhardwaj, N. K., and Singh, A. K. (2011). Optimization of chemical and enzymatic deinking of photocopier waste paper. *BioResources*, *6*(1), 447-463.
- ✓ Phonphuak, N. (2013). Effects of additive on the physical and thermal conductivity of fired clay brick. *Journal of Chemical Science and Technology*, *2*(2), 95-99.
- ✓ Piloyan, G. O., Ryabchikov, I. D., and Novikova, O. S. (1966). Determination of activation energies of chemical reactions by differential thermal analysis. *Nature*, *212*(5067), 1229.
- ✓ Pradhan, D., and Singh, R. K. (2012). Recovery of value added chemicals from waste tyre Pyrolysis. *3rd International conference on solid waste management and exhibition, IconSWM*, Mysore, Karnataka, India.
- ✓ Rao, N. J., Khanna, S. S., Kumar, R., Kannababul, K. (2005). Energy Conservation System in Digester House. *Proc. of the annual seminar of IPPTA on "Developments in Pulping and Chemical Recovery*, 4th-5th March, New Delhi.

- ✓ Rao, N. J., and Kumar, R. (1985). Energy conservation approaches in a paper mill with special reference to the evaporator plant. In *Proc. IPPTA Int. Seminar on Energy Conservation in Pulp and Paper Industry*, 58-70.
- ✓ Rajput, D., Bhagade, S. S., Raut, S. P., Ralegaonkar, R. V., and Mandavgane, S. A. (2012). Reuse of cotton and recycle paper mill waste as building material. *Construction and Building Materials*, *34*, 470-475.
- ✓ Raut, S., Ralegaonkar, R., and Mandavgane, S. (2013). Utilization of recycle paper mill residue and rice husk ash in production of light weight bricks. *Archives of Civil and Mechanical Engineering*, *13*(2), 269-275.
- ✓ Raut, S. P., Sedmake, R., Dhunde, S., Ralegaonkar, R. V., and Mandavgane, S. A. (2012). Reuse of recycle paper mill waste in energy absorbing light weight bricks. *Construction and Building Materials*, *27*(1), 247-251.
- ✓ Reich, L., and Stivala, S. S. (1983). Computer-determined kinetic parameters from TG curves (Part IX). *Thermochimica Acta*, *71*(3), 281-285.
- ✓ Report: Paper (2011). Retrieved April 22, 2015, from http://planningcommission.gov.in/aboutus/committee/wrkgrp12/wg_paper.pdf
- ✓ Saade, R. G., and Koziński, J. A. (1998). Dynamics of physical characteristics of biowaste during pyrolysis. *Journal of Analytical and Applied Pyrolysis*, *45*(1), 9-22.
- ✓ Sadhukhan, A. K., Gupta, P., Goyal, T., and Saha, R. K. (2008). Modelling of pyrolysis of coal–biomass blends using thermogravimetric analysis. *Bioresource technology*, *99*(17), 8022-8026.
- ✓ Sankaralingam, P., Chinnaraj, S. and Subrahmanyam, S. V., (2013). Pulping and light-ECF Bleaching of Bagasse Mixed with Banana Pseudo Stem and Its Impact on Environment. *IPPTA Journal*, 25 (2), 127-130.
- ✓ Shen, D. K., and Gu, S. (2009). The mechanism for thermal decomposition of cellulose and its main products. *Bioresource Technology*, *100*(24), 6496-6504.
- ✓ Singh, R. K., Biswal, B., and Kumar, S. (2013). Determination of activation energy from pyrolysis of paper cup waste using thermogravimetric analysis. *Research Journal of Recent Science*, *2*, 177-182.
- ✓ Singh, R. K., and Shadangi, K. P. (2011). Liquid fuel from castor seeds by pyrolysis. *Fuel*, *90*(7), 2538-2544.
- ✓ Solomon, P. R., Serio, M. A., and Suuberg, E. M. (1992). Coal pyrolysis: experiments, kinetic rates and mechanisms. *Progress in Energy and Combustion Science*, *18*(2), 133-220.

- ✓ Song, X., Bie, R., Ji, X., Chen, P., Zhang, Y., and Fan, J. (2015). Kinetics of reed black liquor (RBL) pyrolysis from thermogravimetric data. *BioResources*, *10*(1), 137-144.
- ✓ Srikanth S. (2014). Pre-treatment of rice husk with acid or base for its effect on pyrolysis products. *M. Tech Thesis*, National Institute of Technology Rourkela, Rourkela.
- ✓ Stefanidis, S. D., Kalogiannis, K. G., Iliopoulou, E. F., Michailof, C. M., Pilavachi, P. A., and Lappas, A. A. (2014). A study of lignocellulosic biomass pyrolysis via the pyrolysis of cellulose, hemicellulose and lignin. *Journal of Analytical and Applied Pyrolysis*, *105*, 143-150.
- ✓ Strezov, V., and Evans, T. J. (2009). Thermal processing of paper sludge and characterisation of its pyrolysis products. *Waste Management*, *29*(5), 1644-1648.
- ✓ Subramanian, R., Fordsmand, H., and Paulapuro, H. (2007). Precipitated Calcium Carbonate (PCC)-Cellulose composite fillers; effect of PCC particle structure on the production and properties of uncoated fine paper. *BioResources*, *2*(1), 91-105.
- ✓ Subramanian, R., Kononov, A., Kang, T., Paltakari, J., and Paulapuro, H. (2008). "*Structure and properties of some natural cellulosic fibrils*," *BioResources*, *3*(1), 192-203.
- ✓ Subramanian, R. and Paulapuro, H. (2006). Effect of PCC-bagasse pulp composites on printing and writing paper properties. *In: Zhan Huaiyu, Chen Fangeng, and Fu Shiyu (editors).New Technologies in Non-Wood Fiber Pulping and Papermaking.Proceedings of the 5th International Non-Wood Fiber Pulping and Papermaking Conference (INWFPPC*). Guangzhou, China, South China University Press, 270-276.
- ✓ Subramanian, S., Rakkiyappan, P., Chinnaraj, S., and Subrahmanyam, S. V. (2012). Evaluation of Erianthus Arundinaceus as a source of non-conventional raw material for pulping and papermaking. *IPPTA Journal*, *24*(3), 41-46.
- ✓ Sutcu, M., and Akkurt, S. (2009). The use of recycled paper processing residues in making porous brick with reduced thermal conductivity. *Ceramics International*, *35*(7), 2625-2631.
- ✓ Sutcu, M., del Coz Díaz, J. J., Rabanal, F. P. Á., Gencel, O., and Akkurt, S. (2014). Thermal performance optimization of hollow clay bricks made up of paper waste. *Energy and Buildings*, *75*, 96-108.
- ✓ Tai, H. S., and Hsu, C. H. (2012). Kinetic analysis of thermal degradation of polypropylene using a modified Gompertz model. *Journal of Hazardous, Toxic, and Radioactive Waste*, *16*(1), 39-50.

- ✓ Tatsumi, D., Higashihara, T., Kawamura, S. Y., and Matsumoto, T. (2000). Ultrasonic treatment to improve the quality of recycled pulp fiber. *Journal of wood science*, *46*(5), 405-409.
- ✓ Vamvuka, D. (1998). Thermogravimetric analysis of beneficiated low-rank coal in oxidative environment. *Mineral Wealth*, 106, 21-28.
- ✓ Vamvuka, D., and Kakaras, E. (2011). Ash properties and environmental impact of various biomass and coal fuels and their blends. *Fuel Processing Technology*, *92*(3), 570-581.
- ✓ Vamvuka, D., Kakaras, E., Kastanaki, E., and Grammelis, P. (2003). Pyrolysis characteristics and kinetics of biomass residuals mixtures with lignite. *Fuel*, *82*(15), 1949-1960.
- ✓ Vamvuka, D., Salpigidou, N., Kastanaki, E., and Sfakiotakis, S. (2009). Possibility of using paper sludge in co-firing applications. *Fuel*, *88*(4), 637-643.
- ✓ Vamvuka, D., and Sfakiotakis, S. (2011). Combustion behaviour of biomass fuels and their blends with lignite. *Thermochimica Acta*, *526*(1), 192-199.
- ✓ Vamvuka, D., and Woodburn, E. T. (1995). Effect of Inorganic Matter on the Devolatilization and Combustion of Low-Rank Coals. *Tech. Chron.*, 15(1-2), 23-33.
- ✓ Varshney, R., Agnihotri, P. K., Sharma, C., and Bansal, M. C. (2007). Flotation Deinking Studies of ONP for Deinking Chemicals and Process Conditions. *IPPTA Journal*, *19*(4), 151-154.
- ✓ Wallberg, P. and Paart, E. (1998). *U.S. Patent No.5,736,622.* Washington DC : U.S. Patent and Trademark Office.
- ✓ Wang, Y. Y., Chen, J. C., and Yang, G. H. (2014). Effect of Heating Rate on the Deinking Sludge Pyrolysis Character. *Applied Mechanics and Materials*, *670*, 205-208.
- ✓ Wang, S., Guo, X., Wang, K., and Luo, Z. (2011). Influence of the interaction of components on the pyrolysis behavior of biomass. *Journal of Analytical and Applied Pyrolysis*, *91*(1), 183-189.
- ✓ Wu, T. Y., Guo, N., Teh, C. Y., and Hay, J. X. W. (2013). Chapter 2 Theory and Fundamentals of Ultrasound. *Advances in ultrasound technology for environmental remediation*. SpringerBriefs in Molecular Science (Green Chemistry for Sustainability), Springer Netherlands.
- ✓ Xie, Z., and Ma, X. (2013). The thermal behaviour of the co-combustion between paper sludge and rice straw. *Bioresource Technology*, *146*, 611-618.
- ✓ Yanfen, L., and Xiaoqian, M. (2010). Thermogravimetric analysis of the co-combustion of coal and paper mill sludge. *Applied Energy*, *87*(11), 3526-3532.

- ✓ Yang, H., Yan, R., Chen, H., Lee, D. H., and Zheng, C. (2007). Characteristics of hemicellulose, cellulose and lignin pyrolysis. *Fuel*, *86*(12), 1781-1788.
- ✓ Yazdi, M. F. A., Zakaria, R., Mustaffar, M., Abd. Majid, M. Z., Zin, R. M., Ismail, M., and Yahya, K. (2014). Bio-composite materials potential in enhancing sustainable construction. *Desalination and Water Treatment*, *52*(19-21), 3631-3636
- ✓ Yu, Y. H., Kim, S. D., Lee, J. M., and Lee, K. H. (2002). Kinetic studies of dehydration, pyrolysis and combustion of paper sludge. *Energy*, *27*(5), 457-469.
- ✓ Zhang, L. (2013). Production of bricks from waste materials–a review. *Construction and Building Materials*, *47*, 643-655.
- ✓ Zhao, Y., Deng, Y., and Zhu, J. Y. (2004). Roles of surfactants in flotation deinking. *Progress in Paper Recycling*, *14*(1), 41-45.
- ✓ Zhenying, S., Shijin, D., Xuejun, C., Yan, G., Junfeng, L., Hongyan, W., and Zhang, S. X. (2009). Combined de-inking technology applied on laser printed paper. *Chemical Engineering and Processing: Process intensification*, *48*(2), 587-591.

Annexure-1

abcdefghijklmnopqrstuvwxyzABCDEFGHIJKLM20123456789!@#$%^&*(){}[]?<>
abcdefghijklmnopqrstuvwxyzABCDEFGHIJKLM20123456789!@#$%^&*(){}[]?<>
abcdefghijklmnopqrstuvwxyzABCDEFGHIJKLM20123456789!@#$%^&*(){}[]?<>
abcdefghijklmnopqrstuvwxyzABCDEFGHIJKLM20123456789!@#$%^&*(){}[]?<>
abcdefghijklmnopqrstuvwxyzABCDEFGHIJKLM20123456789!@#$%^&*(){}[]?<>
abcdefghijklmnopqrstuvwxyzABCDEFGHIJKLM20123456789!@#$%^&*(){}[]?<>
abcdefghijklmnopqrstuvwxyzABCDEFGHIJKLM20123456789!@#$%^&*(){}[]?<>
abcdefghijklmnopqrstuvwxyzABCDEFGHIJKLM20123456789!@#$%^&*(){}[]?<>
abcdefghijklmnopqrstuvwxyzABCDEFGHIJKLM20123456789!@#$%^&*(){}[]?<>
abcdefghijklmnopqrstuvwxyzABCDEFGHIJKLM20123456789!@#$%^&*(){}[]?<>
abcdefghijklmnopqrstuvwxyzABCDEFGHIJKLM20123456789!@#$%^&*(){}[]?<>
abcdefghijklmnopqrstuvwxyzABCDEFGHIJKLM20123456789!@#$%^&*(){}[]?<>
abcdefghijklmnopqrstuvwxyzABCDEFGHIJKLM20123456789!@#$%^&*(){}[]?<>
abcdefghijklmnopqrstuvwxyzABCDEFGHIJKLM20123456789!@#$%^&*(){}[]?<>
abcdefghijklmnopqrstuvwxyzABCDEFGHIJKLM20123456789!@#$%^&*(){}[]?<>
abcdefghijklmnopqrstuvwxyzABCDEFGHIJKLM20123456789!@#$%^&*(){}[]?<>
abcdefghijklmnopqrstuvwxyzABCDEFGHIJKLM20123456789!@#$%^&*(){}[]?<>
abcdefghijklmnopqrstuvwxyzABCDEFGHIJKLM20123456789!@#$%^&*(){}[]?<>
abcdefghijklmnopqrstuvwxyzABCDEFGHIJKLM20123456789!@#$%^&*(){}[]?<>
abcdefghijklmnopqrstuvwxyzABCDEFGHIJKLM20123456789!@#$%^&*(){}[]?<>
abcdefghijklmnopqrstuvwxyzABCDEFGHIJKLM20123456789!@#$%^&*(){}[]?<>
abcdefghijklmnopqrstuvwxyzABCDEFGHIJKLM20123456789!@#$%^&*(){}[]?<>
abcdefghijklmnopqrstuvwxyzABCDEFGHIJKLM20123456789!@#$%^&*(){}[]?<>
abcdefghijklmnopqrstuvwxyzABCDEFGHIJKLM20123456789!@#$%^&*(){}[]?<>
abcdefghijklmnopqrstuvwxyzABCDEFGHIJKLM20123456789!@#$%^&*(){}[]?<>
abcdefghijklmnopqrstuvwxyzABCDEFGHIJKLM20123456789!@#$%^&*(){}[]?<>
abcdefghijklmnopqrstuvwxyzABCDEFGHIJKLM20123456789!@#$%^&*(){}[]?<>
abcdefghijklmnopqrstuvwxyzABCDEFGHIJKLM20123456789!@#$%^&*(){}[]?<>
abcdefghijklmnopqrstuvwxyzABCDEFGHIJKLM20123456789!@#$%^&*(){}[]?<>
abcdefghijklmnopqrstuvwxyzABCDEFGHIJKLM20123456789!@#$%^&*(){}[]?<>
abcdefghijklmnopqrstuvwxyzABCDEFGHIJKLM20123456789!@#$%^&*(){}[]?<>
abcdefghijklmnopqrstuvwxyzABCDEFGHIJKLM20123456789!@#$%^&*(){}[]?<>
abcdefghijklmnopqrstuvwxyzABCDEFGHIJKLM20123456789!@#$%^&*(){}[]?<>
abcdefghijklmnopqrstuvwxyzABCDEFGHIJKLM20123456789!@#$%^&*(){}[]?<>
abcdefghijklmnopqrstuvwxyzABCDEFGHIJKLM20123456789!@#$%^&*(){}[]?<>
abcdefghijklmnopqrstuvwxyzABCDEFGHIJKLM20123456789!@#$%^&*(){}[]?<>
abcdefghijklmnopqrstuvwxyzABCDEFGHIJKLM20123456789!@#$%^&*(){}[]?<>
abcdefghijklmnopqrstuvwxyzABCDEFGHIJKLM20123456789!@#$%^&*(){}[]?<>
abcdefghijklmnopqrstuvwxyzABCDEFGHIJKLM20123456789!@#$%^&*(){}[]?<>
abcdefghijklmnopqrstuvwxyzABCDEFGHIJKLM20123456789!@#$%^&*(){}[]?<>
abcdefghijklmnopqrstuvwxyzABCDEFGHIJKLM20123456789!@#$%^&*(){}[]?<>
abcdefghijklmnopqrstuvwxyzABCDEFGHIJKLM20123456789!@#$%^&*(){}[]?<>
abcdefghijklmnopqrstuvwxyzABCDEFGHIJKLM20123456789!@#$%^&*(){}[]?<>
abcdefghijklmnopqrstuvwxyzABCDEFGHIJKLM20123456789!@#$%^&*(){}[]?<>
abcdefghijklmnopqrstuvwxyzABCDEFGHIJKLM20123456789!@#$%^&*(){}[]?<>
abcdefghijklmnopqrstuvwxyzABCDEFGHIJKLM20123456789!@#$%^&*(){}[]?<>
abcdefghijklmnopqrstuvwxyzABCDEFGHIJKLM20123456789!@#$%^&*(){}[]?<>

Annexure-2

Nomenclature	
A	Mould of brick specimen
B	Raw materials
C	Mixture of raw materials
D	Filling into brick specimen mould
E	Finishing
F	Marking of brick specimen
G	Air drying of brick specimen
H	Laboratory type electrical furnace
I	Brick specimen before firing
J	Brick specimen after firing
K	Final products